

## INFORMATION TO USERS

This manuscript has been reproduced from the microfilm master. UMI films the text directly from the original or copy submitted. Thus, some thesis and dissertation copies are in typewriter face, while others may be from any type of computer printer.

**The quality of this reproduction is dependent upon the quality of the copy submitted.** Broken or indistinct print, colored or poor quality illustrations and photographs, print bleedthrough, substandard margins, and improper alignment can adversely affect reproduction.

In the unlikely event that the author did not send UMI a complete manuscript and there are missing pages, these will be noted. Also, if unauthorized copyright material had to be removed, a note will indicate the deletion.

Oversize materials (e.g., maps, drawings, charts) are reproduced by sectioning the original, beginning at the upper left-hand corner and continuing from left to right in equal sections with small overlaps. Each original is also photographed in one exposure and is included in reduced form at the back of the book.

Photographs included in the original manuscript have been reproduced xerographically in this copy. Higher quality 6" x 9" black and white photographic prints are available for any photographs or illustrations appearing in this copy for an additional charge. Contact UMI directly to order.

# UMI

A Bell & Howell Information Company  
300 North Zeeb Road, Ann Arbor MI 48106-1346 USA  
313/761-4700 800/521-0600



***Soap retention on pulp fibers during recycling:  
A mechanistic study using a packed bed reactor***

by

Claudia Fernandez

A thesis submitted to the Faculty of Graduate Studies and Research  
in partial fulfilment of the requirements for the degree of  
Master of Engineering

Department of Chemical Engineering  
McGill University  
Montreal, Quebec, Canada  
© Claudia Fernandez, 1996

December 1996



National Library  
of Canada

Acquisitions and  
Bibliographic Services

395 Wellington Street  
Ottawa ON K1A 0N4  
Canada

Bibliothèque nationale  
du Canada

Acquisitions et  
services bibliographiques

395, rue Wellington  
Ottawa ON K1A 0N4  
Canada

*Your file Votre référence*

*Our file Notre référence*

The author has granted a non-exclusive licence allowing the National Library of Canada to reproduce, loan, distribute or sell copies of this thesis in microform, paper or electronic formats.

The author retains ownership of the copyright in this thesis. Neither the thesis nor substantial extracts from it may be printed or otherwise reproduced without the author's permission.

L'auteur a accordé une licence non exclusive permettant à la Bibliothèque nationale du Canada de reproduire, prêter, distribuer ou vendre des copies de cette thèse sous la forme de microfiche/film, de reproduction sur papier ou sur format électronique.

L'auteur conserve la propriété du droit d'auteur qui protège cette thèse. Ni la thèse ni des extraits substantiels de celle-ci ne doivent être imprimés ou autrement reproduits sans son autorisation.

0-612-29593-1

Canada



## ABSTRACT

Paper made of recycled fibers often has different properties than that made entirely of virgin pulp. A hypothetical mechanism for the loss of papermaking and printing potential of recycled paper is the adsorption and entrapment of molecules of low surface energy such as oil and soap, on the wood fibers during recycling. The objectives of this study were threefold: first, to develop a technique to quantify contaminant retention during recycling; second, to test this hypothesis; and third, to elucidate the retention mechanisms.

A sensitive technique to quantify the retention of contaminants on the pulp is to follow the dynamics of retention of a concentration pulse generated at the entrance (breakthrough curve, BTC) of a packed bed of fibers. Using this technique, we showed that sodium salts of fatty acids undergo ion-exchange with the calcium present in the pulp. Soap prepared by mixing equimolar amounts of sodium oleate and calcium chloride (1 Meq) do not adsorb on pulp fibers. This behavior goes according to theory as the negatively charged soap particles are repelled from the negatively charged fibers. However, retention of the soap particles increases as the Calcium chloride concentration is increased to 0.164 and 1.48 mmol/L. This is due to a charge screening mechanism expected in the presence of an electrolyte. Two different phenomena can occur: (1) particle deposition above a critical deposition concentration (CDC); and, (2) particle coagulation above a critical coagulation concentration close to the fiber's surface,  $CCC_{\text{surface}}$ . From retention isotherms at different calcium chloride concentrations (0.16 mmol/L calcium oleate), a  $CCC_{\text{surface}}$  of 0.7 mmol/L was estimated.

In the presence of a trivalent cation, such as  $Al^{+3}$ , the mechanism becomes more

complicated as  $\text{Al}^{+3}$  ions undergo adsorption or ion-exchange with the  $\text{Ca}^{+2}$ ; this renders the soap particles positive. The balance between the ion-exchange and charge screening kinetics determine the retention behavior in the presence of aluminum chloride. The effects of the variables studied were analyzed in terms of a mathematical model that simulates particle retention kinetics in packed beds.

## RÉSUMÉ

Les propriétés du papier fabriqué à partir de fibres recyclées sont différentes de celles obtenues en utilisant une pâte vierge. Nous émettons l'hypothèse suivant laquelle la perte du potentiel papetier et d'impression du papier recycle sont dû à l'absorption et le coincement de molécules de faible énergie superficielle (huiles et savons d'acides gras, par exemple) sur les fibres de bois durant le recyclage. Les objectifs de cette étude sont les suivants: primo, développer une technique de quantification de la rétention de contaminants lors du recyclage; deuxio, vérifier cette hypothèse en utilisant des composés modèles de désencrage; et tertio, d'identifier les mécanismes de rétention par les fibres. Une technique sensible de quantification de la rétention de contaminants sur la pâte, consiste à suivre les dynamiques de rétentions à partir d'essais d'impulsions (courbes de fixation) générées à l'entrée de lits de fibres tassées.

Nous avons montré que les sels de sodium d'acides gras sont impliqués dans un échange d'ions avec le calcium présent dans la pâte. Un savon d'acide gras préparé en mélangeant des quantités équimolaires d'oléate de sodium et de chlorure de calcium (1 Meq) ne s'absorbe pas sur les fibres cellulosiques. Le comportement est en accord avec la théorie, car les particules chargées négativement sont repoussées par les fibres papetières, également de charge négative. Cependant, la rétention de particules de savon croît lorsque la concentration de savon est augmentée à 2 Meq et 10 Meq (0,164 et 1,480 mmol/L). Ceci est dû à un mécanisme de masquage de charge, prévisible en présence d'un électrolyte. Deux phénomènes peuvent se produire: (1) Un dépôt de particules au-delà d'une concentration critique de dépôt (CCD); et, (2) La coagulation de particules au-delà d'une concentration critique de coagulation proche de celle de la surface des fibres ( $CCC_{\text{surface}}$ ). A partir



d'isothermes de rétention à différentes concentrations en chlorure de calcium (0,16 mmol/L d'oléate de calcium), une  $CCC_{\text{surface}}$  de 0,7 mmol/L a été estimée.

En présence d' $Al^{3+}$ , le mécanisme se complique. Ce cation peut entraîner une absorption ou un échange d'ions avec  $Ca^{2+}$  (rendant positives les particules de savon). L'équilibre entre cinétiques d'échange d'ions et de masquage de charge, déterminera le comportement rétentionnaire en présence de chlorure d'aluminium. Les effets des variables ont été analysés à travers un modèle mathématique simulant les cinétiques de rétention de particules au sein de lits de fibres tassées.

## ACKNOWLEDGEMENTS

My sincere appreciation goes to my thesis supervisor *Prof. Gil Garnier* for his teaching, understanding, and encouragement.

I would also like to thank Dr. T.G.M. van de Ven for helpful discussions during group meetings. The suggestions and continuous help of my fellow colleagues are warmly appreciated. In particular, I thank: L. Godbout, Dr. L. Yu, Dr. R. Brosseau, Dr. J. Petlicki, Dr. R. Alince, Tom Asselman, Alain Carignan, Ondrej Drabek, Christopher Hammock, Alois Vanerek and Alex Wu.

To the personnel of the McGill Pulp and Paper Research Centre for their kind help. To the personnel of Paprican; in particular, I thank the help received from Photography, Machine shop, Chemical analysis and Physical testing.

I thank the financial support of the National Centres of Excellence - Mechanical and Chemimechanical Wood Pulps Network. Special thanks are due to the Paper Industry Management Association (fellowship), the Pulp and Paper Research Institute of Canada (fellowship), and the National Centres of Excellence (poster award).

To my family for their company, love and support.

Candidates have the option of including, as part of their thesis, the text of one or more papers submitted or to be submitted for publication, or the clearly-duplicated text of one or more published papers. These texts must be bound as an integral part of the thesis.

If this option is chosen, connecting text that provide logical bridges between the different papers are mandatory. The thesis must be written in such a way that it is more than a mere collection of manuscripts; in other word, results of a series of papers must be integrated.

The thesis must still conform to all other requirements of the “Guidelines for thesis preparation”. The thesis must include: A table of contents, an abstract in English and French, an introduction which clearly states the rationale and objectives of the study, a review of the literature, a final conclusion and summary, and a thorough bibliography or reference list.

Additional material must be provided where appropriate (e.g. in appendices) and in sufficient detail to allow a clear and precise judgement to be made of the importance and the originality of the research reported in the thesis.

In the case of manuscripts co-authored by the candidate and others, the candidate is required to make an explicit statement in the thesis as to who contributed to such work and to what extent. Supervisors must attest to test the accuracy of work and to what extend. Supervisors must attest to the accuracy of such statements at the doctoral oral defence. Since the task of the examiners is made more difficult in these cases, it is in the candidate’s interest to make perfectly clear the responsibilities of all the authors of the co-authored papers.

## TABLE OF CONTENTS

ABSTRACT .....	iii
RÉSUMÉ .....	v
ACKNOWLEDGEMENTS .....	vii
LIST OF FIGURES .....	xi
LIST OF TABLES .....	xvi

### CHAPTER 1

INTRODUCTION .....	1
1.1 JUSTIFICATION .....	2
1.2 THE PAPER RECYCLING PROCESS .....	4
1.3 HYPOTHESIS .....	8
1.4 LITERATURE REVIEW .....	8
1.4.1 Retention principles .....	8
1.6 GENERAL OBJECTIVES .....	10
1.7 ORGANIZATION OF THE THESIS .....	11
REFERENCES .....	12

### CHAPTER TWO

#### RETENTION OF FATTY ACID SOAPS DURING RECYCLING:

A STUDY USING PACKED BEDS OF PULP FIBERS .....	14
ABSTRACT .....	15
2.1 INTRODUCTION .....	17
2.2 EXPERIMENTAL TECHNIQUES .....	20
2.3 RESULTS AND DISCUSSION .....	29
2.4 CONCLUSIONS .....	54
REFERENCES .....	56

### **CHAPTER THREE**

#### **RETENTION OF FATTY ACID SOAPS DURING RECYCLING:**

<b>A MECHANISTIC STUDY</b> .....	59
<b>ABSTRACT</b> .....	60
<b>3.1 INTRODUCTION</b> .....	62
<b>3.2 RELATED COLLOID CHEMISTRY DEFINITIONS</b> .....	63
<b>3.3 MODEL OF THE FLOW AND DEPOSITION OF PARTICLES</b> .....	64
<b>3.4 EXPERIMENTAL</b> .....	66
<b>3.5 RESULTS</b> .....	74
<b>3.6 DISCUSSION</b> .....	88
<b>3.7 CONCLUSIONS</b> .....	111
<b>REFERENCES</b> .....	114

### **CHAPTER 4**

<b>CONCLUSIONS</b> .....	117
<b>4.1 Overall conclusions</b> .....	118
<b>4.2 Future work</b> .....	121
<b>4.3 Implications of this study on Paper Recycling</b> .....	123

### **APPENDIX A**

<b>TECHNICAL DESIGN</b> .....	126
<b>I. Experimental strategy</b> .....	127
<b>II. Packed bed design</b> .....	127
<b>III. Trouble-Shooting</b> .....	128

### **APPENDIX B**

<b>PACKED BED TECHNICAL DRAWINGS</b> .....	130
--	-----

## LIST OF FIGURES

	<u>Page</u>
<b>CHAPTER 2</b>	
Fig. 1. Experimental Setup	23
Fig. 2. Calibration curve of the absorbance at 336 nm versus concentration (mM) of calcium oleate suspensions at room temperature.	26
Fig. 3. Breakthrough curve for a ten-minute calcium oleate pulse ( $C_o=0.5$ mmol/l or 0.3 g/l) and sucrose (15 g/l) RTD function on a TMP packed bed (the pulse starts at time 0).	30
Fig. 4. Breakthrough curves of two consecutive sodium oleate (1g/L) pulses on a TMP packed bed.	32
Fig. 5. Calcium and Sodium analyses of TMP samples, before and after a 10-minute Na(Oleate) pulse.	34
Fig. 6. Breakthrough curves of ten-minute sodium oleate pulses on kraft pulp treated with: ( — ) EDTA; ( □ ) HCl washing; and ( ● ) NaCl washing [1N].	36
Fig. 7a. BTC's of consecutive sodium oleate pulses on kraft pulp showing complete sequence.	38
Fig. 7b. BTC's of consecutive sodium oleate pulses on kraft pulp showing detail of the sequence.	39

- Fig. 8. BTC's of consecutive sodium oleate pulses on a kraft pulp bed saturated with sodium oleate (there is no calcium left in the pulp as it was fully exchanged). The curves shown correspond to washing responses using different water quality: ( □ ) deionized water and ( ● ) tap water. 40
- Fig. 9. A simplistic view of the cell wall porosity and the relative sizes of the chemical species involved in this study. 42
- Fig. 10. BTC's of two calcium oleate pulses ( on Kraft pulp) with different levels of calcium concentration: (I) 1 Meq and (II) 10 Meq. 45
- Fig. 11. Calcium oleate mass balance for the 10 Meq calcium oleate pulse showing actual extracted amount. 47
- Fig. 12a. SEM photographs of kraft fibers for the 10 Meq calcium oleate pulse 48
- Fig. 12b. Magnified image 49
- Fig. 13. Contact angle measurements of filter paper samples with (soapy) and without (clean) deposited soap. 52
- Fig. 14. Contact angle measurements of untreated (clean) filter paper samples and the corresponding surface tension measurements of deionized water (71.0 mN/m) and soapy water (49.3 mN/m). 53
- Fig. 15. Proposed scheme of the adsorption-desorption process dynamics between paper and calcium soaps. 55

### CHAPTER 3

- Fig. 1. Particle concentration at the exit of the bed as a function of  $P_1$ .  
Simulation for  $P_2 = P_3 = 1$  and  $Pe = 40$ . 68
- Fig. 2. Particle concentration at the exit of the bed as a function of  $P_2$ .  
Simulation for  $P_1 = 0.1$ ,  $P_3 = 17$  and  $Pe = 40$ . 69
- Fig. 3. Particle concentration at the exit of the bed as a function of  $P_3$ .  
Simulation for  $P_1 = 0.01$ ,  $P_2 = 1.0$  and  $Pe = 40$ . 70
- Fig. 4. BTC's of calcium oleate (0.16 mM) at different  $CaCl_2$  levels. 75
- Fig. 5. BTC of a 10-minute pulse of calcium oleate containing  $AlCl_3$  77
- Fig. 6. BTC's of calcium oleate as a function of consistency for  
[ $CaCl_2$ ] 1.48 mM. 79
- Fig. 7. Effect of consistency on BTC slopes ([ $CaCl_2$ ] = 1.48 mM,  
[Ca(oleate)] = 0.16 mM). 80
- Fig. 8. BTC's at different flowrates ([ $CaCl_2$ ] = 0.16 mM, 0.16 mM Calcium  
oleate). 81
- Fig. 9. BTC's at different flowrates ([ $CaCl_2$ ] = 1.48 mM, 0.16 mM Calcium  
oleate). 82
- Fig. 10. Effect of electrolyte concentration on the zeta potential of pulp fibers. 84



Fig. 11. Effect of calcium chloride concentration on the zeta potential of calcium oleate particles.	85
Fig. 12. Effect of aluminium chloride concentration on the zeta potential of calcium oleate particles.	86
Fig. 13. Effect of calcium chloride concentration on the calcium oleate particle diameter measured by DLS (0.164 mM calcium oleate).	87
Fig. 14. Effect of aluminium chloride concentration on the calcium oleate particle diameter measured by DLS (0.164 mM calcium oleate).	89
Fig. 15. Soap suspension stability (PDA) for 0.16 mM calcium oleate at $[\text{CaCl}_2] = 3.8 \text{ mM}$ .	90
Fig. 16. Retention isotherm for 0.16 mM calcium oleate (10-minute pulses).	92
Fig. 17. Particle concentration polarization at the surface of a membrane.	94
Fig. 18. Schematic of mechanism showing (A, B) piling-up of mobile particles and (C, D) dilution effects causing particle release.	96
Fig. 19. Initial response slope as a function of residence time (1.48 mM $\text{CaCl}_2$ ).	101
Fig. 20. Effect of flowrate on percentage of soap retained.	102
Fig. 21. Number of moles exiting from the packed bed at time $t$ as a function of flowrate.	104

Fig. 22. Rate of soap retention as a function of flowrate for 0.16 mM calcium  
oleate

106

Fig. 23. Effect of consistency on percentage of soap retained.

108

**LIST OF TABLES****CHAPTER 1**

Table I. Deinking chemicals	6
-----------------------------	---

**CHAPTER 2**

Table I. Surface energy of wood and its components.	18
Table II. Pulp Properties	21
Table III. Different levels of calcium ion concentration in the inlet soap suspension for cases I and II.	44
Table IV. Water absorbance test on filter paper for a control ("clean") sample and a sample with deposited calcium soap	51

**CHAPTER 3**

Table I. The physical interpretation of model parameters.	67
Table II. Experimental conditions for retention study.	71
Table III. Rate of soap retention at different flowrates.	105



## **CHAPTER 1**

### **INTRODUCTION**



## 1.1 JUSTIFICATION

Recycled paper often has different properties than paper made of virgin fibers. The paper printing potential can be affected by a decrease in strength, coefficient of friction and water absorbency. Another problem associated with paper recycling is the carryover of process chemicals from one unit to another which contaminates the system and causes runnability problems. These detrimental effects could be caused by: surface morphology changes due to mechanical action or by changes of the surface energy brought by variations in chemical composition. Morphological changes upon recycling and their effect on paper properties have already been reviewed by Howard [1]. Although significant, fibre morphology changes can not account for all observations, especially those concerning the water absorbency and the coefficient of friction. Chemical modification must therefore play a significant role. A hypothetical mechanism we propose to investigate this loss of papermaking and printing potential is the retention of molecules of low surface energy on the wood fibers. Such molecules would drastically change the surface properties of paper, especially the coefficient of friction and the increase in hydrophobicity.

The recycling process consists of two steps: repulping and flotation. During repulping, ink particles are detached from the fibers by a combination of mechanical and chemical action. This process unit is analogous to the soil laundering process. Once ink particles are detached from the fibers, they are separated by flotation with the use of fatty acid collectors. The ink aggregates are removed with the froth whereas the clean fibers are directed to the papermachine. Surface active agents are used in large quantities throughout the process. The most widely used deinking chemicals are fatty acid soaps because they are cheap and because they have been used for many decades for mineral flotation applications. In addition, fatty

and resin acids are part of ink formulations and may even originate from the natural wood extractives. The complexity of the deinking chemical system represents a drawback for this study in terms of analytical techniques and competing processes.

The aim of this thesis is not to simulate the actual deinking system but to obtain fundamental information on the mechanism that can contribute to the understanding of the real process. Our experimental strategy consists of working within a well defined model system. Thus, we will focus on the interactions between a model chemical and the wood fibers, in the absence of ink particles. It is also desired to study the main variables (kinetics aspects) affecting the surfactant adsorption/desorption phenomena. These findings can form a basis for future research work such that a mathematical model will be developed for simulation purposes.

The overall objectives of this thesis are:

1. To develop an analytical technique that can be used to quantify contaminant retention in general, fatty acid soaps in specific.
2. To test if our hypothesis of surfactant retention on wood fibers is correct.
3. To propose a retention mechanism.

In this study, pulp retention of fatty acid soaps is considered as a combination of adsorption and mechanical entrapment. Mechanical entrapment is primarily a function of the size of the eluting molecule, relative to the dimension of the void spaces in the pulp network. Adsorption results from the balance between the attractive van der Waals forces, the electrostatic forces and the hydrodynamic forces. This phenomena can best be quantified by using a packed bed made of wood fibres and following the exit stream dynamics

(breakthrough curve) of a soap concentration pulse generated at the entrance. The soap concentration at the effluent stream can be monitored on-line by light scattering of the soap particles.

Retention studies on the packed bed can be complemented with other methods such as: scanning electron micrographs, atomic absorption analysis of residual inorganic material, gas chromatographic analysis of fatty acids, streaming potential measurements ( to measure the charge on the fibers), zeta potential (charge of the soap particles), dynamic light scattering (effective diameter of soap particles), photodispersion analysis (stability of soap suspension) and dynamic contact angle (Surface energy of paper samples). Finally, our results can be compared in terms of existing mathematical models of particle deposition in packed beds in order to define the parameters that should be included in a mathematical model to simulate the complete retention mechanism for soaps.

The remainder of this chapter consists of: an overview of the industrial problem, a proposed hypothesis, relevant colloidal chemistry and engineering principles, general objectives and organization of this thesis.

## **1.2 THE PAPER RECYCLING PROCESS**

### **1.2.1 Ink removal and separation**

Defibering and removal of ink from waste paper is accomplished primarily in the repulper, similar to a laundry washer. Mechanical action is sufficient to remove and disperse most inks, but the level of energy that is required can not be achieved without the help of chemicals, analogous to laundry detergents. Repulping may be a batch or a continuous process. The batch process is preferred because it allows for better operational control [2].

Once the ink is removed from the fibers, cleaning and screening units remove large ink agglomerates and coarse contaminants such as staples. The ink contaminants are then separated from the stock by either washing or froth flotation. Washing consists of a series of dilution and thickening units. The specific design of a washer is decided upon according to the type of ink to be removed. For efficient washing of the pulp, it is required that the ink particles be finely dispersed so that they can pass through the fibre network and washing screens. Froth flotation is a process that has been used by the mining industry for many decades in the mineral concentration field. The mineral-containing froth that is recuperated corresponds to the agglomerated ink that is disposed of during recycling. The flotation cell is a tank where air bubbles are forced through the pulp slurry. A fatty acid collector fed with the slurry will cause the ink particles to agglomerate and adhere to the air bubbles by hydrophobic interactions. As the bubbles rise to the surface, they collect and remove the agglomerated ink particles.

### **1.2.2 Deinking chemistry**

Paper recycling involves the use of several types of deinking chemicals. Table I outlines the basic deinking chemicals and their role in the process [3, 4]. Surfactants are used in order to detach ink particles from fibres, to disperse ink suspensions (washing), to agglomerate ink particles and to attach them to air bubbles (flotation). Detergency is the removal of soils and inks from fiber surfaces (eg. Laundering). It is believed that the main detergency mechanism is the solubilization of oily stains into the interior of surfactant micelles [5,6]. Although many studies have been done on detergency [7-10], the exact mechanism of ink removal and detachment during recycling is not known.



**TABLE I**  
**DEINKING CHEMICALS [3,4]**

NAME	FUNCTION	FORMULA
Sodium Hydroxyde	swells fibers, activates $H_2O_2$	NaOH
Sodium silicate	prevents ink redeposition, stabilizes $H_2O_2$	$NaSiO_x$
Sodium carbonate	water softening, buffering, alkalinity	$NaCO_3$
Complexing agent	chelates metallic ions, stabilizes $H_2O_2$	e.g. DTPA
Non-ionic surfactant	wetting, emulsification, ink removal	e.g. Alkyl phenol ethoxylates
Collector	attaches to air bubble for froth flotation	e.g. calcium oleate
Hydrogen peroxide	bleaching agent, prevents alkaline yellowing	$H_2O_2$

Although it would be ideal that all the extraneous substances (chemical input) be used efficiently and leave the system with the ink, several studies have shown that it is impossible to remove all contaminants from the pulp fibers and it could even build up as the proportion of recycled fibre increases. The pulp fibers may adsorb dissolved substances from the process water either by ionic or van der Waals interactions.

### **1.2.3. Problems associated with the use of waste paper**

The strength, the coefficient of friction and water absorbency decrease by incorporating recycled fibers into paper. This results in problems achieving quality printing. There is also a maximum number of times that a fiber can be recycled while preserving its paper making integrity. The tensile strength of paper is a measure of how strong the fibre-fibre bond is.

Aside from detrimental properties, paper recycling presents runnability problems. Chemical carryover is the entrainment of process chemicals by the pulp slurry. These chemicals are transported from one process unit to the next one, contaminating the process and causing the deposition of resinous “sticky” (pitch deposition) material on equipment such as paper rolls [11]. These deposits may accumulate and eventually stick on the paper resulting in dirt specks. Numerous studies on pitch deposition suggest that the severity of the problem increases with the recycle content [12]. Studies have also been done on the composition of the deposits [13-15] and concluded that about 25% was resin and fatty acid material.

Machine breaks are also a problem in recycling mills. If the paper repels water in localized places, these may constitute “weak spots” where the paper fails to stand the tension

of the paper machine.

### **1.3 HYPOTHESIS**

A hypothetical mechanism for the loss of papermaking and printing potential is the retention of molecules of low surface energy on the fibers during recycling. Such molecules would size the paper and could be responsible for chemical carryover in other unit operations when subjected to a shock in pH, temperature or ionic strength. Oils, waxes, but especially fatty acid soaps, are present in significant concentration during recycling and could fulfill the sizing criteria.

Soaps could conceivably alter the fibre-fibre hydrogen bonding and cause changes in conformability thus reducing the paper strength. These surfactants could also act as a 'lubricant' on the surface of the fiber in such a way as to lower the coefficient of friction. The coefficient of friction is known to be partially dependent on the surface energy and partially, on morphology [16]. If fatty acid soaps are adsorbed onto paper, they would likely reduce the surface energy of fibers. This would result in an increase of hydrophobicity.

Thus, the loss of papermaking and printing potential of recycled fibers can be due to the retention of soap on the wood fibers.

### **1.4 LITERATURE REVIEW**

#### **1.4.1 Retention principles**

Pulp retention of fatty acid soaps is considered as a combination of adsorption and mechanical entrapment. Mechanical entrapment is primarily a function of the size of the eluting molecule, relative to the dimension of the interstitial spaces (porosity) in the pulp

slurry. While the soap particle diameter should vary by less than an order of magnitude, the pore size is a strong function of the consistency and the properties of the fibers. Adsorption results from the balance between the attractive van der Waals forces, the electrostatic forces and the hydrodynamic forces between particles and fibers.

The *van der Waals* forces are weak attractive forces, effective only at small particle-fibre distances. Thus, particles and fibers must be first brought to close approach by hydrodynamic forces which promote particle-fibre collisions. Whether the collisions result in physical adsorption or not depends on the electrostatic forces. The *electrostatic forces* could be either attractive or repulsive depending on the surface charges of particles and fibers. Fatty acid soaps are negatively charged particles. The surface charge on the fiber depends on the surface chemical composition, on the pH, and the amount of adsorbed substances. The ionization of the surface carboxyl and sulphonate groups in de-ionized water renders the fiber surface negative [17]. This ionization behavior is strongly dependent on the pH of the suspension water. Since most of the dissolved material in a recycling furnish is anionic (commonly called “anionic trash”), the retention of these substances makes the fiber charge even more negative. Furthermore, it is the nature of the fiber charge that determines its capacity to *ion-exchange*. The ion-exchange kinetics, affinity of different ions to pulp fibres, and the effects on the process and paper properties have been studied extensively [17-20].

As the amount of surfactant material accumulates on the surface, the fiber will become *hydrophobic* by a similar process as sizing. Once the fibers are covered by a monolayer of hydrophobic molecules or particles, the surface will tend to attract more hydrophobic material. Rogan’s work on the sequential adsorption of triolein on negative mineral surfaces

is a good example of this phenomenon [21]. It was found that a first layer of the triglyceride enhances the adsorption rates of consecutive layers by a “cooperative adsorption” mechanism.

Adsorption may be reversible in nature. The balance between colloidal forces and hydrodynamic forces determine the desorption kinetics.

#### **1.4.2 Retention studies**

Lindstrom et al studied the adsorption of fatty acid soaps on pulp fibers [22]. It was suggested that an increase in consistency during “cake formation” resulted in higher amounts of soap adsorption compared to the amounts found on dilute pulp suspensions. Ben *et al* investigated ink washing in a packed bed [23]. They found that ink retention in a pulp mat was highly dependent on electrolyte concentration. They explained that this was due to the coagulation of ink aggregates on the fiber surface irregularities.

Al-Jabary et al studied the deposition kinetics of clay particles in packed beds of pulp fibers both experimentally [24] and theoretically [25]. They developed a mathematical model based on the plug flow transport equation and a modified Langmuir adsorption kinetics. The simulation results obtained agreed well with their clay deposition data.

### **1.6 GENERAL OBJECTIVES**

The overall objectives of this thesis are:

1. To develop an analytical technique that can be used to quantify contaminant retention in general, fatty acid soaps in specific. It is preferable to be able to measure fatty acid concentration in a continuous fashion to reduce the time taken to analyze samples. This

technique, once built and debugged will be useful in future research studies on contaminant retention on pulp fibers.

2. To test if our hypothesis of surfactant retention on wood fibers is correct. Once this objective is fulfilled, we will know whether fatty acids can be retained by the pulp fibers, to what extent, and under which conditions.
3. To propose a retention mechanism. The mechanism will encompass the combined effect of selected variables, and will constitute the basis for a mathematical simulation of the contaminant retention phenomena during paper recycling.

## 1.7 ORGANIZATION OF THE THESIS

Chapters two and three are written in the format of separate manuscripts that will be submitted for publication following the submission of the thesis. Chapter two contains the description of the analytical technique developed for this study (objective one) and preliminary experimental results. Chapter three contains the detailed study of fatty acid soap retention in fibre networks and a complete mechanism is proposed (objectives two and three). There is a logical continuation between these chapters and the necessary links are drawn within the introductory sections. The thesis supervisor, Gil Garnier, will be the co-author of both papers.

## REFERENCES

1. HOWARD, R.C. and BICHARD, W., "The basic effects of recycling on pulp properties", *Paprican*. PPR # 864: 5-23 (1991).
2. WOODWARD, T.W., "Deinking chemistry", *TAPPI Wet-end Operations short course*: 473 (1992).
3. MAK, N., "Characteristics of fatty acids as an effective flotation deinking collector", *CPPA 2<sup>nd</sup> Research Forum on Recycling*: 145-146 (1993).
4. MORELAND, R., "Changes in deinking chemistry", *PIMA* : 50-52 (1992).
5. PUTZ, H.J., SCHAFFRATH, H.J. and GÖTTSCHEING, L., "De-inking of oil- and water-borne printing inks: a new flotation de-inking model", *Pulp Pap. Canada* 94 (7): 16-21 (1993).
6. BORCHARDT, J.K., "Possible deinking mechanisms and potential analogies to laundering", *Prog. Pap. Recycling*: 47-53 (1993).
7. EVANS, P.G. and EVANS, W.P., "Mechanism for the Anti-redeposition action of Sodium Carboxymethylcellulose with Cotton. I. Radiotracer studies", *J. Appl. Chem.* 17:276-282 (1967).
8. JOHNSON, G.A. and LEWIS, K.E., "Mechanism for the Anti-redeposition action of Sodium Carboxymethylcellulose with Cotton. II. Colloid-stability Theory applied to the Fibre-soil system", *J. Appl. Chem.* 17:283-287 (1967).
9. JOHNSON, G.A. and BRETLAND, A.C., "Mechanism for the Anti-redeposition action of Sodium Carboxymethylcellulose with Cotton. III. Electrophoresis and Sedimentation studies" *J. Appl. Chem.* 17:288-292 (1967).
10. JOHANSON, B., WICKMAN, M. and STRÖM, G., "Surface chemistry of Flotation deinking: Agglomeration Kinetics and Agglomerate Structure", *Nordic pulp Pap. Res. J.* 2:74-85 (1996).
11. DOUEK, M. and ALLEN, L.H., "Calcium soap deposition in kraft mills", *Paprican Reports*, PPR # 255: 1-13 (1979).
12. OLSON, C. and LETSCHER, M.K., "Increasing the use of secondary fibre: an overview of deinking chemistry and stickies control", *Appita* 45(2): 125-130 (1992).

13. SITHOLÉ, B., TRAN, T.N. and ALLEN, L.H., "Quantitative determination of Aluminum Soaps in pitch deposits", *Nordic pulp Pap. Res. J.* 1:64-69(1996).
14. DOUEK, M. and ALLEN, L.H., "Calcium soap deposition in kraft mills", *Paprican* PPR # 255 (1979).
15. DORRIS, G.M., DOUEK, M. and ALLEN, L.H., "Analysis of metal soaps in kraft mill brownstock pitch deposits", *Paprican* Report # 375 (1982).
16. INOUE, M., GURNAGUL, N. and AROCA, P., "Static friction properties of linerboard", *Tappi* 73(4):81-85 (1990).
17. SCOTT, W.E., in *Pulp and Paper Manufacture*, "VII. Papermaking Chemistry":140-191 (1990).
18. CROW, R.D. and STRATTON, R.A., "The chemistry of Aluminum salts in Papermaking I: Aluminum adsorption", *TAPPI Papermakers Conf. (Denver) Proc.*, 183-187 (1985).
19. TOWERS, M. and SCALLAN, A.M., "Predicting the Ion-Exchange of Kraft Pulps Using Donnan Theory", *Paprican Report*, PPR # 1170 (1995).
20. LINDSTRÖM, T., SÖREMARK, C., HEINEGÅRD, C. and MARTIN-LÖF, S., "The importance of Electrokinetic properties of Wood Fiber for Papermaking", *TAPPI* 57 (12):94-96 (1974).
21. ROGAN, K.R., "Adsorption of oleic acid and triolein onto various minerals and surface treated minerals" *Colloid. Polym. Sci.* 272: 82-98 (1994).
22. LARSSON, A., STENIUS, P. and ODBERG, L., "Surface chemistry in flotation deinking. Part 3. Deposition of ink and calcium soap particles on fibers", *Svensk Papperstidning* 3: R2-R7 (1985).
23. BEN, Y., PELTON, R. and DORRIS, G.M., "Displacement washing deinking of water-based inks", *Paprican* PGRLR (1995).
24. AL-JABARI, M., VAN HEININGEN, A.R.P. and VAN DE VEN, T.G.M., "Modeling the flow and the Deposition of Fillers in Packed beds of Pulp Fibers", *J. Pulp Pap. Sci.* 20(9):J249-J253 (1994).
25. AL-JABARI, M., VAN HEININGEN, A.R.P. and VAN DE VEN, T.G.M., "Experimental Study of Deposition of Clay Particles in Packed Beds of Pulp Fibers", *J. Pulp Pap. Sci.* 20(1):J289-J295 (1994).



## **CHAPTER TWO**

### **RETENTION OF FATTY ACID SOAPS DURING RECYCLING:**

#### **A STUDY USING PACKED BEDS OF PULP FIBERS**

## ABSTRACT

*Paper made of recycled fibers often has different properties than that made entirely of virgin pulp. A hypothetical mechanism for the loss of papermaking and printing potential of recycled paper is the adsorption and entrapment of molecules of low surface energy (such as oil and soap) on the wood fibers during recycling. This hypothesis was tested with a packed bed of wood fibers by following the dynamics of retention of a concentration pulse generated at the entrance (breakthrough curve, BTC). This study investigated the retention of model deinking chemicals in packed beds. The variables studied include the type of fibre (Kraft, TMP), the type of adsorbate (calcium and sodium oleate), and the ionic strength. The objectives of this study were threefold: first, to develop a sensitive technique to quantify contaminant retention during recycling; second, to elucidate the mechanisms of soap retention by the fibers; and third, to assess the effects of soap retention on product quality.*

*A sensitive technique to quantify the retention of contaminants on the pulp is to measure the area under a breakthrough curve (BTC) of a packed bed of fibers. We showed that sodium salts of fatty acids undergo ion-exchange with the calcium present in the pulp. The availability of calcium within the pulp for ion-exchange is diffusion-controlled. When tap water was used during washing stages, calcium ions from the tap water were retained by the pulp, replacing some of the sodium ions.*

*Soaps prepared by mixing equimolar amounts of sodium oleate and calcium chloride (1 Meq) did not adsorb on pulp fibers. This behavior goes according to theory as the negatively charged soap particles are repelled from the negatively charged fibers. However, complete retention of the particles occurred at high calcium concentration (10 Meq). We*

*propose a mechanism by which calcium soap particles deposit on the fibers at salt concentrations above a critical coagulation concentration (CCC). Dynamic contact angle and surface tension experiments confirm the important role of soap retention in sizing and carryover phenomena.*

## 2.1 INTRODUCTION

Paper made of recycled fibers often has different properties than that made entirely of virgin pulp [1]. The strength, the coefficient of friction and the water absorbency can all decrease by incorporating recycled fibers into paper. This results in problems achieving quality printing. It also raises concerns as to the maximum number of times a fiber can be recycled while preserving its paper making integrity. Such modifications are due to alterations of the physical and chemical characteristics at the fiber level, more specifically, at its surface. The physical changes of a fiber submitted to recycling consist of the collapse of lumen and defibrillation. This leads to an increase of density and perhaps modifications of the mechanical and frictional properties.

A change of the fiber's surface chemistry can be rationalized in two ways: first, by the selective removal of a wood component and, second, by the adsorption of a process chemical. A simplistic view of deinking consists of repulping, for detaching ink particles from the fibers, and flotation/washing, for their removal. The first step is best carried out by strong mechanical forces applied to paper under alkaline conditions. Any selective extraction would preferentially occur at this stage. Wood extractives (such as fatty acids, resin acids and pectin), hemicellulose, and even some lignin could be partially solubilized [2]. However, the surface energy of wood and its constituent polymers, measured by contact angle or inverse gas chromatography [3-7], were found to be relatively similar (Table I). It is unlikely that a moderate extraction of any of these wood polymers would modify the surface energy to such an extent as to affect its surface properties [6]. These predictions are supported by the experimental work of Eriksson [8] and Chatterjee [9] wherein the surface energy of pulp fibers, repeatedly submitted to a sequence of recycling treatments, was measured after each

**TABLE I**  
**SURFACE ENERGY OF WOOD AND ITS COMPONENTS**

COMPONENT	CRITICAL SURFACE TENSION $\gamma$ (mJ/m <sup>2</sup> )	REFERENCE	COMMENTS
Cellulose			
avicell	36	4,5	function of humidity and physical state
regenerated	36 - 49	3,6	
Hemicellulose			
arabinogalactan	33	4	
galactoglucomannanyl	36.5	4	
softwood (white pine)	35	4	
hardwood (white birch)	36	4	
Lignin	36	5	
Wood Pulp (CTMP)	37	7	

cycle. No correlation was demonstrated within the experimental error. Thus, any selective extraction of a wood component can be discarded as phenomenon governing the surface energy of recycled fibers.

A hypothetical mechanism for the loss of papermaking and printing potential is the retention of molecules of low surface energy on the fibers during recycling. Such molecules would size the paper and could be responsible for chemical carryover in other unit operations when subjected to a shock in pH, temperature or ionic strength [10, 11]. Oils, waxes, but especially surfactants and soaps, are present in significant concentration during recycling and could fulfill the sizing criteria.

Metallic soaps of fatty acids are the most widely used for recycling by flotation in the Canadian paper industry [12]. The reasons being their effectiveness and stability, their low cost and decennary use in the mining industry. The mechanisms of soil removal and detergency on cotton and synthetic textiles are relatively well documented [13-19]. However, despite the apparent simplicity of the process and its popularity, relatively little is known about the physical chemistry of fatty acid soaps in a recycling mill, and less about their retention on pulps [20, 21].

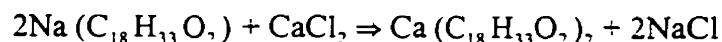
The objectives of this article are threefold: to develop a sensitive technique to measure the retention of contaminants, to characterize the retention of fatty acid soaps on pulps, and to assess the effects of soap retention during recycling. In this study, pulp retention of fatty acid soaps is considered as a combination of adsorption and mechanical entrapment. Mechanical entrapment is primarily a function of the size of the eluting molecule, relative to the dimension of the average pulp pore. While the soap particle diameter should vary by less than an order of magnitude, the pore size is a strong function of the consistency and the

properties of the fibers. Adsorption results from the balance between the attractive van der Waals forces, the electrostatic forces and the hydrodynamic forces. Retention can best be quantified by using a packed bed made of wood fibres and following the exit stream dynamics of a soap concentration pulse generated at the entrance. Flow and deposition of colloidal particles in such packed beds of pulp fibers were rigorously derived by Al-Jabari, van Heiningen and van de Ven [22].

## 2.2 EXPERIMENTAL TECHNIQUES

### 2.2.1 Materials

A never-dried black spruce bleached kraft pulp (Domtar Q-90) and a never-dried black spruce TMP pulp (Paprican) were used. Both pulps were washed extensively with deionized water over a 200 mesh size stainless steel filter to remove the fines. The mechanical pulp was extracted with acetone in a soxhlet to obtain a fatty acid-free pulp. The fatty acid and ash content of the pulps are shown in Table II. A commercial grade of sodium oleate (Sigma Co.) was used, as received, to prepare solutions of 0.1, 0.3 and 1.0 g/L in deionized water (solution pH=9). The calcium oleate suspension was prepared by mixing a stoichiometric amount of sodium oleate and calcium chloride as follows:



### 2.2.2 Packed Bed

The fixed bed reactor consists of a 7.5cm i.d. × 21cm height plexiglass vessel closed by a 200 mesh size screen at the bottom to prevent pulp fibers from exiting. The liquid

**TABLE II**  
**PULP PROPERTIES**

Type of Pulp	Total Fatty acids before extraction (mg/kg)	Total Fatty acids after extraction (mg/kg)	Ash content		
			Ca	Na (mg/kg)	Mg
Mechanical	28	8	1350	34	n/a
Kraft	n/a	n/a	535	22.3	79.9



distribution piston at the top is connected to a Masterflex peristaltic pump (Figure 1). An average flowrate of 140 mL/min, developing a superficial velocity of 35 mm/min (residence time of 1.3 minutes) was selected for all experiments. Appendices A and B contain details on the packed bed design.

### 2.2.3 Pulp Pad Preparation

Prior to an experiment, the pulp suspension (17.6 g. o.d., 1 % consistency, pH≈6) was degassed under a vacuum pump for 15 minutes and then slowly poured into the reactor through a funnel extension. Water was allowed to drain until the suspension level reached the bed height required (4 cm) to give a 10% consistency packing. The funnel was then replaced by the upper piston providing an air-tight fixed bed. The fiber bed was never allowed to run dry. All experiments were carried out at room temperature and at the equilibrium pH of the soap solution (pH 10 for calcium oleate and pH 9 for sodium oleate). To characterize the fiber distribution in each bed formed, a 15 g/L sucrose solution was used as an inert tracer so as to obtain a Residence Time Distribution (RTD) curve.

### 2.2.4 Absorbance and particle light scattering

A Varian CARY 1 UV/VIS Spectrophotometer equipped with a flow-through quartz cell (10 mm optical length, volume = 0.6 ml) was used to measure the absorbance of the eluent at the bed exit (Figure 1). The angle between the detector and the beam of light is 180°. The wavelength was kept at 195 nm to measure the sucrose tracer concentration while the calcium and sodium soap measurements were carried out at 336 nm.

The reduction of intensity that occurs when light of intensity  $I_0$  passes through a

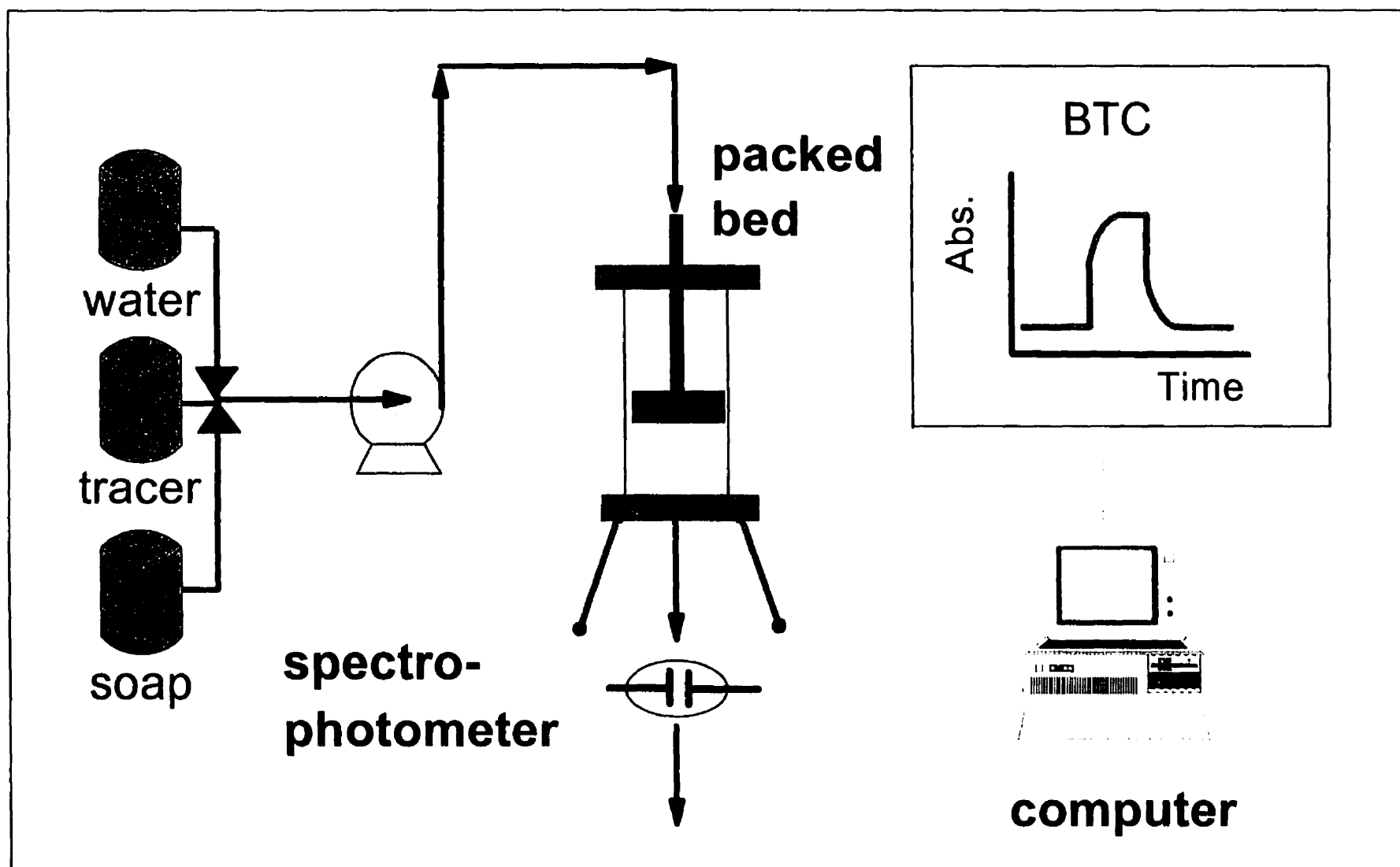


Fig. 1 Experimental Setup

solution of thickness,  $\Delta x$ , which contains an absorbing species at a concentration,  $C$ , is described by the Beer-Lambert law [23]:

$$\frac{I_t}{I_o} = \exp (- C \varepsilon \Delta x ) \quad [1]$$

where  $I_t$  is the intensity of the light transmitted and  $\varepsilon$  is the molar absorption coefficient defined as:

$$\varepsilon = \pi r^2 Q_{\text{abs}} \quad [2]$$

$$Q_{\text{abs}} = f ( \lambda, r, n, \theta ) \quad [3]$$

where  $r$  is the hydrodynamic radius of the absorbing molecule, and  $Q_{\text{abs}}$  is the absorbance efficiency factor. The magnitude of the efficiency factor is a function of the wavelength of the light ( $\lambda$ ), the molecule size ( $r$ ), the refractive index ( $n$ ), and the angle of observation ( $\theta$ ).

When light passes through a colloid suspension, a reduction in light intensity also results from particle scattering. For a non-absorbing suspension, the intensity decrease is related to the suspension turbidity ( $\tau$ ) as follows:

$$\frac{I_t}{I_o} = \exp (- C \tau \Delta x ) \quad [4]$$

where the turbidity is a function of the particle radius ( $R$ ) according to:

$$\tau = \pi R^2 Q_{\text{sca}} \quad [5]$$

where  $Q_{sca}$  is the scattering efficiency factor. As for the absorbance factor,  $Q_{sca}$  also depends on the wavelength ( $\lambda$ ), the particle size ( $R$ ), the refractive index ( $n$ ), and the angle of observation ( $\theta$ ). For a specific chemical species and a given instrument, the index of refraction and the angle of observation are usually fixed. Thus, the scattering efficiency is often reported as a function of a size parameter ( $\alpha$ ):

$$Q_{sca} = f(\lambda, R, n, \theta) \quad [6]$$

$$\alpha = 2 \pi \frac{R}{\lambda} \quad [7]$$

For a system which presents both absorption and scattering effects, the Beer-Lambert equation becomes:

$$\frac{I_t}{I_o} = \exp [- C ( \varepsilon + \tau ) \Delta x ] \quad [8]$$

Where we define the total reduction of light intensity as a *modified absorbance* ( $A$ ). Thus:

$$A = \ln \frac{I_o}{I_t} = C ( \varepsilon + \tau ) \Delta x \quad [9]$$

A calibration curve shows the direct relationship between the absorbance,  $A$ , and concentration,  $C$ , for a suspension of calcium oleate particles (for which  $\varepsilon \ll \tau$ ) (Figure 2). The Beer-Lambert law was also found valid for micellar solutions of sodium oleate (CMC= 0.48 mmol/l) where the decrease of light intensity is due to a combined mechanism of

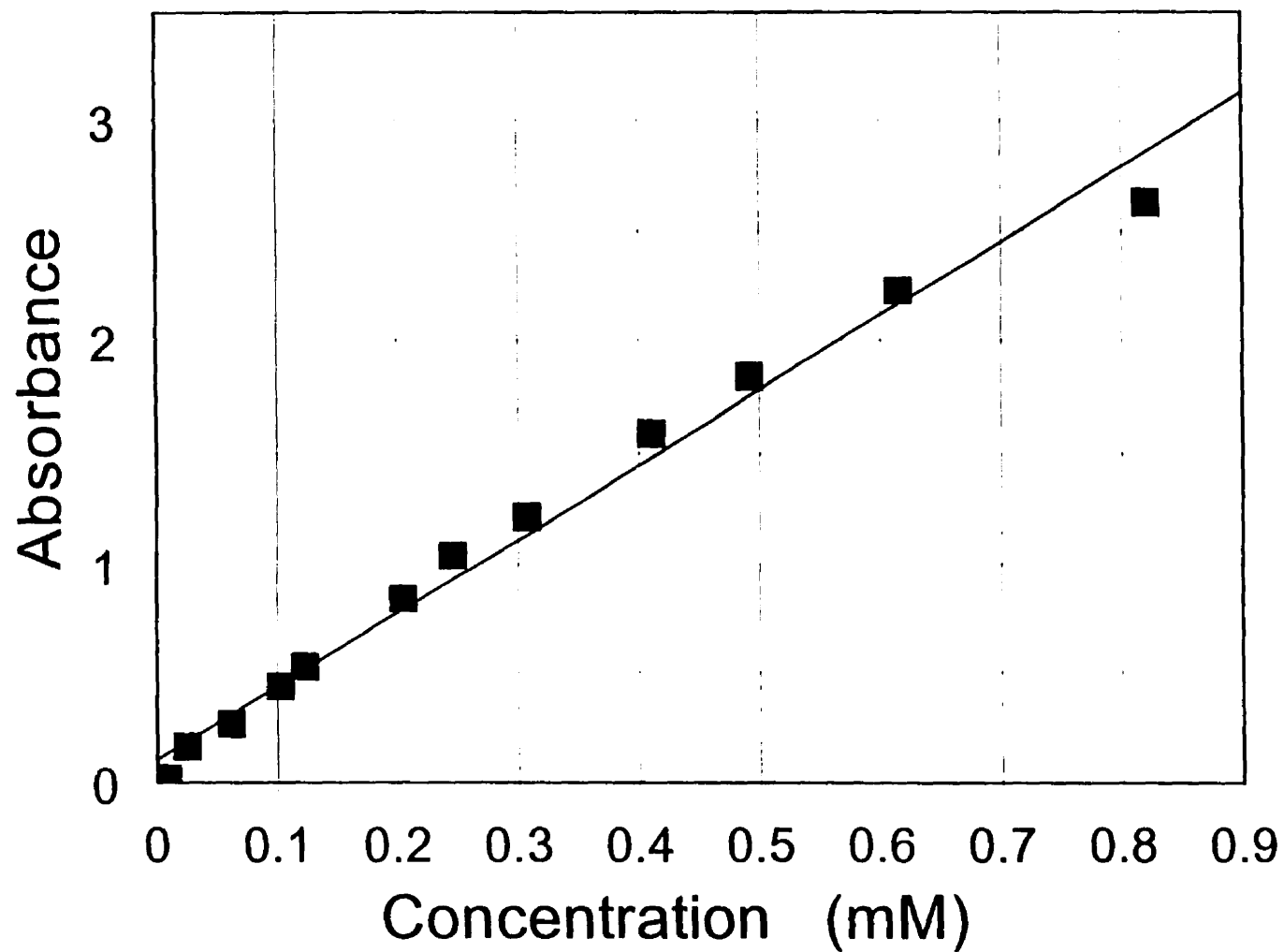


Fig 2. Calibration curve of the absorbance at 336 nm versus concentration (mM) of calcium oleate suspensions at room temperature.

absorption and light scattering ( $\varepsilon \approx \tau$ ).

### 2.2.5 Breakthrough curves and retention

The breakthrough curves (BTC's) were obtained by normalizing the soap outlet stream concentration with respect to the inlet concentration and plotted against time. The dimensionless concentration therefore ranges from 0, when there is no fatty acid soap in the exit stream, to 1 when the outlet concentration finally reaches that of the inlet. The interaction of the soap with fibers can be quantified in two ways: first, by performing a mass balance and, second, from the slope and inflection point of the pulse front of the BTC. The soap mass balance is calculated from:

$$N_p = Q \times C_o \times \Delta t - Q \times C_o \int \frac{C}{C_o} dt = Q \times C_o (\Delta t - \int \frac{C}{C_o} dt) \quad [10]$$

*accumulation   inlet pulse   outlet BTC*

where  $N_p$  is the number of moles of soap retained within the pulp,  $C_o$  is the soap concentration in the feed stream (mol/L),  $Q$  is the volumetric flowrate (L/min),  $C$  is the soap concentration of the exiting stream (mol/L), and  $\Delta t$  is the pulse duration. When a component deposits on the fibers, its BTC also shifts in the time axis with respect to the Residence Time Distribution (RTD) of the tracer. Sucrose, a small non-adsorbing and easily measurable molecule, is an ideal tracer [24-26].

### 2.2.6 Sizing

In order to test the sizing effects of soap, paper samples were made in a standard handsheet machine. When a calcium oleate suspension was added to the 7 liter pulp suspension in the handsheet machine, the resulting slurry had 1, 4 and 10 Meq of calcium chloride. The handsheets were pressed following the CPPA standard procedure [27].

Another approach was to deposit soap onto a filter paper stack packed within the packed bed. A series of filter paper was cut in circular shapes to fit the cross sectional area of the packed bed. Whatman No. 4 filter paper was used as the packing material at about 12% consistency. This “fast filtration” type was chosen to avoid retention by mechanical entrapment of the soap particles.

Both the filter paper and handsheets were dried in a drum type drier at 85° C for 2 minutes with the soap deposition surface facing away from the heating surface. The level of sizing of the samples was measured using a Hercules™ Sizing Tester (HST) with a 10% formic acid ink solution and taking the 80% reflectance endpoint.

The dynamic contact angle of the filter paper samples was also measured. A Sigma 70 (KSV Instruments Ltd.) computerized contact angle meter was used to characterize the wettability of the filter paper. The rate of liquid rise was measured at room temperature by a microbalance with a resolution of 0.01  $\mu$ N. Paper strips of 5 x 2.5 cm were used. The pulling rate was 20 mm/min and the area dipped was 0.75 cm<sup>2</sup>.

The contact angle is calculated from [28]:

$$\cos \theta = \frac{F}{P \cdot \gamma} \quad [11]$$

where  $F$  is the force measured by the microbalance [mN],  $P$  is the perimeter of the sample [m], and  $\gamma$  is the surface tension at the liquid-vapour interface [mN/m].

## 2.3 RESULTS AND DISCUSSION

### 2.3.1 Mechanical Pulp

The interaction of **calcium** soap particles with fibers was investigated first. A 10-minute pulse of *calcium oleate* suspension (0.3 mM) was passed through the TMP pulp. Its outlet response superimposed on the tracer RTD shows no indication of retention either from a mass balance or a time-shift in the BTC (Figure 3). This goes according to theory. No adsorption is expected as the negatively charged soap particles [29] are repelled from the negatively charged fibers [30]. Mechanical entrapment is also very unlikely since the diameter of the soap particles (230 nm, measured by Photon Correlation Spectroscopy) is a few orders of magnitude smaller than that of the average bed pore size.

In most recycling mills, the soap is introduced in its sodium form directly into the pulper and prior to the flotation cell, to facilitate ink removal. Calcium chloride is then added for the formation of calcium soap particles, bridging ink fragments to air bubbles. It is therefore of interest to characterize as well the affinity of a **sodium** soap with the mechanical pulp fibers.

When a 10-minute pulse containing 1 g/L [3.3 mM/L] of *sodium oleate* was introduced



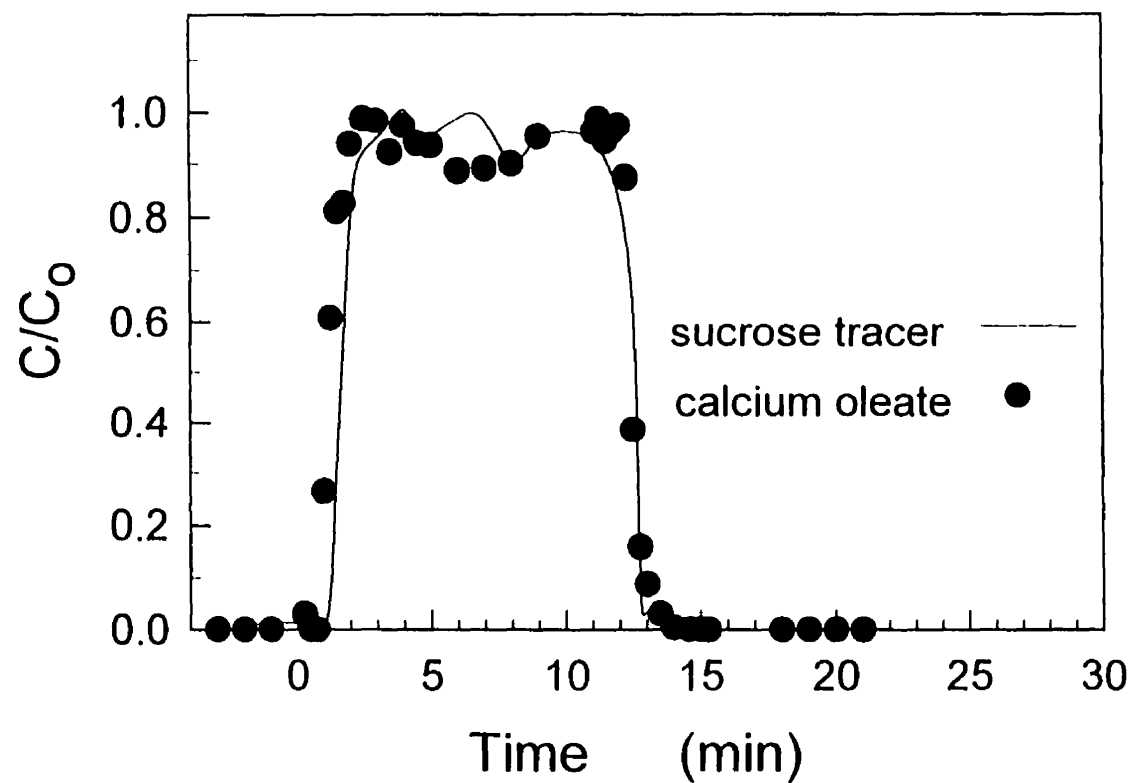


Fig. 3. Breakthrough curve for a ten-minute calcium oleate pulse( $C_0=0.5$  mmol/l or 0.3 g/l) and sucrose (15 g/l) RTD function on a TMP packed bed (the pulse starts at time 0).

to the fiber bed, the outlet stream absorbance increased to 23 times that of the inlet (Figure 4). The effluent exiting from the bed became very cloudy in appearance, unlike the clear feed solution. This turbid solution was very similar to the calcium soap suspension used in the previous experiment. A second 10-minute Na(Oleate) pulse was passed through the packed bed and another absorbance overshoot was recorded (Figure 4).

Two explanations could account for the absorbance overshoot following the two sodium oleate pulses:

1. Two or more cations from the pulp were ion-exchanging with the sodium from the soap.
2. Pulp cations diffuse from the bulk of the fibre toward its surface during the time elapsed between the two pulses .

A model and well characterized fiber, such as clean kraft pulp, is best suited to elucidate this behavior.

### 2.3.2 Kraft Pulp

As the chemical reaction between sodium oleate and wood goes to completion, there is a transformation from a micellar structure of sodium oleate to a solid particulate structure of calcium oleate, which explains the large differences in the measured absorbances between these species. The chemical species and their light scattering properties are very different. The absorbance is therefore not only a function of concentration, but also of the particle size and the efficiency factors ( $Q_{scat}$ ,  $Q_{abs}$ ). Thus, until the nature and the extent of the reaction are better known, it is preferable to describe the response of sodium oleate in terms of dimensionless absorbance ( $A/A_0$ ) instead of concentration. The ordinate of all the

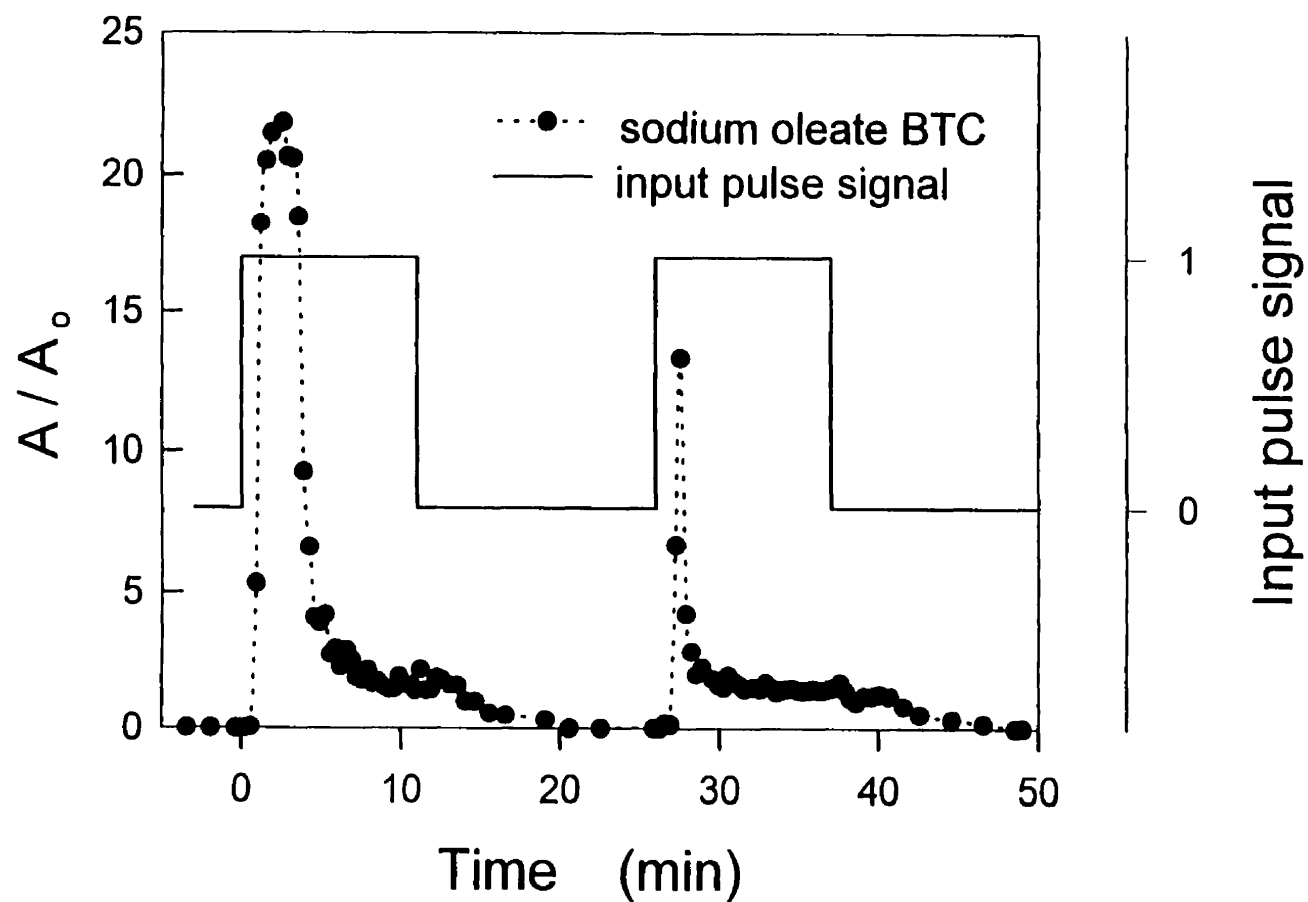


Fig. 4. Breakthrough curves of two consecutive sodium oleate (1 g/l) pulses on a TMP packed bed.

breakthrough curves (BTC's) are expressed in terms of dimensionless absorbance from now on.

The same sequence of sodium oleate cycles was repeated on kraft pulp beds and the same behavior as with TMP was observed. Again, the first overshoot reached an absorbance ratio of 23. The BTC obtained is characteristic of a very fast reaction: once the dead volume of the reactor is excluded, the absorbance overshoot corresponds exactly to the pulse of sodium oleate created at the inlet. This leaves very little time for a slow reaction and diffusion to occur.

Bivalent cations, such as Calcium (Ca), Magnesium (Mg) and Manganese (Mn) or even trivalent cations (such as Aluminum and Iron ) from the pulp could exchange with the sodium of the soap [31]. However, calcium ions are reported to outnumber by far any cation present in the pulp. A sample of the original pulp and another of the fiber bed submitted to a Na(Oleate) pulse were analyzed for their Na and Ca content. The results led to two observations (Figure 5).

First, almost the total amount of calcium initially present reacted upon contact with the sodium oleate micelles during 10 minutes of reaction (34 out of 35 mmole  $\text{Ca}^{+2}$ ). This would imply that the calcium ions from the pulp are all readily accessible to the micelles. Because of the low  $\text{Ca}^{+2}$  content, it can also be concluded that no  $\text{Ca(Oleate)}_2$  soap particles were retained within the pores of the cell wall.

The second observation concerns the molar ratio of reacted calcium to sodium. The sodium increase of 78 mmole per kg of pulp, coupled with a 34 mmole/kg calcium decrease, corresponds very closely to the 1:2 stoichiometric ratio expected when the ion-exchange from the pulp is due solely to calcium ions. This evidence confirms the ion-exchange

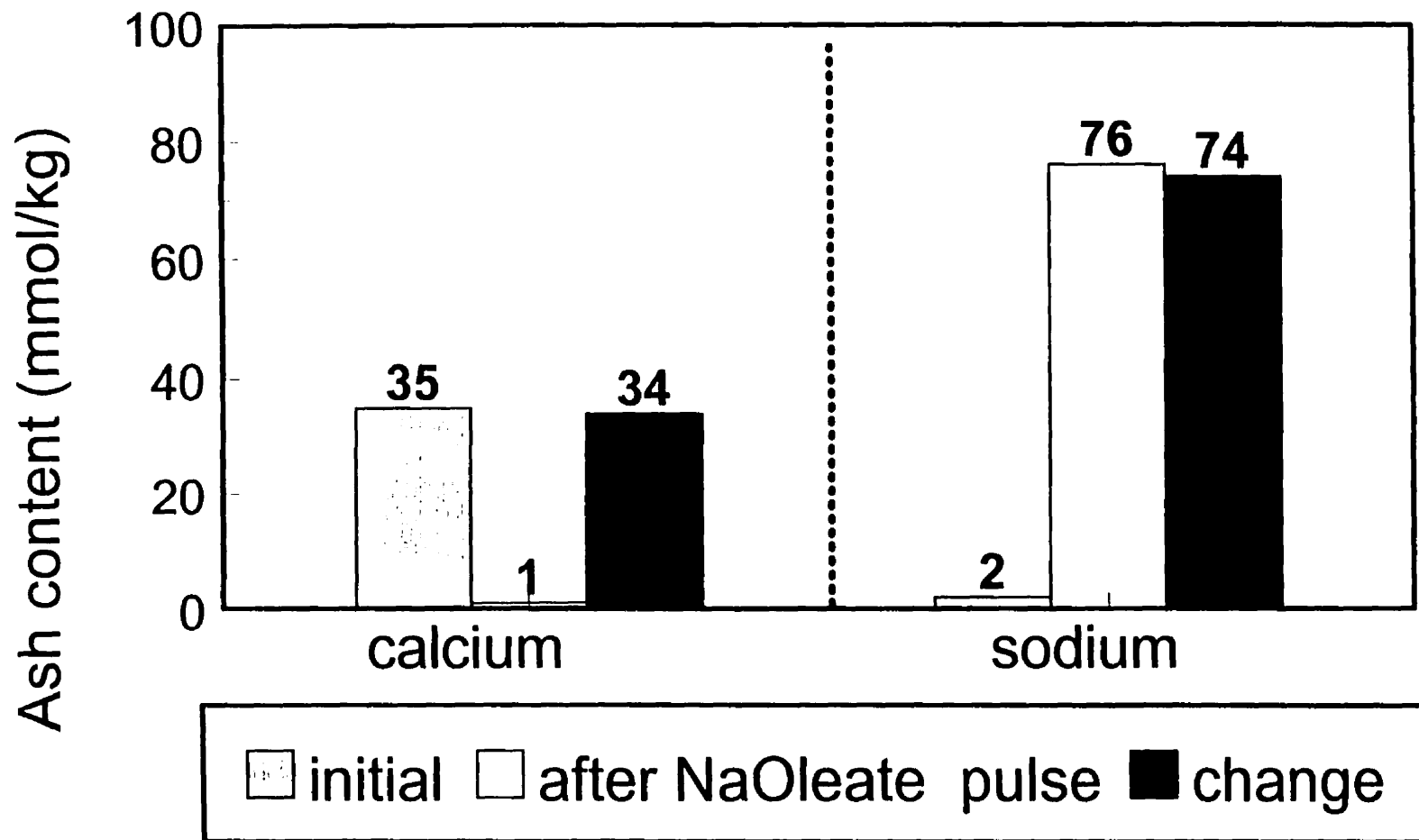


Fig. 5. Calcium and Sodium analyses of TMP samples, before and after a 10-minutes Na(Oleate) pulse.

mechanism between the sodium of the soap and the calcium of the pulp. It is arguable whether the 10 mmol/kg sodium excess from the stoichiometric ratio of the  $\text{Na}^+/\text{Ca}^{2+}$  ion-exchange mechanism is due to experimental errors, to the adsorption of some sodium oleate micelles within the cell wall, or to the exchange with the other cations present in the pulp.

A predominant sodium/calcium ion-exchange mechanism between the soap and the pulp would also predict a direct relationship between the maximum absorbance and the amount of calcium present in the pulp for a given pulse of Na-oleate. It is therefore desirable to decrease the calcium content of the pulp to confirm this mechanism. Three techniques were used. The pulp was either (i) washed with a chelating agent (EDTA), (ii) treated with HCl, or (iii) mixed with excess NaCl to yield a pulp mainly under its hydrogen (i or ii) and sodium (iii) form. Identical Na-oleate pulses were introduced at the inlet of reactors containing each of the three treated pulps. The normalized absorbance maxima ( $A/A_0$ ) were reduced from a value of 23 for the initial pulp, down to 7 for the acid and chelating agent washing, and 1.5 for sodium chloride (Figure 6). It should be noted that neither the acid nor the EDTA washing was optimized. Therefore, the efficiency of these three calcium removal processes can not be compared with each other in Figure 5. However, it clearly demonstrates that as the calcium concentration of the pulp decreases, its ability to form calcium soap decreases, confirming the proposed ion-exchange mechanism. The BTC of a sodium oleate pulse on the NaCl treated fibers also exhibits an important peak at 12 minutes, which corresponds exactly to the end of the 10-minute soap pulse. This phenomena is analyzed further.

Because the ion-exchange reaction is very fast, the rate of calcium soap formation within the packed bed depends on the rate at which calcium ions are made available to react. Therefore, it is of interest to investigate the diffusion of calcium ions to the surface of the

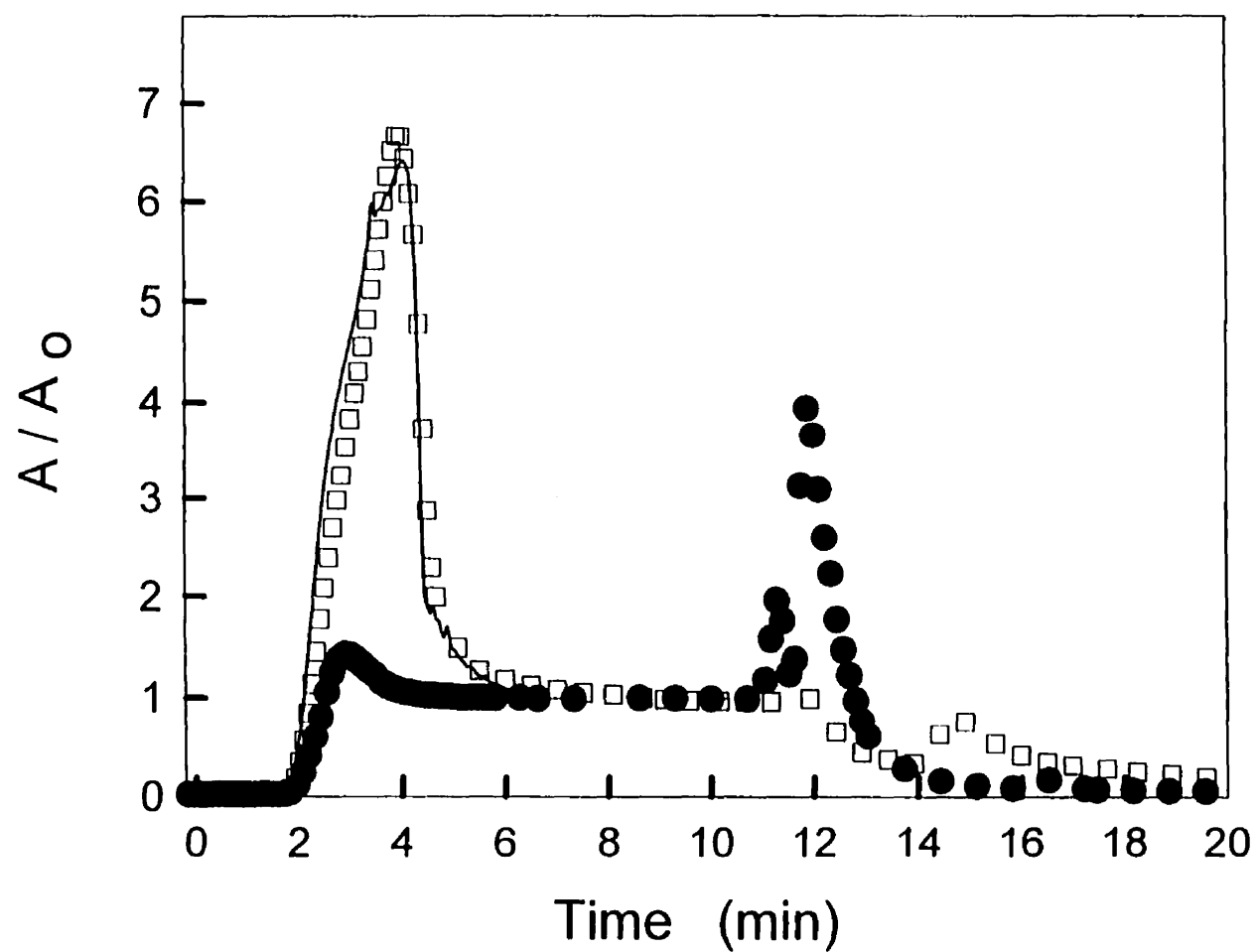


Fig. 6. Breakthrough curves of 10-minute sodium oleate pulses on kraft pulp treated with: (-) EDTA; ( $\square$ ) HCL washing; and ( $\bullet$ ) Na Cl washing [1N].

fibers. This was studied by controlling the duration of the inlet pulse and the time elapsed between two such signals. Once the readily available  $\text{Ca}^{+2}$  ions were depleted, a narrow pulse of Na-Oleate (2 minutes) was introduced after 10, 15, 20 and 25 minute-rinsing intervals. The longer the water washing intervals, the higher the absorbance peaks are (Figure 7). The last peak (D) is even higher than the first peak (A) in spite of its lower initial calcium concentration ( $\text{Ca}^{+2}$  was previously consumed by three pulses of sodium oleate). The results corroborate the mechanism by which ions diffuse from the bulk of the fiber to easily accessible areas during the rinsing periods.

The washing water could also be a calcium source. To investigate this possibility, the pulp pad previously exchanged with sodium oleate was rinsed for 7 minutes with the same deionized water used for the rinsing intervals. The next sodium oleate pulse introduced did not generate an overshoot as there was no calcium left within the pulp to ion-exchange with sodium. A second rinsing period followed, this time using tap water. It resulted in an absorbance overshoot (Figure 8). This proves that the calcium ions present in the tap water can also ion-exchange some of the sodium ions in the pulp.

The results so far indicate that: (1) readily available calcium ions from the pulp are depleted quickly, also observed when preparing the calcium oleate suspensions; (2) once the readily available calcium ions are consumed, the outlet signal slowly decreases, accompanied by the slow diffusion of particles out of the bed, until it reaches equilibrium with the inlet concentration signal ( $C/C_0=1$ ); and, (3) during the rinsing period, calcium ions diffuse to the more accessible areas so that the next pulse of Na(Oleate) will generate an absorbance overshoot due to ion-exchange.

From these observations, we propose a mechanism illustrated by Figure 9. In a simplistic



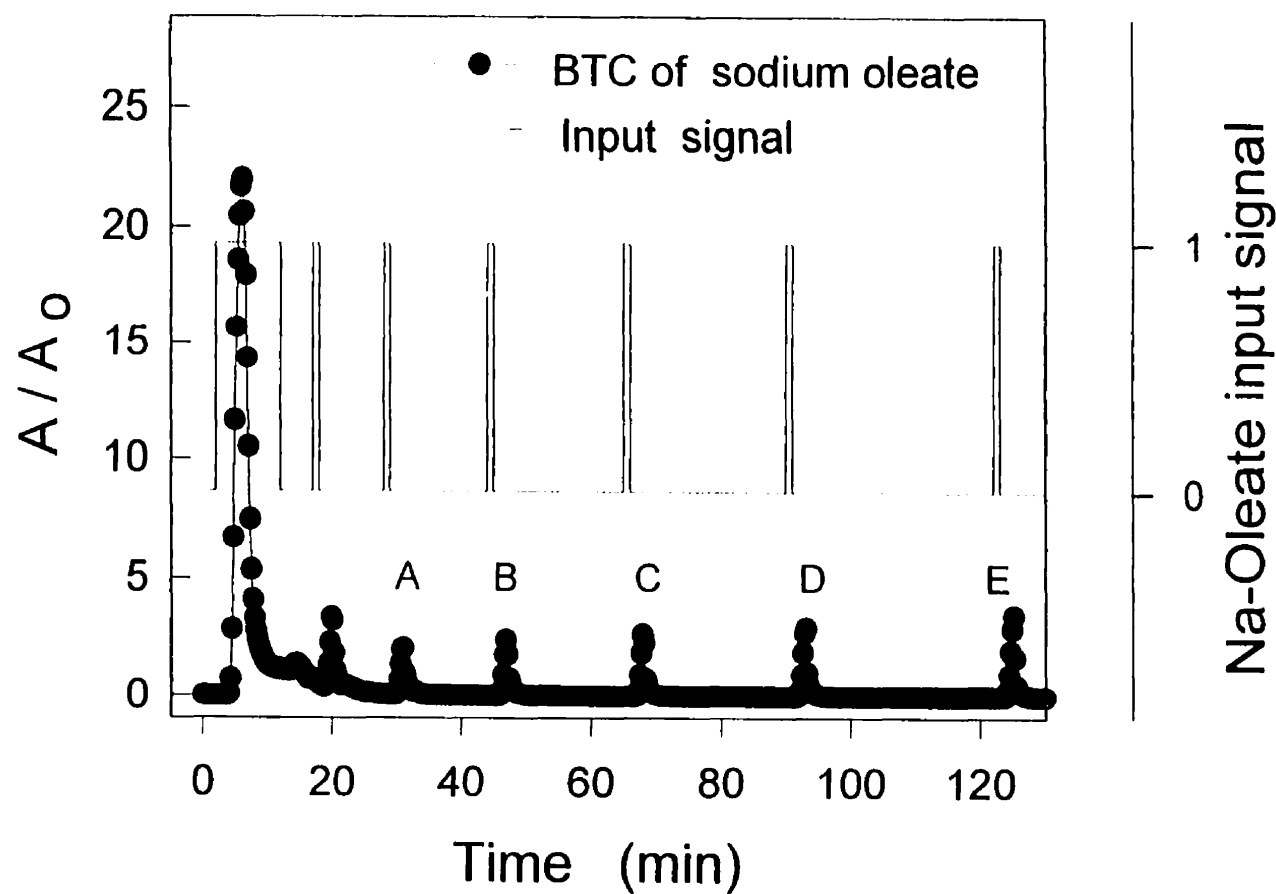


Fig. 7a. BTC's of consecutive sodium oleate pulses on kraft pulp showing the complete sequence.

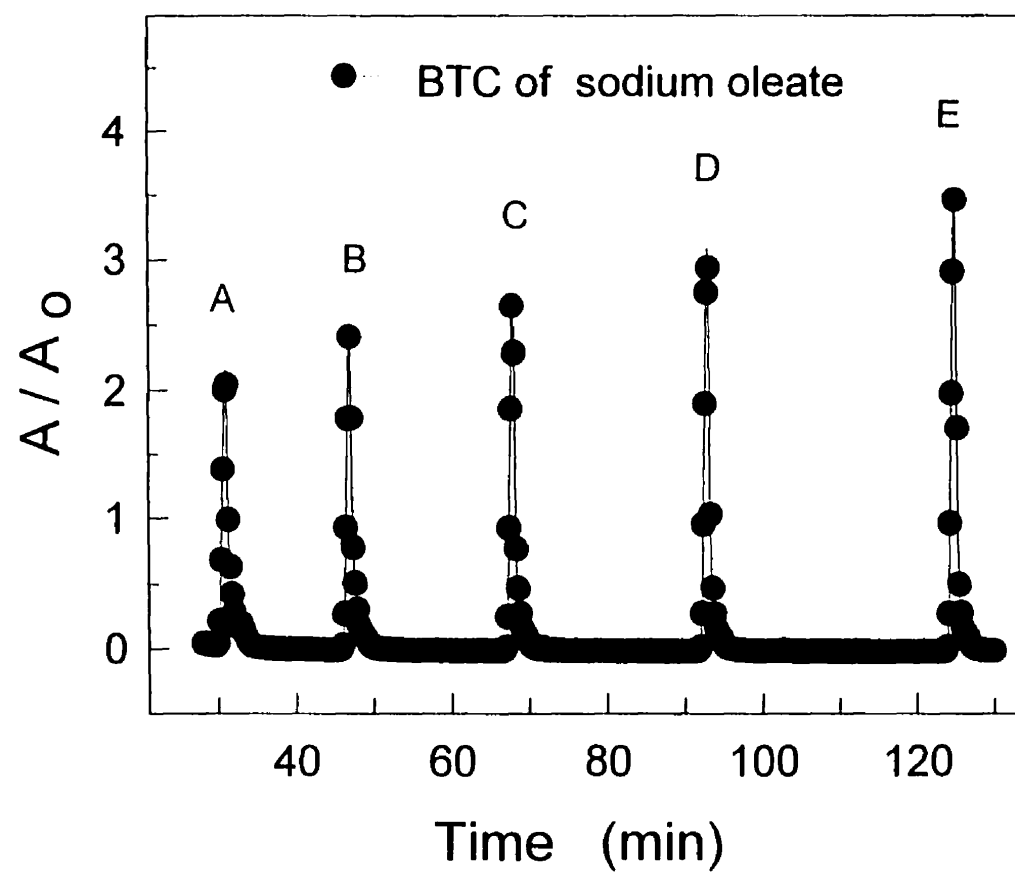


Fig. 7b. BTC's of consecutive sodium oleate pulses on kraft pulp showing a detail of the sequence.

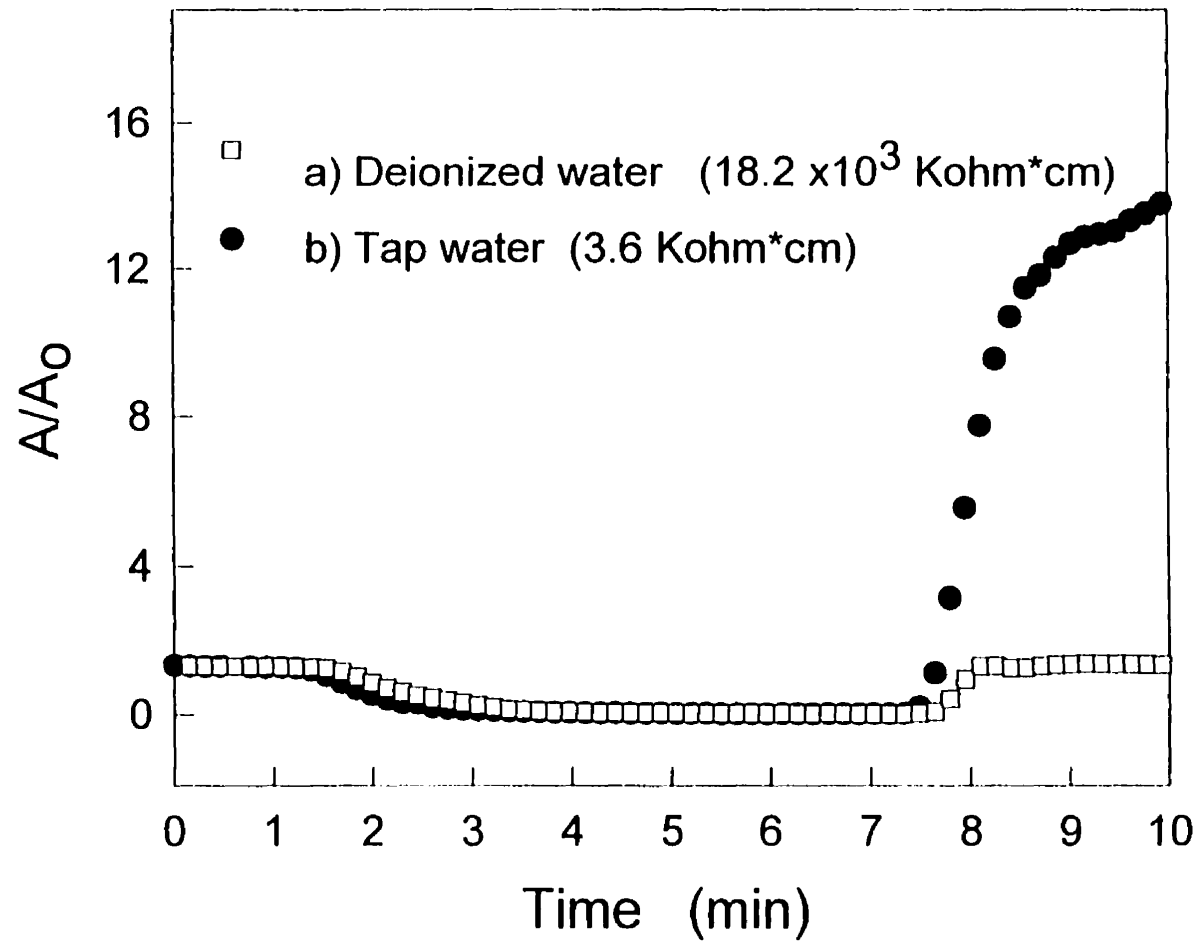


Fig. 8 BTC's of 6-minute pulses on a bed saturated with sodium oleate ( no calcium left ). The washing responses to (  $\square$  ) deionized water and (  $\bullet$  ) tap water are shown.

way, the porosity of the cell wall can be viewed as a bimodal function made of macropores of diameter up to 30 nm and micropores of the order of 0.3 nm (Pine bleached kraft pulp) [32]. The interfibril distance could hypothetically form the macropores while the fibril-fibril space could be viewed as a micropore. Although there is also the concept of a pore as a continuum medium, here a “pore” is considered as tube through which the components can diffuse. With an average hydrodynamic diameter of 230 nm, the calcium oleate soap particles cannot diffuse through the macropores. However, molecules of sodium oleate ( $\ell \approx 2$  nm) [21] and their micelles ( $d \approx 7$  nm, CMC = 0.48 mmole/L [21]) can. Only small ions can move through the micropores. The calcium ion has a bare diameter of 0.20 nm, but once fully hydrated by six molecules of water its diameter increases to 0.82 nm. [33]. Whether or not calcium ions can freely diffuse through the micropore is arguable and would certainly require more accurate measurements.

Two molecules of sodium oleate colliding with one of calcium would react to produce one of calcium oleate. This forward reaction is believed to be very rapid and many orders of magnitude faster than its counterpart. Calcium oleate molecules can crystallize by a yet poorly understood mechanism [29]. If this phenomena happens inside a macropore, the soap is entrapped within the cell wall. The calcium present at the surface of a macropore can be considered as “easily accessible”. Upon reaction, a concentration gradient is created, forming the driving force for the calcium ions to diffuse from the areas of higher concentration of the fiber’s bulk. The calcium transport from the bulk can be visualized either as diffusion through micropores or by considering the fiber network as a gel.

### **2.3.3 Effect of Calcium concentration**

Most often, the addition of calcium chloride in a deinking plant is higher than the

Calcium ion  
0.2 nm

Hydrated Calcium ion  
0.8 nm

Na(oleate) micelle  
7 nm

Ca(oleate)<sub>2</sub> particle  
230 nm

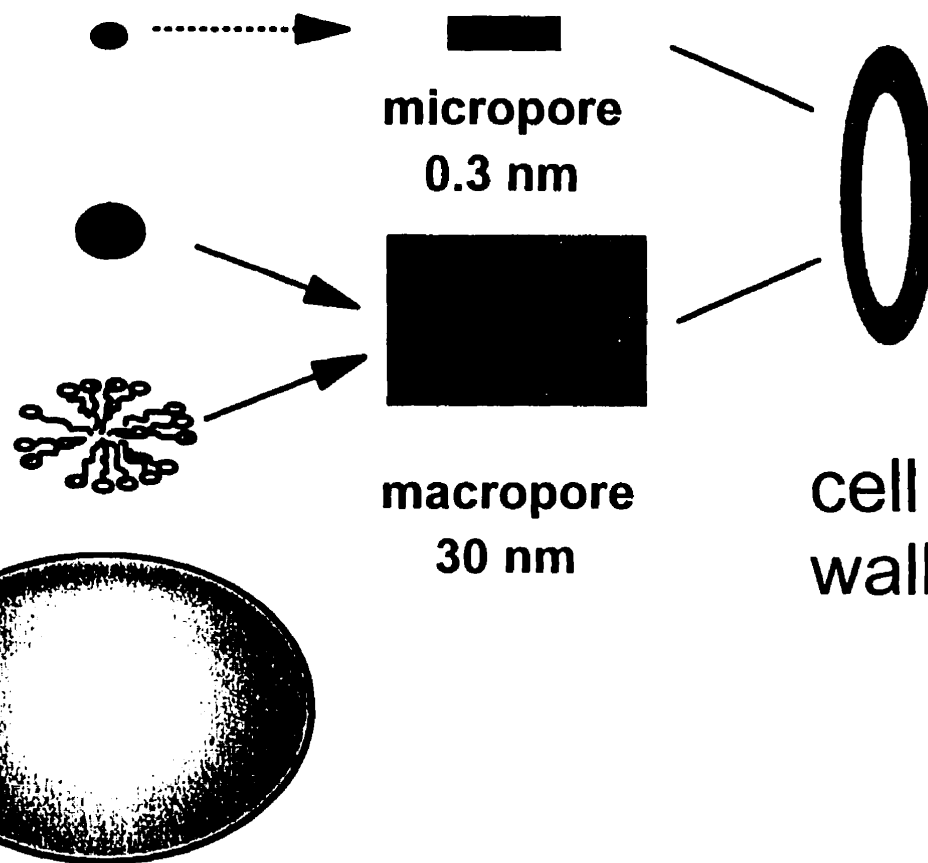


Fig. 9 A simplistic view of the cell wall porosity and the relative sizes of the chemical species involved in this study.

stoichiometric amount required to react the sodium oleate into its calcium form. Excess calcium could well be a variable of importance in a mill. Three calcium oleate suspensions of identical soap concentration were prepared by mixing the same sodium oleate solution with different amounts of calcium chloride. The  $\text{CaCl}_2$  required for equimolar (1 Meq) and tenfold (10 Meq) stoichiometry were mixed with a 100 ppm (0.33 mM) sodium oleate solution. The exact composition of each of these soap suspensions is presented in Table III. The effect of the concentration of  $\text{Ca}^{+2}$  on the retention of calcium soap particles on kraft pulp was studied (Figure 10 ). As for the mechanical pulp, there was no retention of calcium oleate on kraft pulp for the soap suspension without calcium excess (1 Meq). However, markedly smaller BTC's resulted for the passage through the bed of calcium soap suspensions with excess of calcium (10 Meq).

Such behavior can result either from adsorption of soap on the pulp at the 10 Meq, or from an artifact of our analytical technique. Indeed, a direct effect of calcium excess could have been to increase the light scattering and absorbance by the soap particle due to a change in particle size or its refractive index. This was not the case as each absorbance ratio was normalized with respect to its own inlet absorbance. Furthermore, the light absorbance of the inlet suspensions proved to be independent of the calcium excess. Therefore, the decrease in BTC intensity with increasing amounts of calcium can only be caused by soap adsorption on the fibers. We can now wonder if the area under the BTC is a direct measurement of the calcium oleate eluded from the packed bed [Equation 10]. A mass balance was performed for the pulse containing a tenfold calcium stoichiometry (10 Meq). BTC analysis predicted that 1.2 mmol of calcium oleate stayed within the fiber bed after the 10-minute pulse. The predicted retention amount was confirmed by Soxhlet extraction of the pulp (chloroform),

<b>TABLE III</b> <b>DIFFERENT LEVELS OF CALCIUM ION CONCENTRATION IN THE INLET SOAP SUSPENSION FOR CASES I AND II</b>		
LEVEL	Na(Oleate) mmol/l	Ca <sup>+2</sup> mmol/l
I) 1 Meq	0.34	0.16
II) 10 Meq	0.34	1.64

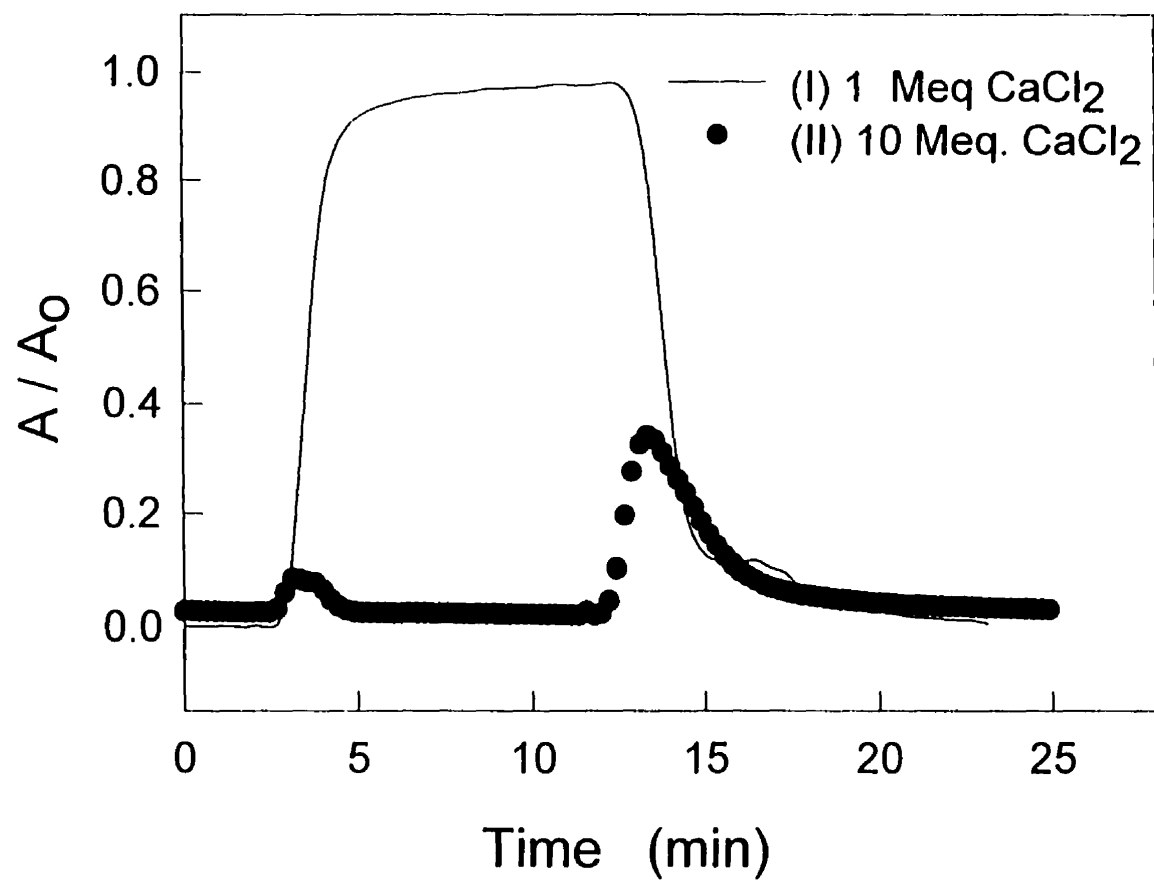


Fig. 10 BTC's of two calcium oleate pulses ( on kraft pulp) with different levels of calcium concentration: (I) 1 Meq, and (II) 10 Meq.



which removed 1.0 mmol of calcium oleate (Figure 11). Furthermore, scanning Electron micrographs of individual fibers after the 10 Meq pulse experiment showed soap particles retained in the form of large aggregate patches on the surface of the fibers (Figure 12), suggesting a coagulation mechanism.

Deposition of soap particles on the fibers at excess calcium levels is in agreement with theory. Soap retention could occur either by charge reversal or by coagulation (screening of the electrostatic forces). Electrophoretic mobility measurements of calcium oleate particles were conducted by Matijević at oleate to  $\text{CaCl}_2$  molar ratios ranging from 0.05 to 0.5 [29]. He concluded that calcium oleate particles retain their negative charge in spite of the  $\text{Ca}^{+2}$  excess. According to the DLVO theory, an excess of calcium ions would also suppress the electrostatic repulsion between fibers and soap particles. The van der Waals forces can easily overcome the energy barrier resulting in heteroflocculation, i.e., deposition of individual soap particles on the fibers. Soap particles can also coagulate within the fiber network above a Critical Coagulation Concentration (CCC) and deposit as soap flocs onto the fiber surface. A retention mechanism which involves flocculation of the soap particles was therefore investigated and is the subject of an accompanying paper.

#### **2.3.4 Effect of adsorbed Calcium Soaps on Sizing and Carryover**

Since it is now proven that soaps can be retained on the pulp during recycling, it is of interest to quantify how this phenomenon affects the surface properties of paper. Surface sizing was first tested with a Hercules Sizing Tester (HST) from handsheets made at different calcium levels. All samples gave nearly zero minutes, thus no measurable sizing. Such behavior suggests either that a minute amount of soap was retained on the fibers' surface

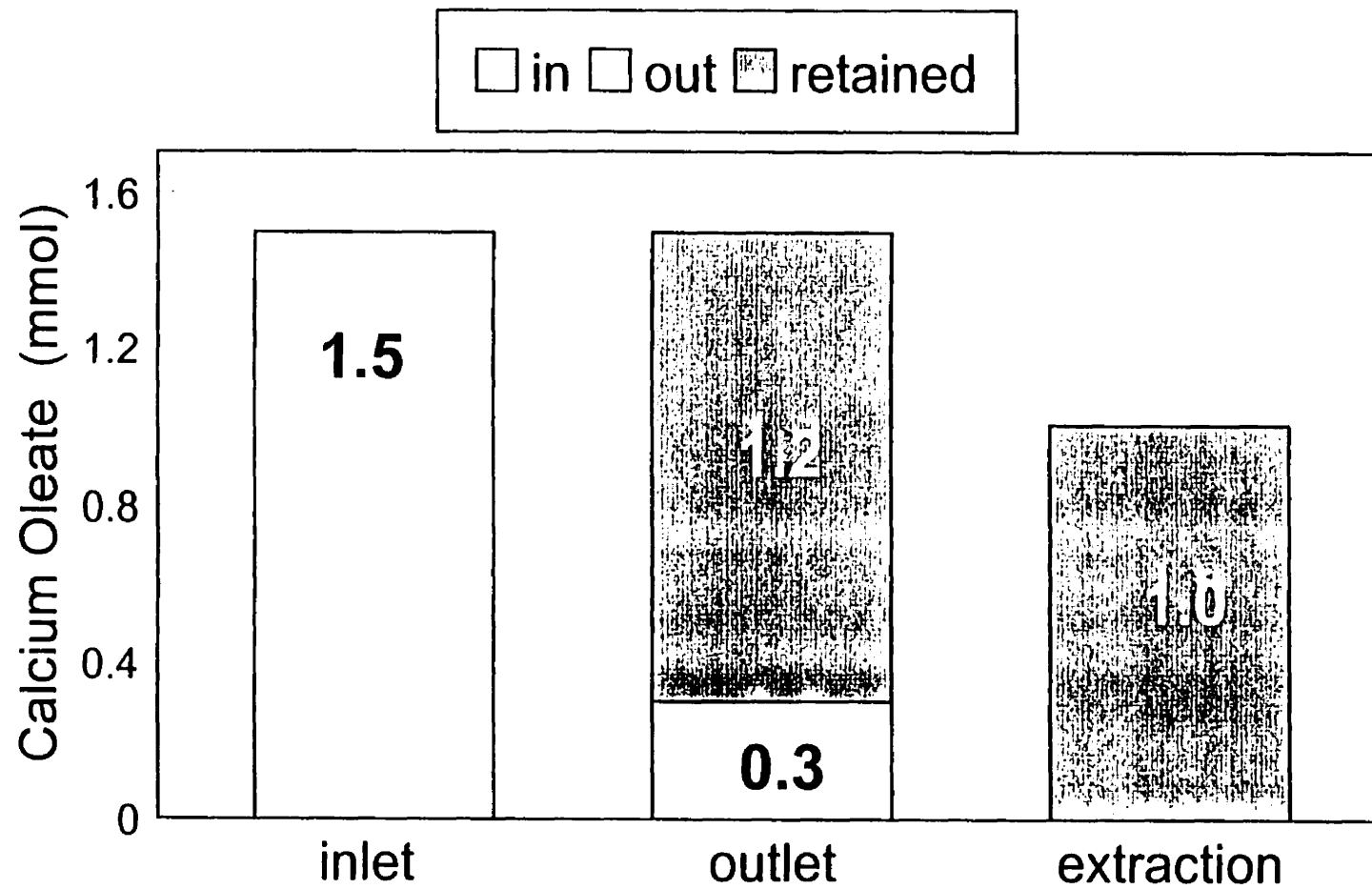


Fig. 11 Soap mass balance for the 10 Meq calcium oleate pulse (10 minutes) showing actual extracted amount.

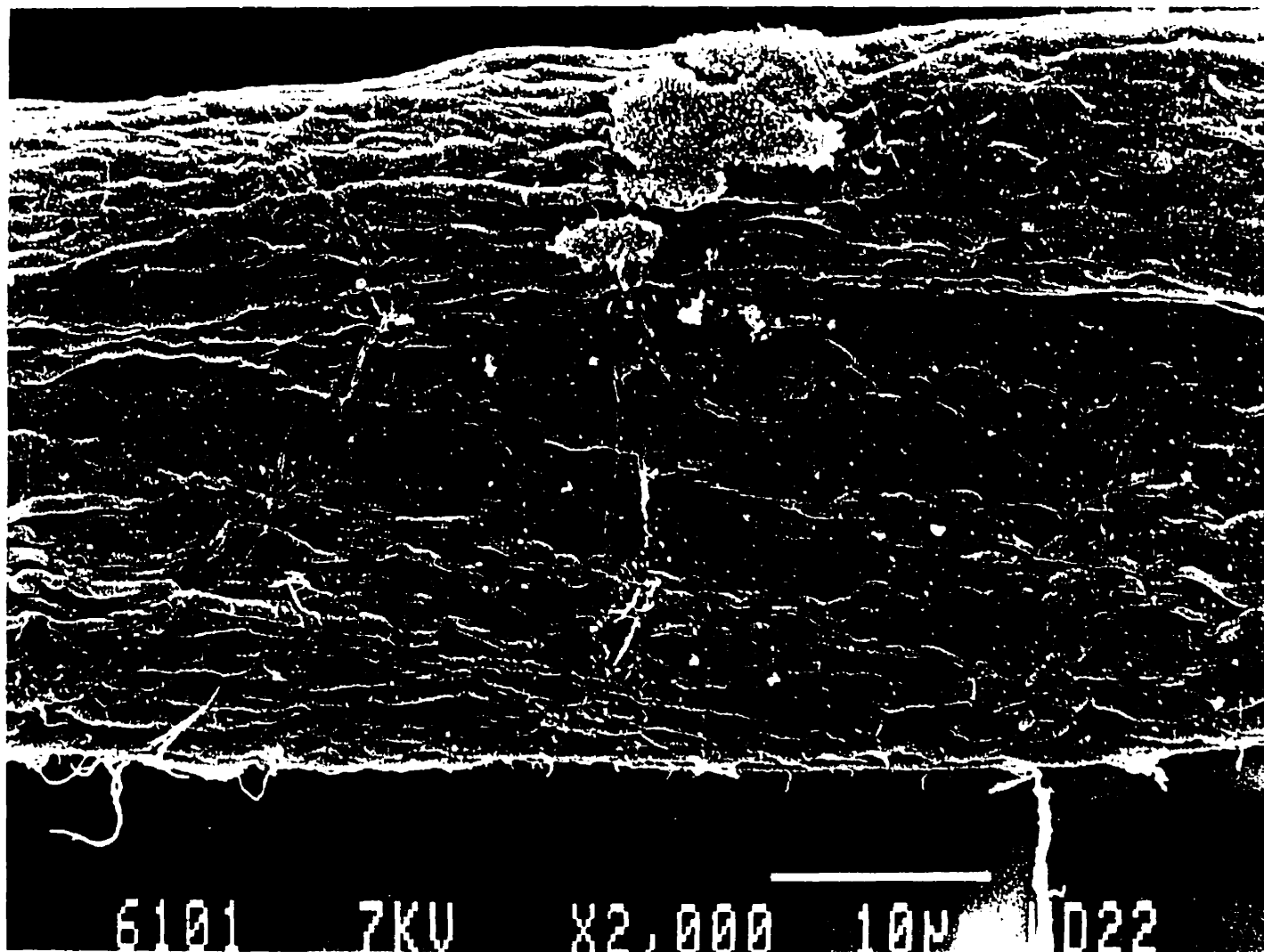


Figure 12a. SEM photograph of a wood fiber for the 10 Meq Calcium Oleate pulse BTC.



Figure 12b. Magnified image (white bar indicates 100 nm).

(i.e., less than monolayer deposition), that the soap has no effect on sizing, or that the paper's high porosity hides any sizing effect. The first hypothesis is the most likely because of the short contact time and low consistency during handsheet formation. To overcome these potential problems, soap deposition was carried out in the packed bed directly onto filter paper cut in circles to fit the reactor. Again, no measurable sizing effects were found with the HST on these samples.

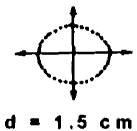
In spite of the HST results, the filter paper samples felt and smelled "soapy". Thus, another simple test was designed. It consists of measuring the time required to spread a drop of deionized water up to a circular area of 1.5 cm diameter marked on the samples. The results for treated filter papers are shown in Table IV. A significant difference between the blank sample without soap (0.5 sec) and the "soapy" sample (3.2 sec) was observed. This test indicates the sizing effect of the soap retained.

To eliminate the effect of porosity, the behavior of sizing agents is best studied on smooth surfaces such as a microscope slide coated with a cellulose film [28] by following the spreading of a water drop. For a given paper morphology, any variation in contact angle would be a direct measurement of a change in surface composition. The contact angle of water over filter paper strips submitted to pulses of calcium soap were therefore measured. Figures 13 and 14 show the contact angle as well as the liquid surface tension results. For a given paper porosity, a large increase in the advancing contact angle between untreated and soap-treated paper (from 20 to 148 °) indicates an important hydrophobization caused by the retained soap. The surface tension of the water was measured before and after contact angle measurements with a soapy paper. The decrease in water surface tension from 71 mN/m to 49 mN/m prior and after contact indicates that the soap retained on the paper can be readily

---

**TABLE IV**  
**WATER ABSORBANCE TEST ON FILTER PAPER FOR A**  
**CONTROL ("CLEAN") SAMPLE AND A SAMPLE WITH**  
**DEPOSITED CALCIUM SOAP**

---

Time required to spread a drop of water to 1.5 cm.	Clean sample (sec)	Sample with soap (sec)
 <p>d = 1.5 cm</p>	0.38	2.84
	0.41	3.84
	0.68	3.08

---

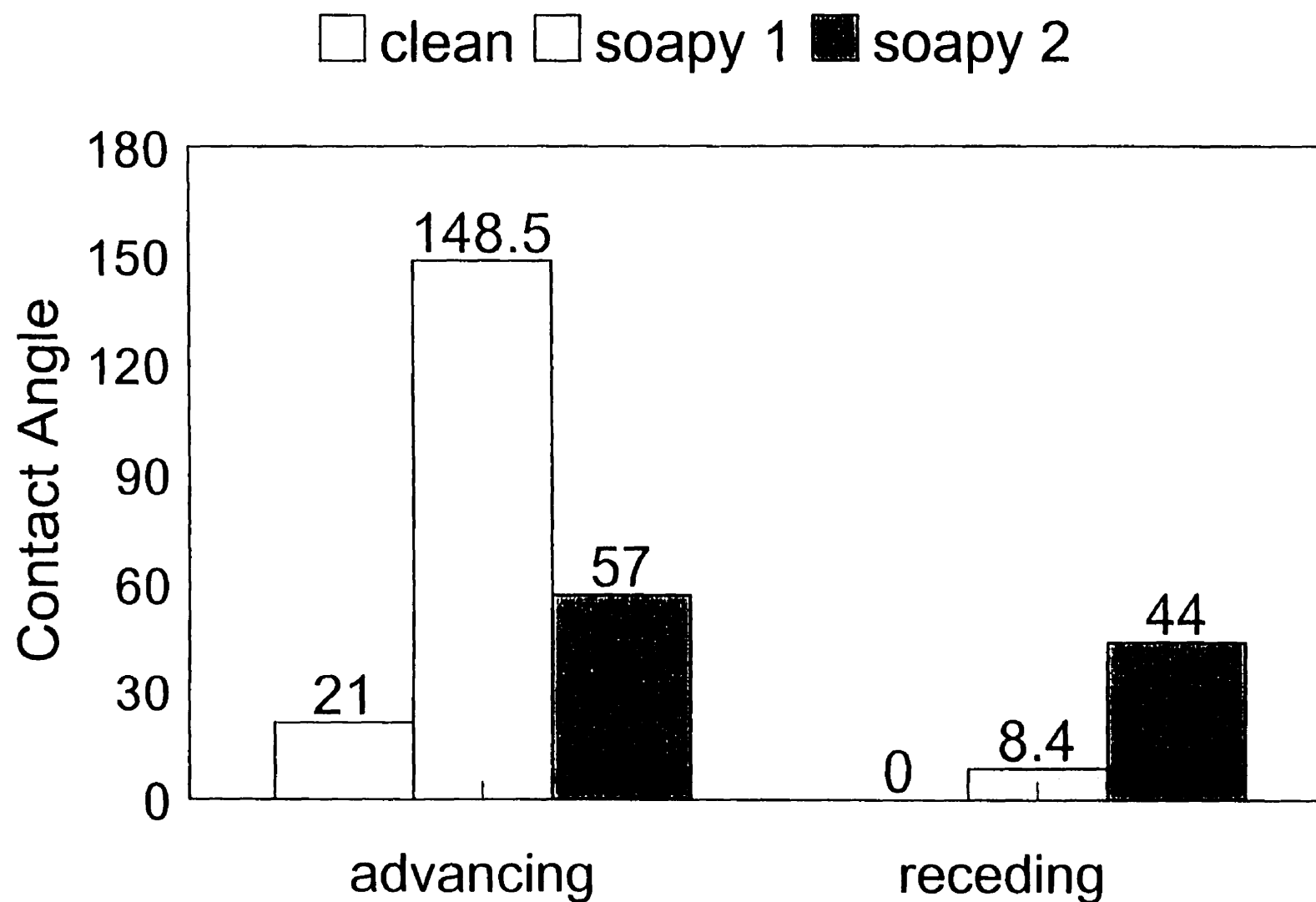


Fig. 13 Contact angle measurements of filter paper samples with (soapy) and without (clean) deposited soap.

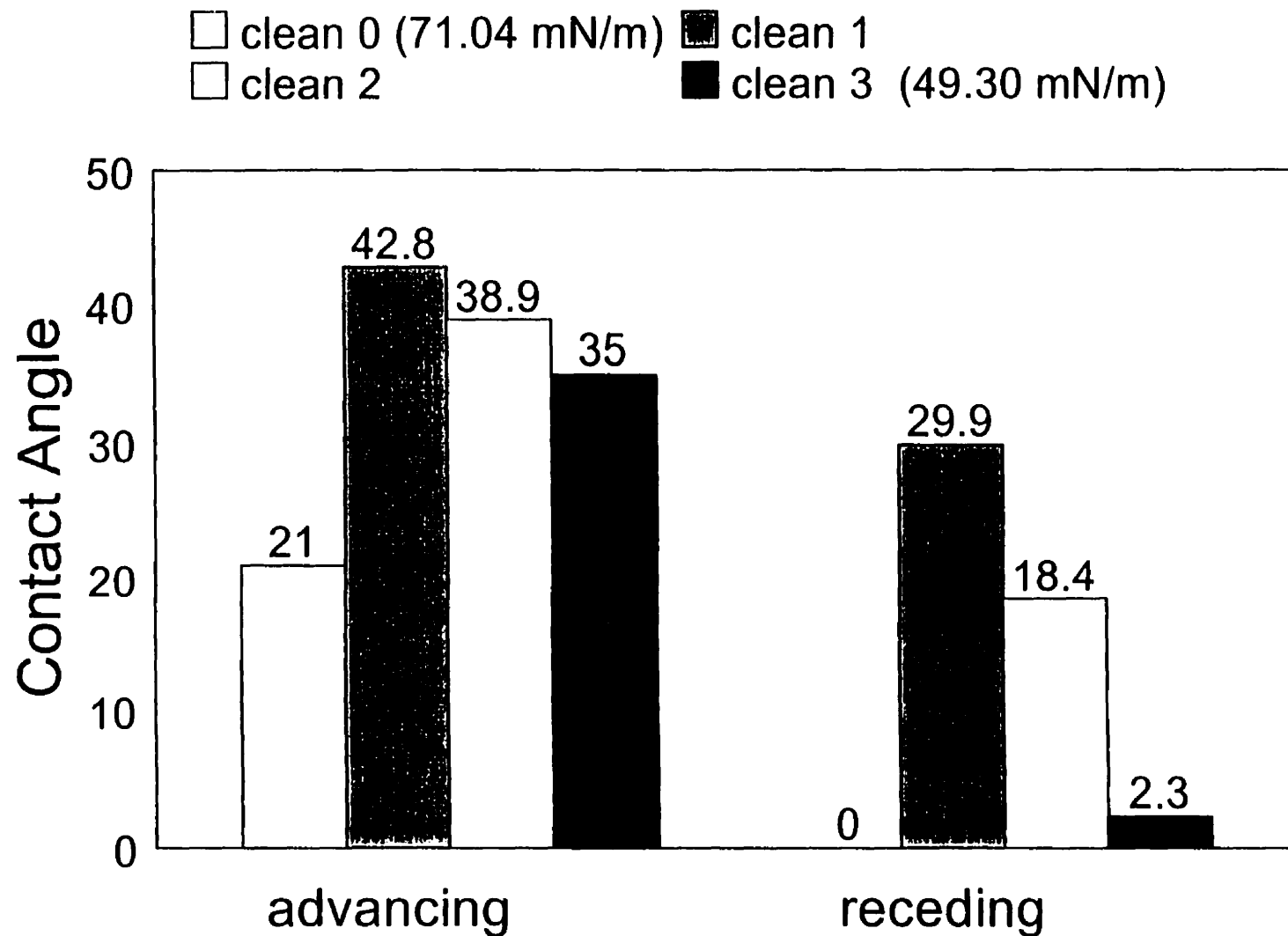


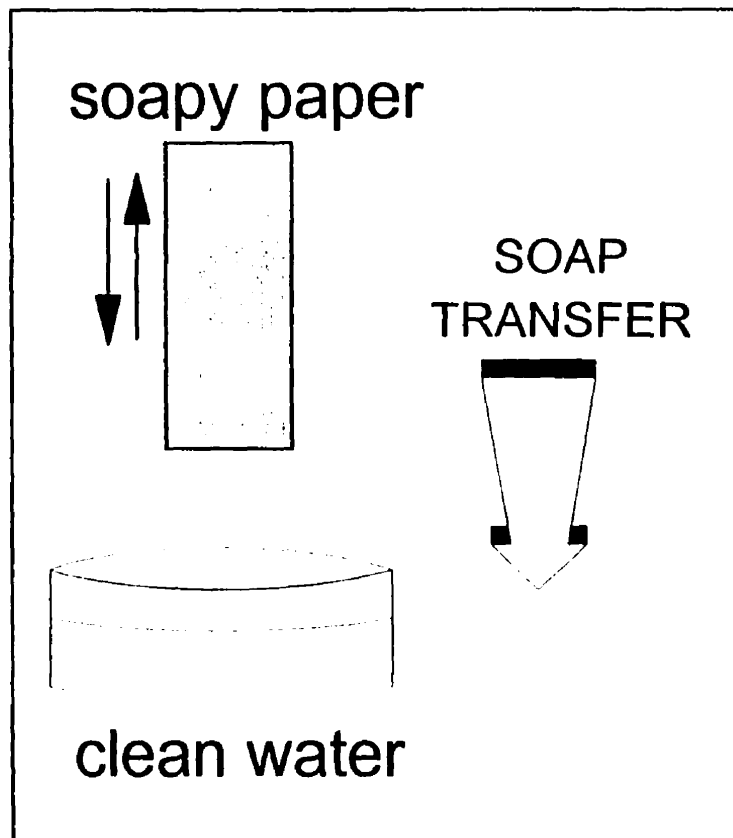
Fig. 14 Contact angle measurements of untreated (clean) filter paper samples and the corresponding surface tension measurements of deionized water (71.0 mN/m) and soapy water (49.3 mN/m).



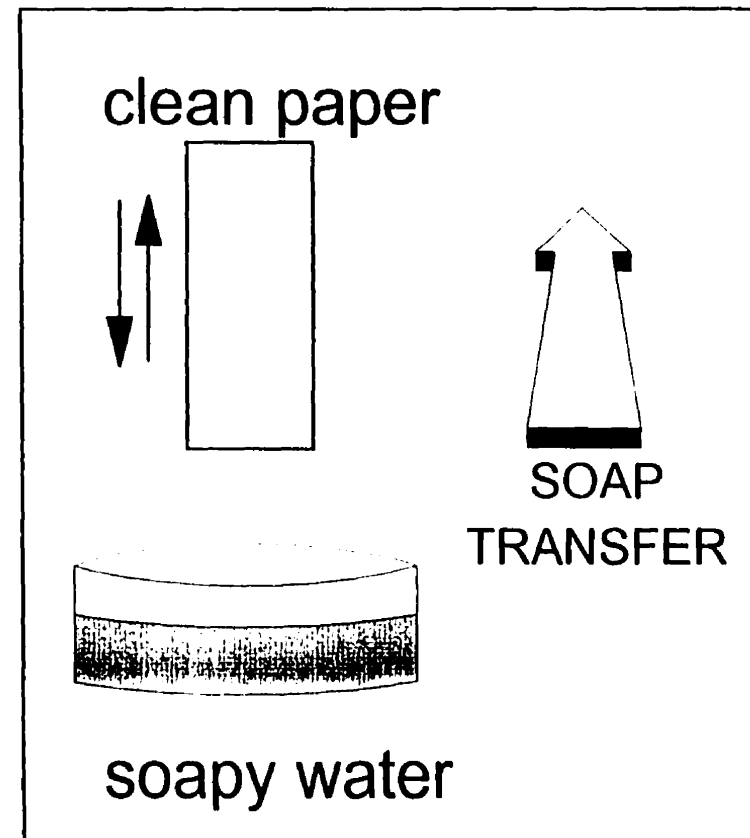
desorbed into the clean distilled water. Conversely, when “clean” papers (soap-free) were introduced into the soapy water, the surface tension showed a steady increase as more “clean” paper samples re-adsorbed the calcium soap from the water (Figure 15). These trends highlight the dynamics of this adsorption-desorption process. Furthermore, these observations suggest a weak adhesion between the soap particles and the paper. The adsorption and desorption rate constants must also be high and of similar magnitude.

## 2.4 CONCLUSIONS

1. Calcium soap particles may deposit on the fibers at salt concentrations above the critical coagulation concentration (CCC).
2. We proposed a diffusion mechanism by which the fibers micropores would be inaccessible to all species. The macropores could allow diffusion of hydrated calcium and micelles of sodium oleate.
3. Soap retention on the pulp increases the hydrophobicity of paper.
4. The weak adhesion strength of soap particles on paper combined with high adsorption and desorption rate constants of similar magnitude explain the carryover mechanism of fatty acid soaps.
5. Sodium salts of fatty acids undergo ion-exchange with the calcium present in the pulp (forming calcium soaps).
6. Calcium ions present in tap water can be retained by the pulp.
7. The availability of calcium within the pulp for ion-exchange is diffusion controlled.
8. The area under a BTC is a sensitive measure of contaminant retention on the pulp.



Surface tension of water  
decreases upon contact



Surface tension of water  
increases upon contact

Fig. 15 Proposed scheme of the adsorption-desorption process dynamics between paper and calcium soaps.

## REFERENCES

1. DORRIS, G., *Paprican Report: Recycling and the Canadian Pulp and Paper Industry*, Part II, Sept. (1989).
2. FENGEL, D. and WEGENER, G., *Wood: Chemistry, Ultrastructure, Reactions*, de Gruyter Ed., New York, 613 (1984).
3. LUNER, P. and SANDELL, M., J., "The Wetting of Cellulose and Wood Hemicelluloses" *Polymer Sci.*, Part C, Polymer Symp., 28:115-142 (1969).
4. BROWN, P.F. and SWANSON, J.W., "Wetting Properties of Cellulose treated in a Corona Discharge", *Tappi J.* 54(12):T2012-T2018 (1971).
5. GARNIER, G. and GLASSER, W.G., "Measurement of the Surface Energy of Amorphous Cellulose by Alkane Adsorption: A critical evaluation of Inverse Gas Chromatography (IGC)" *J. Adhesion* 46:165-183 (1994).
6. GARNIER, G. and GLASSER, W.G., "Measuring the Surface Energies of Spherical Cellulose Beads by Inverse Gas Chromatography", *J. Polymer Eng. Sci.* 36(6):885-894 (1996).
7. JACOB, P. N. and BERG, J.C., "Zisman analysis of three Pulp Fiber furnishes", *Tappi J.* 76(2):105-107 (1993).
8. ERIKSSON, I. et al, "Recycling Potential of Printed Thermomechanical Fibres for Newsprint", *CPPA 3rd Res. Forum on Recycling*, 163-169 (1995).
9. CHATTERJEE, A., ROY, D.N. and WHITING, P., "Effect of Recycling on the Surface characteristics of Paper, *Preprints, Int. Phys. Conf.*, 129-141 (1991).
10. HEDBORG, F., and LINDSTRÖM, T., "Alkaline Rosin Sizing using Microparticulate Aluminum-based Retention Aid system", *Nordic Pulp Paper Res. J.* 3:331-336 (1993).
11. MARTON, J., "Practical Aspects of Alkaline Sizing", *Tappi J.* :139-143 (1990).
12. ORTNER, H.E., "Flotation Deinking", Ch. XVIII, *Secondary Fibers and Non-wood Pulping, Pulp and Paper Manufacture*, Monograph Series 3:208 (1987).
13. EVANS, P.G. and EVANS, W.P., "Mechanism for the Anti-redeposition action of Sodium Carboxymethylcellulose with Cotton. I. Radiotracer studies", *J. Appl. Chem.* 17:276-282 (1967).

14. JOHNSON, G.A. and LEWIS, K.E., "Mechanism for the Anti-redeposition action of Sodium Carboxymethylcellulose with Cotton. II. Colloid-stability Theory applied to the Fibre-soil system", *J. Appl. Chem.* 17:283-287 (1967).
15. JOHNSON, G.A. and BRET LAND, A.C., "Mechanism for the Anti-redeposition action of Sodium Carboxymethylcellulose with Cotton. III. Electrophoresis and Sedimentation studies" *J. Appl. Chem.* 17:288-292 (1967).
16. FORT, T. Jr. , BILLICA, H.R. and GRINDSTAFF, T.H., "Studies of Soiling and Detergency. Part II: Detergency experiments with model Fatty Soils", *Textile Res. J.* 36:99-111 (1966).
17. GRINDSTAFF, T.H., PATTERSON, H.T. and BILLICA, H.R., "Studies of Soiling and Detergency. Part III: Detergency experiments with Particulate Carbon Soils ", *Textile Res. J.* 37:564-573 (1967).
18. GRINDSTAFF, T.H., PATTERSON, H.T. and BILLICA, H.R., "Studies of Soiling and Detergency. Part IV: Deposition and Transfer experiments with Fatty Soils", *Textile Res. J.* 40:35-42 (1970).
19. HSIAO, L. and DUNNING, H.N., "A Comparative Study of Non-Ionic Detergent Adsorption by Radioactive, Spectrophotometric and Surface Tension Methods", *J. Phys. Chem.* 59:362-366 (1955).
20. LARSSON, A., STENIUS, P. and ÖDBERG, L., "Surface Chemistry in Flotation Deinking: Part 3. Deposition of ink and calcium soap particles on fibers", *Svensk Papperstidn.* 3:R2-7 (1985).
21. STRÖM, G., *et al*, "Surface Chemical aspects of the behavior of Soaps in Pulp Washing", *Nordic Pulp Paper Res. J.* 1:44-51 (1990).
22. AL-JABARI, M., VAN HEININGEN, A.R.P. and VAN DE VEN, T.G.M., "Modeling the flow and the Deposition of Fillers in Packed beds of Pulp Fibers", *J. Pulp Pap. Sci.* 20(9):J249-J253 (1994).
23. HIEMENZ, P., *Principles of Colloid and Surface Chemistry*, 2nd ed., Marcel Dekker Inc., New York 815 (1986).
24. ALI, O., *Dynamic Chlorination of Kraft Pulps*, Ph.D. Thesis, McGill University (1990).

25. AL-JABARI, M., VAN HEININGEN, A.R.P. and VAN DE VEN, T.G.M., "Experimental Study of Deposition of Clay Particles in Packed Beds of Pulp Fibers", *J. Pulp Pap. Sci.* 20(1):J289-J295 (1994).
26. PICARO, T. and VAN DE VEN, T.G.M., "The Flow of Dilute Polyethylene Oxide Solutions through Packed Beds of Pulp Fibers", *J. Pulp Pap. Sci.* 21(1):J13-J18 (1995).
27. CPPA, Technical Section CPPA Standard Testing Methods, C4 (1994).
28. VAN OSS, C., Interfacial Forces in Aqueous Media, Marcel Dekker Inc., New York, 440 p. (1994).
29. MATIJEVIĆ, E., LEJA, J. and NEMETH, R., "Precipitation Phenomena of Heavy Metal Soaps in Aqueous Solutions. I. Calcium Oleate", *J. Colloid Interface Sci.* 22:419-429 (1966).
30. ALINCE, B., PETLICKI, J. and VAN DE VEN, T.G.M., "Kinetics of Colloidal Particle Deposition on pulp Fibers. 1. Deposition of Clay on Fibers of Opposite Charge", *Colloids Surfaces* 59:265-277 (1991).
31. TOWERS, M. and SCALLAN, A.M., "Predicting the Ion-Exchange of Kraft Pulps Using Donnan Theory", *Paprican Report*, PPR # 1170 (1995).
32. STONE, J.E. and SCALLAN, A.M., "A Structural Model for the Cell Wall of Water-Swollen Wood Pulp Fibres based on their Accessibility to Macromolecules", *Cellulose Chem. Tech.* 2:343-358 (1968).
33. ISRAELCHVILI, J. N., Intermolecular and Surface Forces, 2nd. Ed., Academic Press 450 (1992).

## **CHAPTER THREE**

### **RETENTION OF FATTY ACID SOAPS DURING RECYCLING: A MECHANISTIC STUDY**

## ABSTRACT

*Soap retention on wood fibers during recycling can play an important role in sizing and carryover phenomena. Sizing is the treatment of paper that renders it hydrophobic. Unintended sizing may occur during paper recycling and have detrimental effects on the surface properties of paper. Carryover is the undesirable transport of process chemicals by the pulp from one unit to another causing contamination problems. This study investigated the retention of fatty acid soaps on the pulp with a packed bed of wood fibers by following the dynamics of retention of a concentration pulse generated at the entrance (breakthrough curve, BTC). A proposed mechanism by which calcium soap particles deposit on the fibers at salt concentrations above a critical coagulation concentration (CCC) was tested. The variables studied include: electrolyte concentration (0-1.64 mM/L), cation valence ( $\text{Ca}^{+2}$ ,  $\text{Al}^{+3}$ ), pulp consistency (5-15%) and flowrate (30-180 mL/min). All tests were carried out at room temperature using bleached Kraft pulp (black spruce) and calcium oleate at 0.16 mmol/L (100 ppm), the common industrial concentration. The objective of this study was to investigate a soap retention mechanism.*

*Soaps prepared by mixing equimolar amounts of sodium oleate and calcium chloride (1 Meq) do not adsorb on pulp fibers. This is explained by the electrostatic repulsion between the negatively charged soap particles and fibers. However, retention of the particles increases as the Calcium chloride concentration is increased (0.164 and 1.48 mmol/L). This is due to a charge screening mechanism expected in the presence of an electrolyte. Two*

different phenomena can occur: (1) particle deposition above a critical deposition concentration (CDC); and, (2) particle coagulation close to the fiber surface above a critical coagulation concentration ( $CCC_{surface}$ ) close to the fiber's surface. A  $CCC_{surface}$  value of 0.7 mmol/L, lower than the critical coagulation concentration of 3.8 mmol/L for a particle suspension system in the absence of fibers was estimated. The fiber surface can depress the CCC by a reverse osmosis pressure. The  $CCC_{surface}$  was estimated from the soap retention isotherms at different calcium chloride concentrations, and constant pulp consistency (10%) and feed flowrate (130 mL/min ).

The rate of soap coagulation in the presence of pulp fibers was calculated for different flowrates from the BTC's. It is suggested that soap retention occurs via orthokinetic coagulation. At high flowrates (above 100 mL/min), the rate of coagulation becomes ion-diffusion controlled, and it slows down. The critical residence time (minimum contact time) for complete surface coagulation was found to be 6.4 minutes.

If the excess electrolyte contains a trivalent cation, such as  $Al^{+3}$ , the retention mechanism becomes more complicated because  $Al^{+3}$  may undergo ion-exchange or adsorption with the  $Ca^{+2}$  ions which render the soap particles positive. The balance between the ion-exchange and charge screening kinetics is the key factor that determines the retention behavior.

The effects of the variables studied were analyzed in terms of a mathematical model that simulates particle retention kinetics in packed beds. The parameters studied include the average residence time ( $\theta_{avg}$ ), bed porosity ( $\epsilon$ ), equilibrium deposition constant ( $K$ ) and maximum surface coverage ( $N_{max}$ ).



### 3.1 INTRODUCTION

Soap retention on wood fibers during paper recycling can play an important role in sizing and carryover phenomena [1-8]. Sizing is the treatment of paper that renders it hydrophobic for specific applications. Unintended sizing may occur during paper recycling and have detrimental effects on the surface properties of paper such as fibre-fibre bond, friction coefficient, ink penetration time, etc. Carryover is the undesirable transport of process chemicals by the pulp from one unit to another causing contamination problems such as pitch (sticky material) deposition on equipment surfaces.

In order to reduce potential losses due to soap retention, it is necessary to understand the fundamentals of the soap-fiber interactions. Soap retention can occur due to mechanical entrapment and adsorption. Mechanical entrapment is the filtration mechanism of “large” particles through the fibre web. *Chemisorption* is the retention by chemical bond (covalent or ionic) formation whereas *physisorption* is associated with weak reversible forces such as the van der Waals interactions. Adsorption may occur on the fibre surface, inside the lumen and within the pores on the fibre wall. In order for particles to adsorb they must be brought in close proximity such that the colloidal forces become predominant. Thus, conditions that improve the collision frequency also improve the particle-fibre adsorption.

On a previous study of soap retention on wood fibers [9], we found that soap is retained on wood fiber surfaces in the presence of excess electrolyte, possibly by a particle coagulation mechanism. Contaminant retention on the pulp was investigated with a packed bed of wood fibers by following the response dynamics a concentration pulse generated at the entrance (breakthrough curve, BTC). The objectives of this paper are threefold: (1) to

further investigate the effects of electrolyte valence and concentration, pulp consistency, and flowrate; (2) to compare the experimental data to a mathematical simulation of particle flow and deposition in packed beds of pulp fibers; and (3) to identify a retention mechanism of fatty acid soaps on pulp fibers.

### 3.2 RELATED COLLOID CHEMISTRY DEFINITIONS

This article refers to *homogeneous coagulation* when a stable suspension of particles forms aggregates (destabilizes) upon the addition of an electrolyte salt above a critical coagulation concentration (CCC) [10]. At high electrolyte concentrations, the electrical double layer is compressed to such an extent that the particle-particle repulsion is minimized (charge screening mechanism). According to the *Schultze-Hardy rule*, the CCC for negatively charged particles is inversely proportional to the sixth power of the cation valence [11]. This general rule applies only for symmetric electrolyte systems (eg.  $\text{Al}(\text{PO}_4)_3$ ). Thus:

$$\text{CCC}(\text{Al}^{+3}) = 0.1 \text{ CCC}(\text{Ca}^{+2}) \quad [1]$$

Coagulation is *heterogeneous* when different particles aggregate either (1) spontaneously due to net attractive forces (eg. a positive particle-negatively particle); or (2) by a charge neutralization mechanism (eg. negative particle-negative particle). One form of heterogeneous coagulation is the *deposition* of individual soap particles on the fiber surface at an electrolyte concentration above the Critical Deposition Concentration (CDC) through

a charge screening (neutralization) mechanism [12].

*Soap retention* denotes the total amount of soap retained in the fibre network. This term does not describe specifically the mode(s) of retention.

### 3.3 MODEL OF THE FLOW AND DEPOSITION OF PARTICLES

The mathematical simulation of clay particle deposition in packed beds of pulp fibers was previously studied by Al-Jabary *et al* [12,13]. The model consists of two coupled partial differential equations describing the transport and the deposition kinetics. The transport equation represents the flow of particles through a porous medium neglecting the diffusion term [14,15]:

$$\begin{array}{ccccc} & \text{transient} & & \text{convective} & \\ \varepsilon \frac{\partial n}{\partial t} + (1 - \varepsilon) \rho \frac{\partial N}{\partial t} + U \frac{\partial n}{\partial x} = 0 & & & & [2] \\ \text{liquid} & \text{solid} & & \text{liquid} & \end{array}$$

where  $n$  and  $N$  are the concentrations of the particles in suspension and on the fibers respectively,  $\varepsilon$  is the void fraction,  $\rho$  is the density of the fibers.  $t$  refers to the time and  $x$  to the spatial coordinate. The particle concentration on the fibers was modelled by a modified Langmuir deposition kinetics equation [9]:

$$\frac{\partial N}{\partial t} = k_1 \frac{\varepsilon}{\rho (1 - \varepsilon)} n \left(1 - \frac{N}{N_{\max}}\right) - k_2 \frac{N}{N_{\max}} \quad [3]$$

where  $k_1$  is the forward (deposition) rate coefficient,  $k_2$  is the backward (detachment) rate coefficient; and  $N_{\max}$  is the maximum amount of particles that can deposit on the fibers.

When the variables are non-dimensionalized, equations [2] and [3] become:

$$\frac{\partial n}{\partial t} + \frac{1}{P_1} \frac{\partial N}{\partial t} + \frac{\partial n}{\partial x} = 0 \quad [4]$$

$$\frac{\partial N}{\partial t} - \frac{1}{P_2} \left( P_1 n \left(1 - \frac{N}{N_{\max}}\right) - \frac{1}{P_3} N \right) = 0 \quad [5]$$

$$P_1 = \varepsilon \frac{n_o}{(1 - \varepsilon) \rho N_{\max}} \quad [6]$$

$$P_2 = \frac{1}{k_1 \theta_{avg}} \quad [7]$$

$$P_3 = \frac{\kappa_1}{\kappa_2} N_{\max} = K N_{\max} \quad [8]$$

Table I outlines the physical meaning of these parameters.

This system of PDE's was solved numerically by Al-Jabary *et al* [13] using the Galerkin finite element method (GFEM). Their simulation results showing the effects of  $P_1$ ,  $P_2$  and  $P_3$  are presented in figures 1, 2 and 3 respectively to better analyze our current experimental results.

### 3.4 EXPERIMENTAL

This section is subdivided into three parts: (i) retention studies, where the kinetics and amount of soap retention are measured from BTC's; (ii) particle characterization to measure size (soap) and charge (soap and fibers); and (iii) stability study to measure the particle coagulation kinetics. Table II outlines the experimental conditions for part (i).

#### 3.4.1 Materials

A never-dried *Black Spruce* bleached kraft pulp (Domtar Q-90) was used. The pulp was washed extensively with deionized water over a 200 mesh size stainless steel filter. This was done in order to remove the smaller fiber fraction (fines) that could interfere with the analytical technique. Commercial grades of sodium oleate and calcium chloride were used

**TABLE I**  
**THE PHYSICAL INTERPRETATION OF MODEL PARAMETERS [13]**

PARAMETER	PHYSICAL MEANING	EFFECT ON RETENTION AS PARAMETER INCREASES
$P_1$	<u>( number of particles suspended in the bed )</u> $N_{\max}$	<i>decreases</i>
$P_2$	<u>( forward deposition time )</u> $\theta_{\text{avg}}$	<i>decreases</i>
$P_3$	<i>dimensionless steady state constant</i>	<i>increases</i>

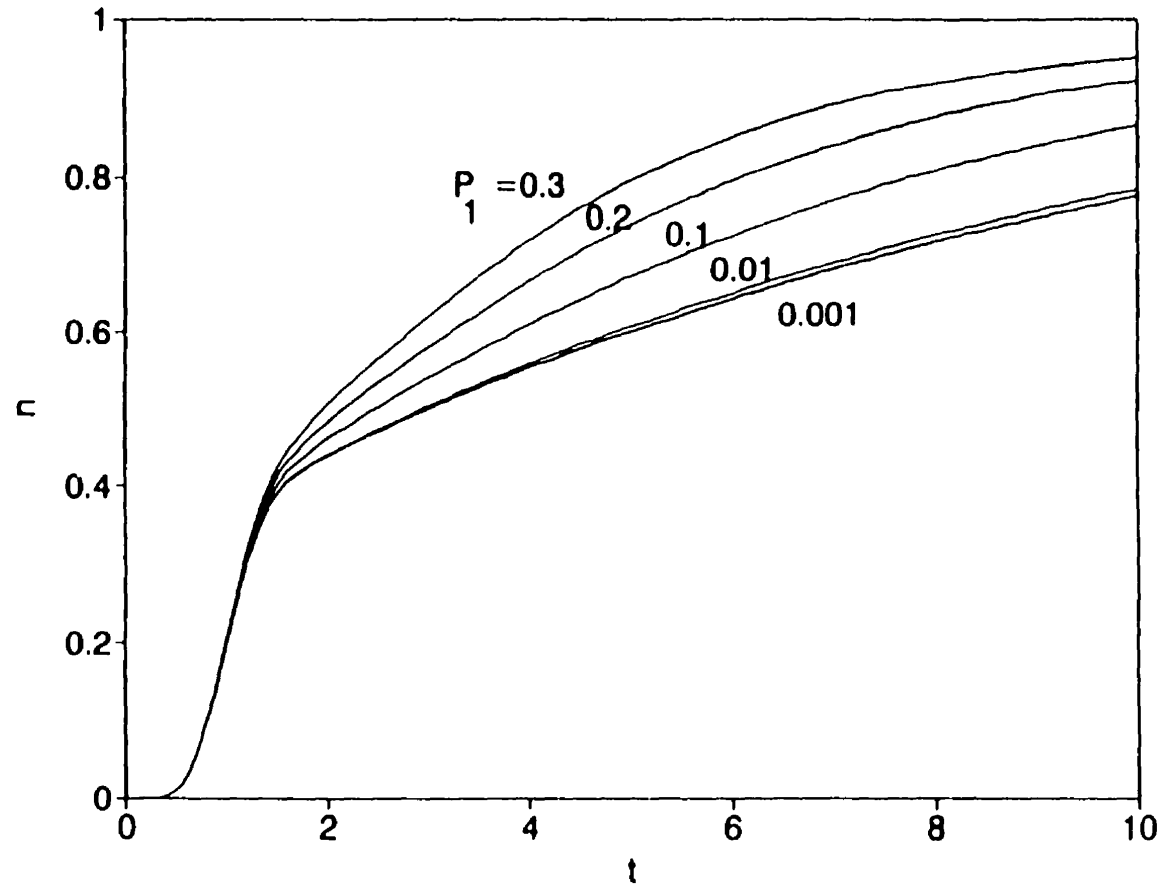


Fig. 1 Particle concentration at the exit of the bed as a function of  $P_1$ . Simulation for  $P_2 = P_3 = 1$  and  $Pe=40$  [13].

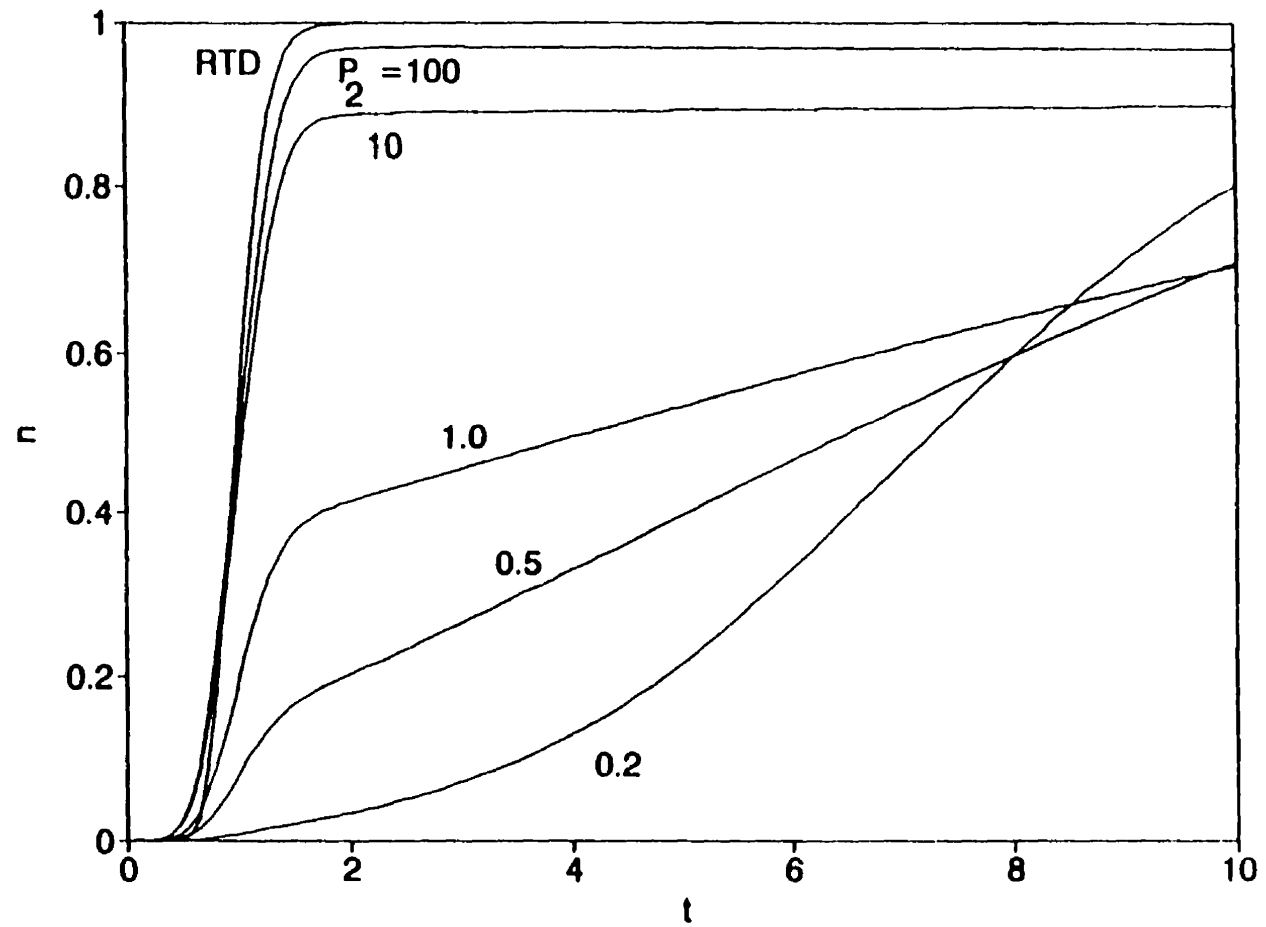


Fig. 2 Particle concentration at the exit of the bed as a function of  $P_2$ . Simulation for  $P_1 = 0.1$ ,  $P_3 = 17$  and  $Pe = 40$  [13].



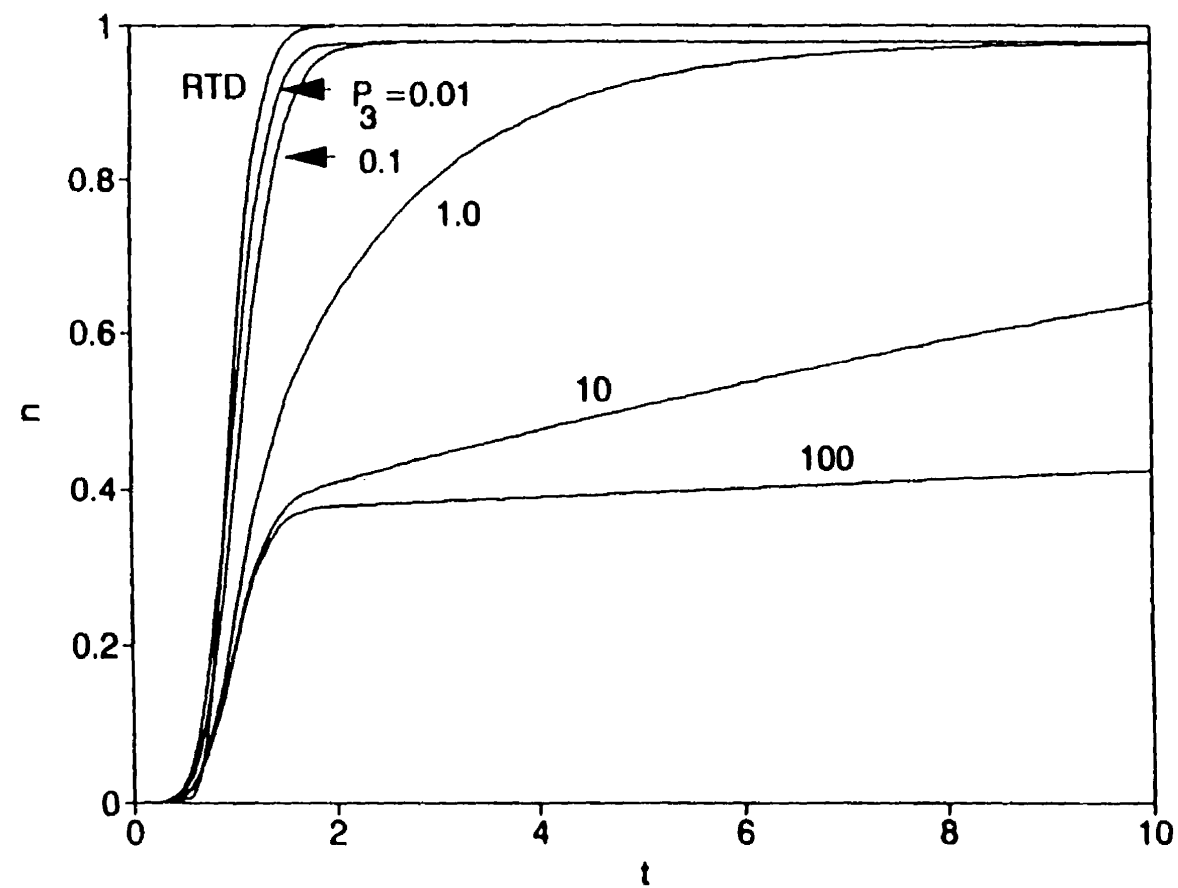
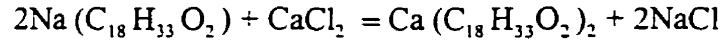


Fig. 3 Particle concentration at the exit of the bed as a function of  $P_3$ . Simulation for  $P_1 = 0.01$ ,  $P_2 = 1.0$ , and  $Pe = 40$  [13].

**TABLE II**  
**EXPERIMENTAL CONDITIONS**  
**FOR RETENTION STUDY**

VARIABLE STUDIED	Calcium oleate mmol/L	Consistency %	Flowrate mL/min	calcium chloride mmol/L	aluminum chloride mmol/l
CaCl <sub>2</sub> concentration	0.16	10	130	0, 0.16, 1.48	0
Valency	0.16	10	130	0	0, 0.1, 2.0
Consistency	0.16	5, 10, 15	96-130	1.48	0
Flowrate	0.16	10	32-180	0.16, 1.48	0

(Sigma Co.), as received, to prepare a calcium oleate suspension by mixing a stoichiometric amounts as follows:



### 3.4.2 Breakthrough curves

A packed bed reactor was used to carry out retention studies. For a detailed description of the analytical technique please refer to Chapter 2. Soap retention can be quantified by following the exit stream dynamics of a soap concentration pulse generated at the entrance. The breakthrough curves (BTC's) were obtained by normalizing the soap outlet stream concentration with respect to the inlet concentration and plotted against time. The dimensionless concentration therefore ranges from 0, when there is no fatty acid soap in the exit stream, to 1 when the outlet concentration finally reaches that of the inlet. The retention of soap on the fibers can be quantified by performing a soap mass balance :

$$M_p = \frac{N_p \times MW_s}{W} = \frac{Q}{W} \times C_o \times MW_s \times \Delta t - \frac{Q}{W} \times C_o \times MW_s \int \frac{C}{C_o} dt \quad [9]$$

*accumulation*                      *inlet pulse*                      *outlet BTC*

where  $M_p$  is the mass of calcium soap retained within the fiber bed (mg/g),  $N_p$  is the amount of calcium soap retained (mol),  $W$  is the oven dry weight of pulp fibers in the

reactor (g),  $MW_s$  is the molecular weight of the calcium soap (mg/mol),  $C_o$  is the soap concentration in the feed stream (mol/L),  $Q$  is the volumetric flowrate (L/min),  $C$  is the soap concentration of the exiting stream (mol/L), and  $\Delta t$  is the pulse duration.

### 3.4.3 Zeta potential

A Laser-Zee (Penkam) Zeta potential meter was used to measure the charge of the soap particles at different concentrations of  $CaCl_2$  and  $AlCl_3$ . The soap particle concentration was kept constant at 0.164 mmol/L. It should be pointed out that at this concentration the suspension was very blurry, making the measurements somewhat difficult.

### 3.4.4 Electrokinetic analyzer (EKA)

An electrokinetic analyzer (Brookhaven Instruments) was used to measure the streaming potential of the pulp fibers. A Calcium chloride solution is pumped through the wood fiber plug at increasing flowrates (pressure drops), the streaming potential (associated with the electric field established across the plug) is measured with electrodes placed on each end. The zeta potential is then calculated from the Chang-Robertson equation [16].

### 3.4.5 Dynamic light scattering (DLS)

Dynamic light scattering measurements were performed with a Helium-Neon laser (Spectral Physics) at a wavelength of 632.8 nm; and a Photon Correlator Spectrometer BI-2030 (Brookhaven Instruments). The effective diameter of the soap particles was measured

at different calcium chloride concentrations. The soap concentration was kept at 0.16 mmol/L. Three replicates were done for each sample at an angle of detection (observation) of  $90^\circ$ . For a description of the apparatus and principle of operation see [ref. 17].

### **3.4.6 Photodispersion analyzer (PDA)**

A photodispersion analyzer, PDA-2000 (Rank Brothers Ltd.), was used to measure the flocculation rate of a calcium oleate suspension at a  $\text{CaCl}_2$  concentration of 3.8 mmol/L (measured CCC of the soap in suspension). The apparatus is equipped with a flow cell, a high intensity light-emitting diode (led) at 820 nm and a sensitive photodiode (detector). The DC gain was kept at 10 mV, the flow was maintained at 50 mL/min, and the stirring at 100 rpm. This instrument derives the root mean square (rms) value of the fluctuating transmittance signal, which is a sensitive measure of the state of aggregation of the soap suspension [18].

## **3.5 RESULTS**

### **3.5.1 Calcium concentration**

A ten minute pulse of a 0.164 mmol/L calcium oleate suspension was fed to the bed at the inlet of the packed bed at a flowrate of 130 mL/min. The bed was packed with 17.6 g (oven dry) kraft pulp at a 10 % consistency. Calcium chloride was added to a stock soap suspension to yield excess amounts of 0.16, 0.50 and 1.48 mmol/L. The results are shown in Figure 4. For the case where no  $\text{CaCl}_2$  was added, the amount of soap particles retained was negligible. Its BTC superimposed a sucrose (tracer) pulse response which confirms the

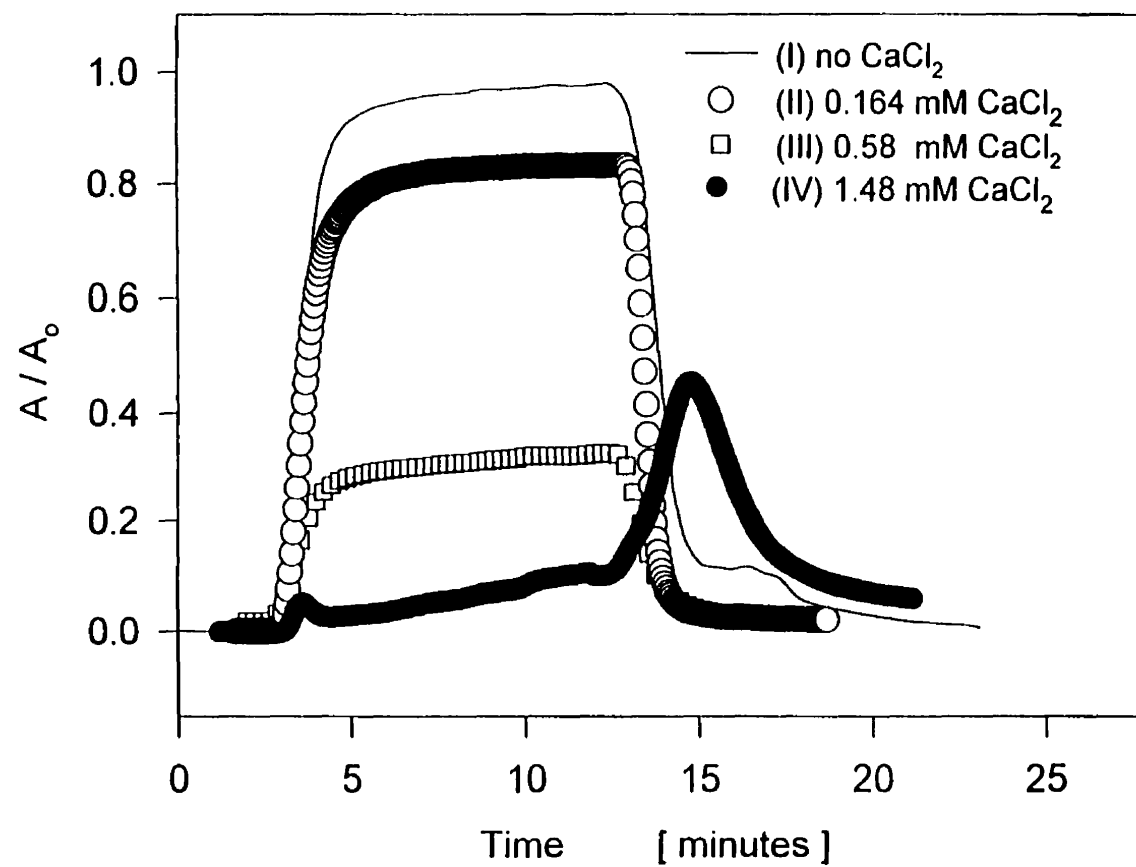


Fig. 4 BTC's of calcium oleate (0.16 mM) at different  $\text{CaCl}_2$  levels.

absence of retention. The retention level increases steadily as the  $\text{CaCl}_2$  concentration is augmented.

The marked differences in shapes between the BTC's at 0.16 and 1.48 mmol/L should be noticed. The BTC for the first case has a smooth shape and a plateau at a normalized exit concentration of 0.80. Under high salt concentration, the soap BTC exhibits a unique behavior with almost complete retention. A small peak is first eluted; although soap is continuously fed to the packed bed, there is a decrease in outlet concentration. There is also a tailing peak at the end of the 10-minute pulse when the feed stream is switched to deionized water. SEM pictures taken of the fiber pad after the ten minute pulse provide evidence of the formation of aggregates (Chapter 2).

### 3.5.2. Aluminum chloride

The experiments described above were carried out this time using  $\text{AlCl}_3$  as the excess electrolyte (in the feed soap suspension) at 0.1 and 2 mmol/L. The results are shown in Figure 5. These BTC's also exhibit the two types of behavior observed in the presence of calcium ion. Unlike the calcium chloride results, the 2 mmol/L BTC does not display a tailing peak at the end of the soap concentration pulse when deionized water replaces the soap stream which implies an irreversible particle retention at this concentration.

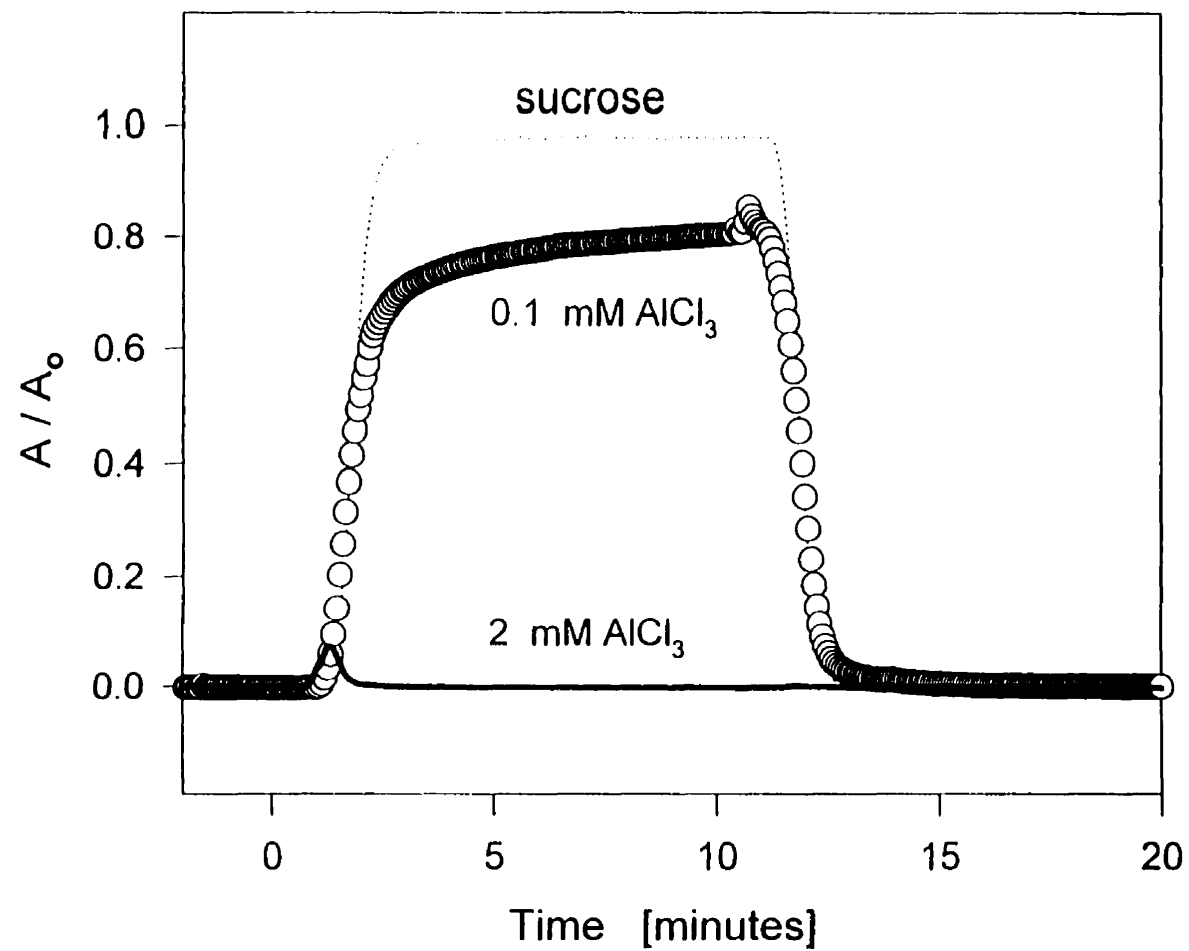


Fig.5 BTC of a 10-minute pulse of calcium oleate containing  $\text{AlCl}_3$



### 3.5.3 Pulp pad consistency

The effect of pulp pad consistency was tested by keeping constant the surface area available for soap deposition. That is, using the same amount of dry pulp (17.6 g ) the consistency of the packing was changed by varying the height (volume) of the pulp suspension in the bed. The results for a ten-minute pulse of a 0.16 mmol/L calcium oleate with 1.48 mmol/L of  $\text{CaCl}_2$  are shown in Figure 6 for a 5, 10, and 15 % consistency. It can be seen that as the bed consistency is increased, the soap retention also increases. All BTC's display a tailing peak. Finally, the BTC's slope following the first eluted peak decreases with increasing consistency (see Figure 7).

### 3.5.4 Feed flowrate

The effect of feed flowrate on soap retention was studied at two levels of excess calcium chloride: 0.16 and 1.48 mmol/L. In both cases the bed consistency was 10% and the feed calcium oleate concentration was 0.16 mmol/L. These results are shown on Figures 8 and 9 respectively. The fact that each concentration level exhibits a very different response to flowrate changes supports the existence of two different retention mechanisms. The BTC's for the soap suspension containing only 0.16 mmol/L excess  $\text{CaCl}_2$  is not a function of the flowrate; the plateau fluctuates between 0.8 and 1, but no general trend is observed. On the other hand, the BTC's for the soap at 1.48 mmol/L  $\text{CaCl}_2$  show a consistent tendency. As the flowrate increases, the soap retention decreases as measured by the area under the BTC. Also the outlet soap concentration slope becomes constant after an initial small peak, and it decreases in magnitude as the flowrate decreases. In general, the tailing peak of this series

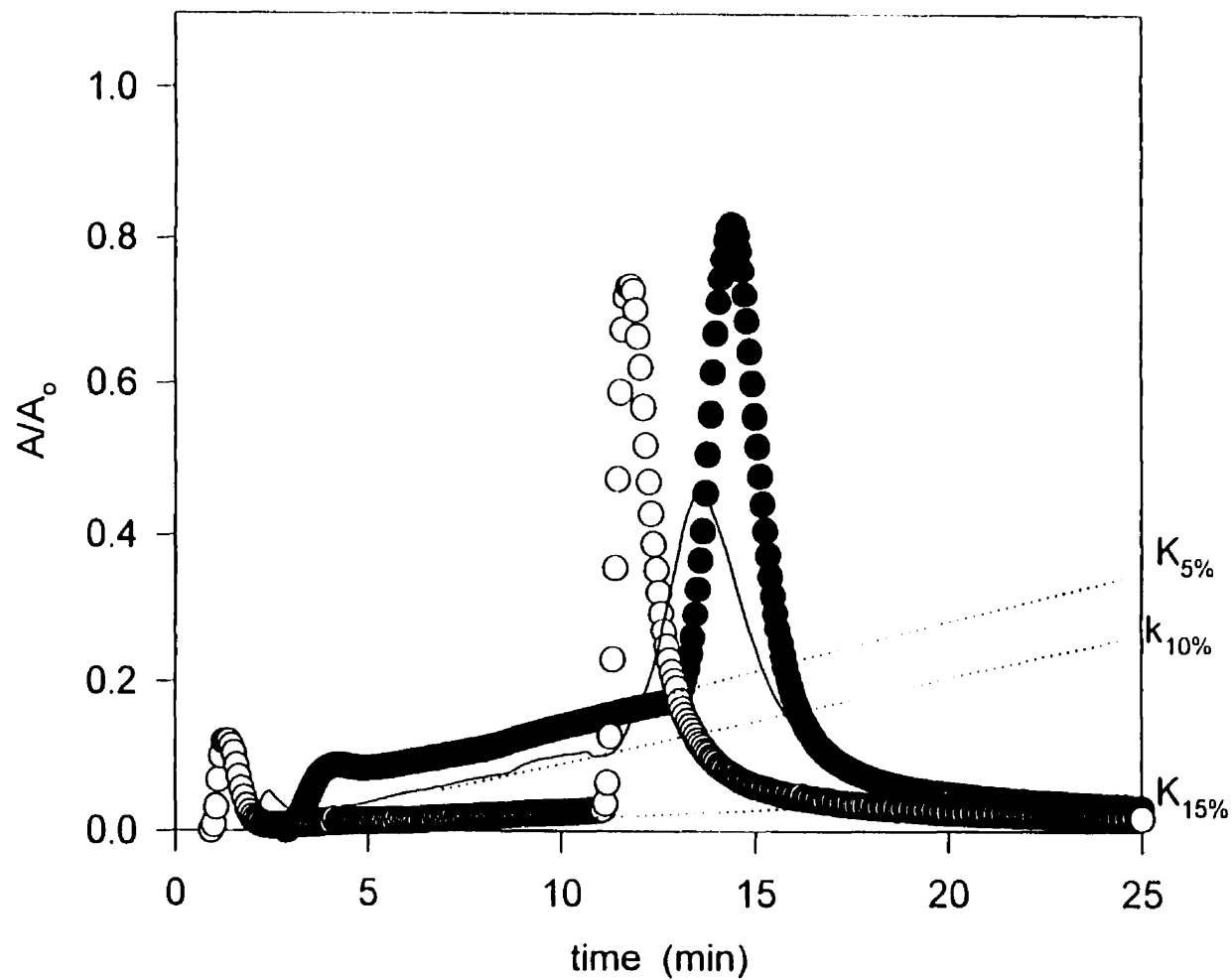


Fig.6 BTC's of calcium oleate as a function of consistency for  $[CaCl_2]=1.48$  mM

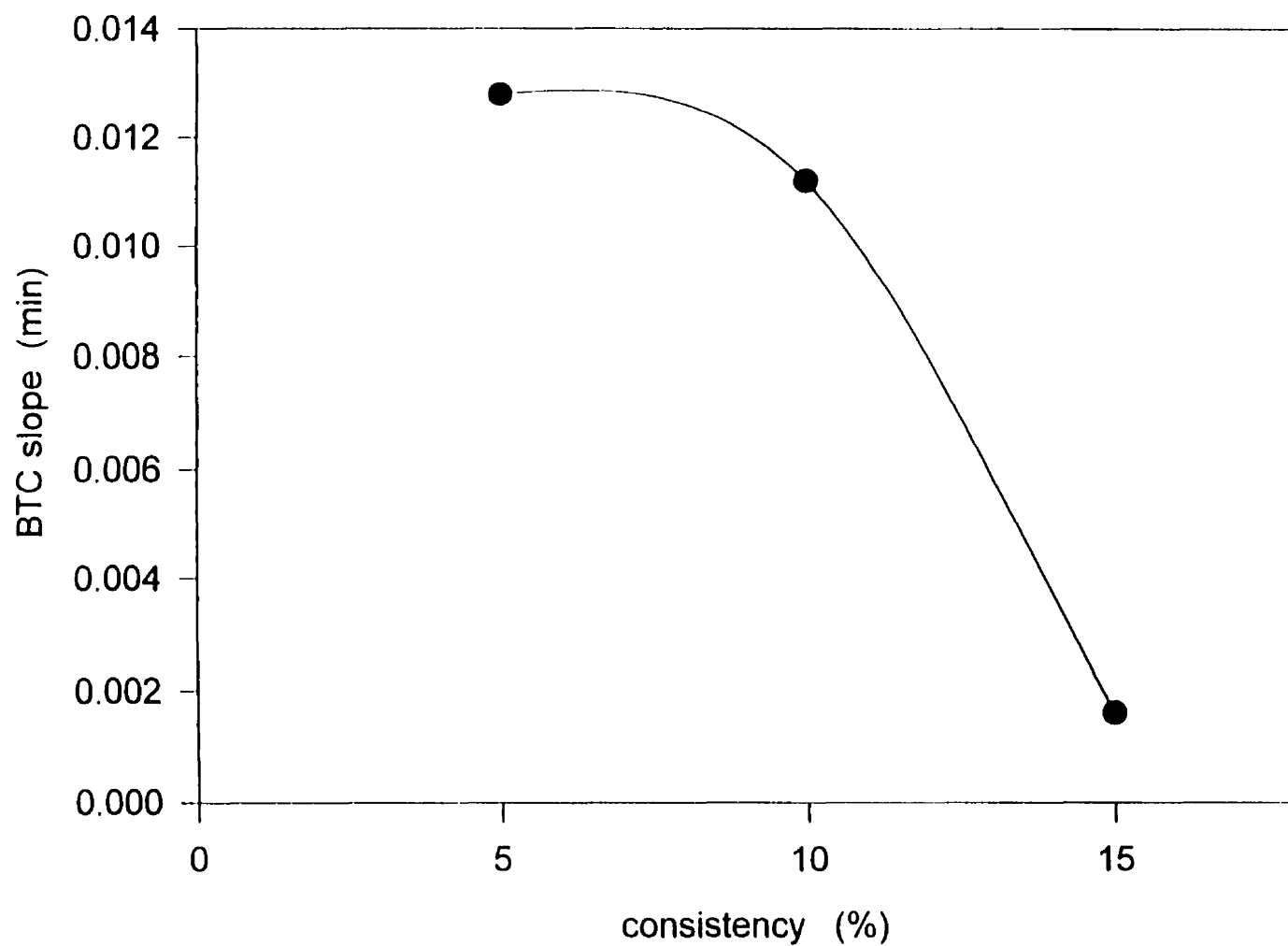


Fig. 7 Effect of consistency on BTC slopes ( $[\text{CaCl}_2]=1.48 \text{ mM}$ ,  $[\text{Ca(oleate)}]=0.16 \text{ mM}$  ).

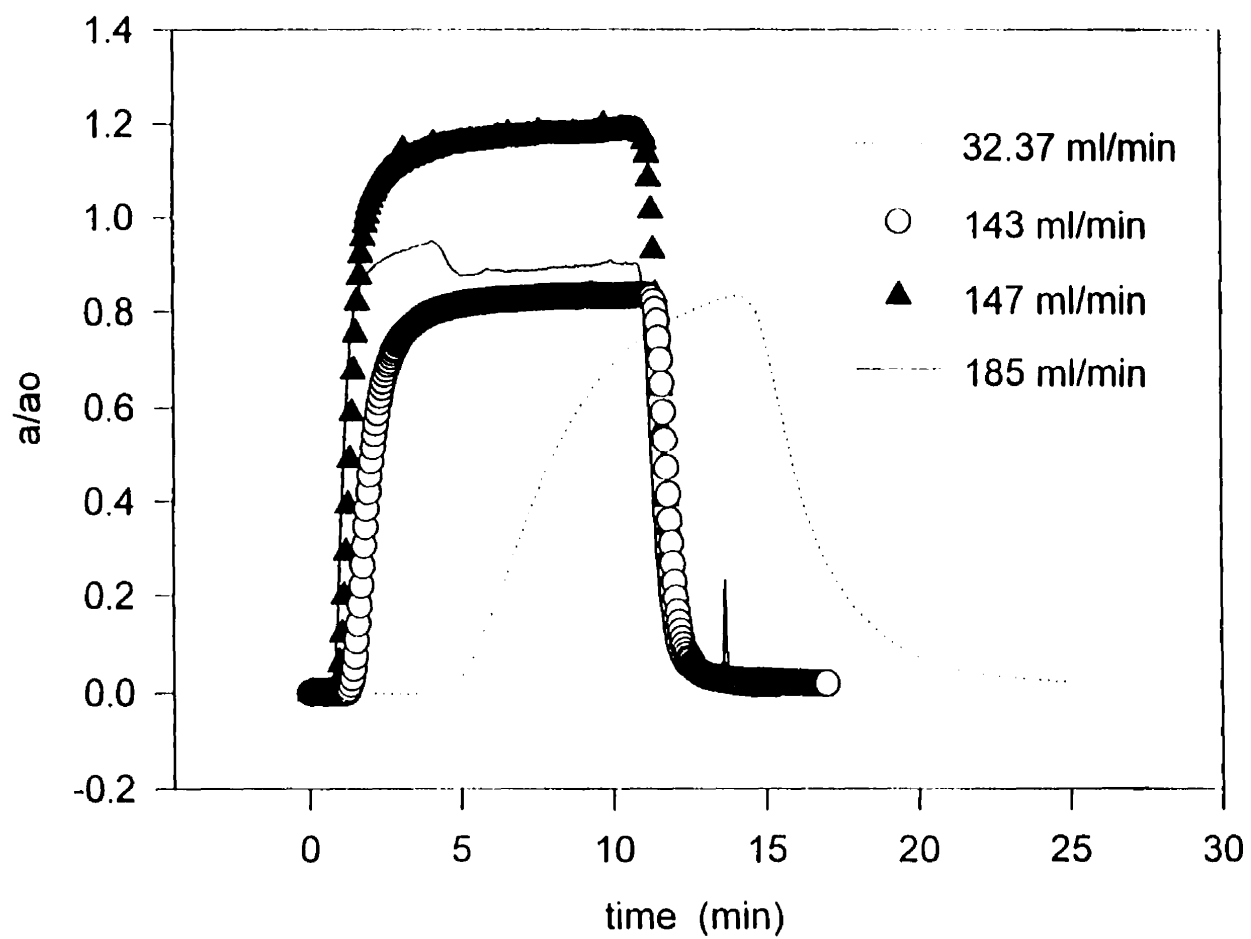


Fig.8 BTCs at different flowrates (  $[\text{CaCl}_2] = 0.16 \text{ mM}$ ,  $0.16 \text{ mM}$  Calcium oleate).

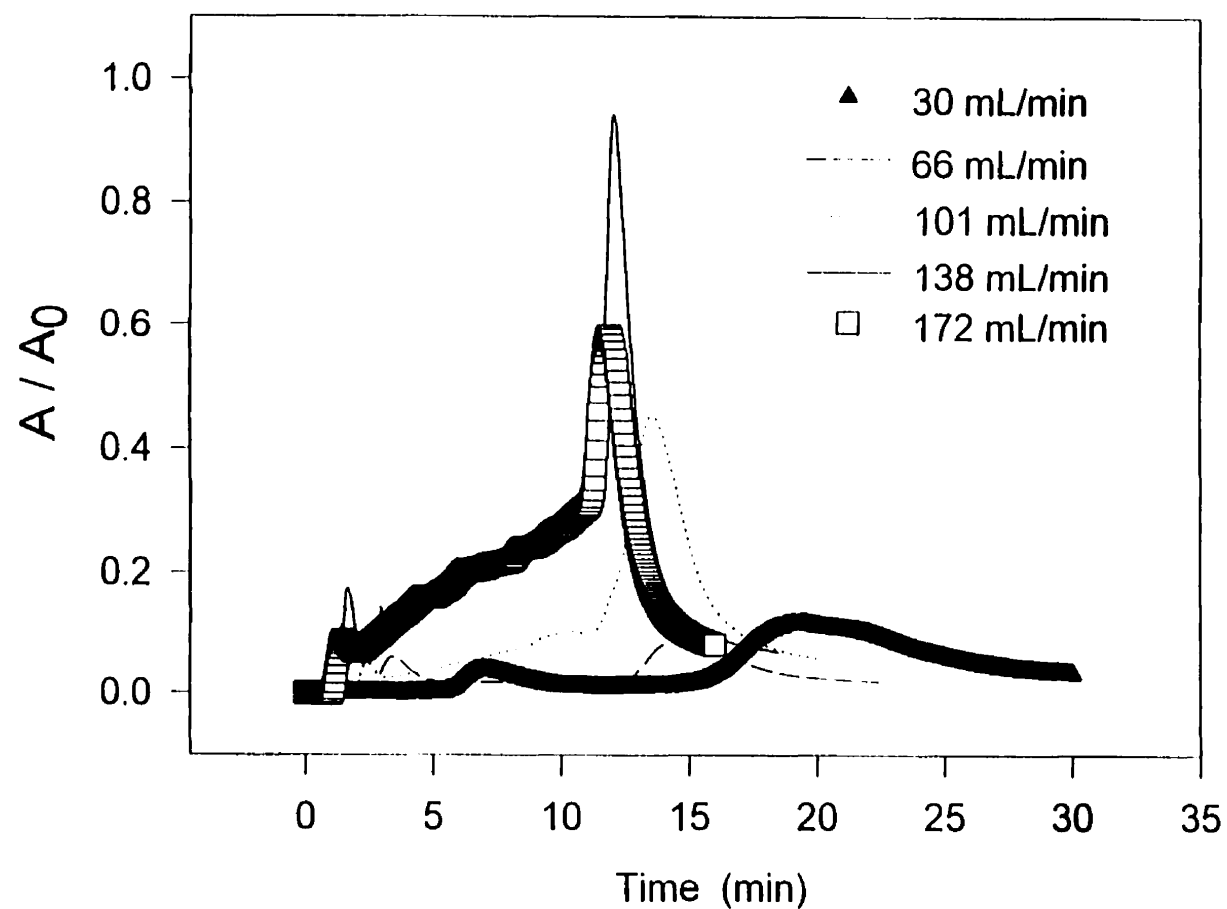


Fig. 9 BTC's at different flowrates ( $[\text{CaCl}_2]=1.48 \text{ mM}$ ,  $0.16 \text{ mM}$  calcium oleate)

also decreases as the flowrate decreases.

### 3.5.5 Fiber Charge

The effect of electrolyte concentration on the equilibrium zeta potential of the fibers was investigated. Figure 10 shows the results obtained for the addition calcium chloride salt.

All experiments were carried out using the same pulp as the one used for our retention studies. The most salient result is that calcium chloride does not reverse the charge sign of the fibers' surface but it consistently neutralizes its charge.

### 3.5.6 Particle charge

The zeta potential of calcium oleate suspensions was measured at different addition levels of calcium chloride. Clearly, the soap particles remain negatively charged (Figure 11). However, the soap suspension containing aluminum chloride undergo charge reversal at a  $\text{AlCl}_3$  concentration around 0.02 mmol/L (Figure 12). At concentrations higher than 0.5 mmol/L, the charge converges to +50 mV.

### 3.5.7 Particle size

The effective diameter of the soap particles was found to be nearly constant for all the calcium chloride concentrations of interest except for the 1.48 mmol/l, probably an indication of the onset of particle coagulation (Figure 13). The results for the soap suspensions with aluminum chloride show a different trend, starting off at 230 nm (no aluminum), rising to 400 nm (at about 0.05 mmol/L) and then levelling off to the initial

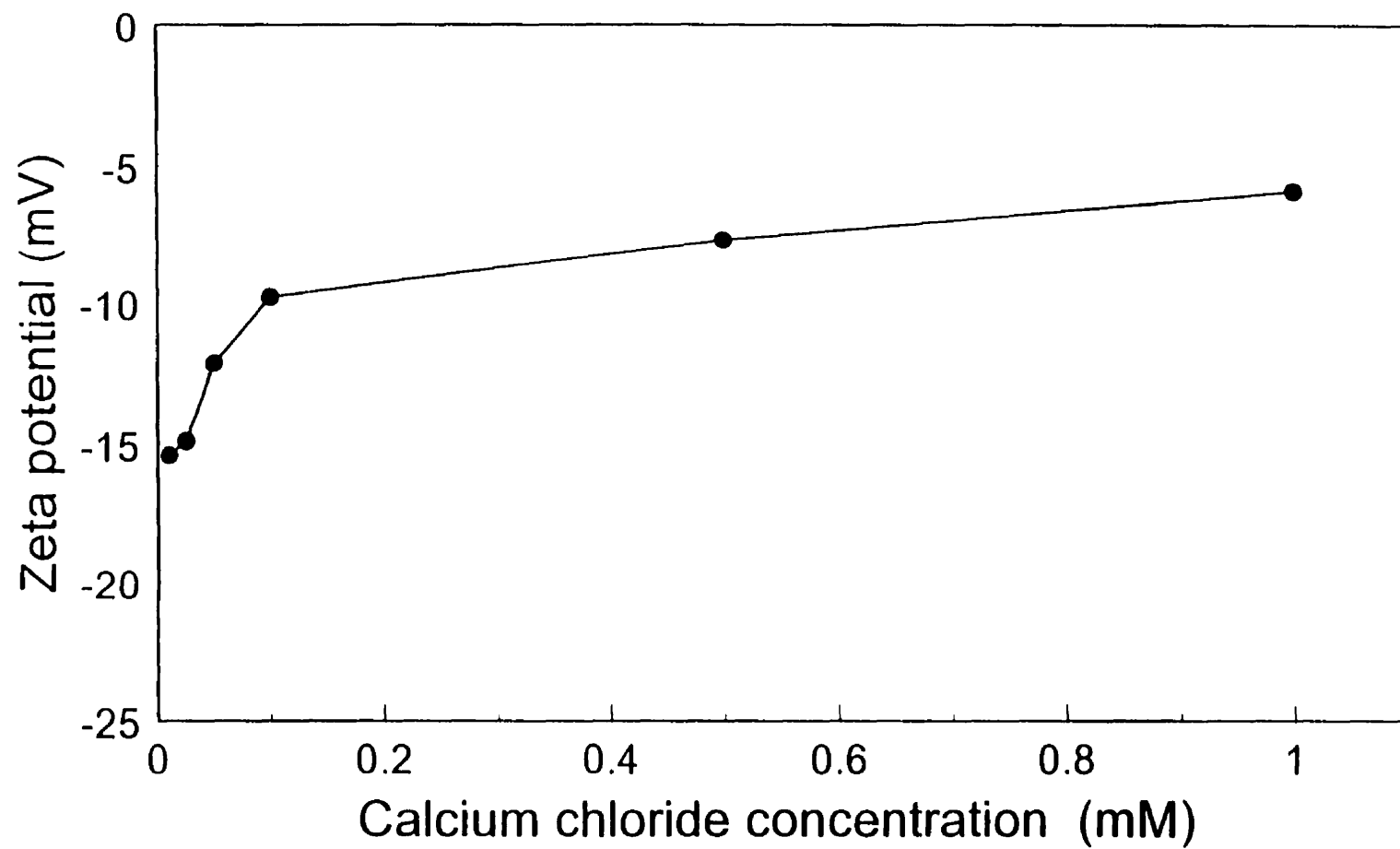


Fig.10 Effect of electrolyte concentration on the zeta potential of pulp fibers

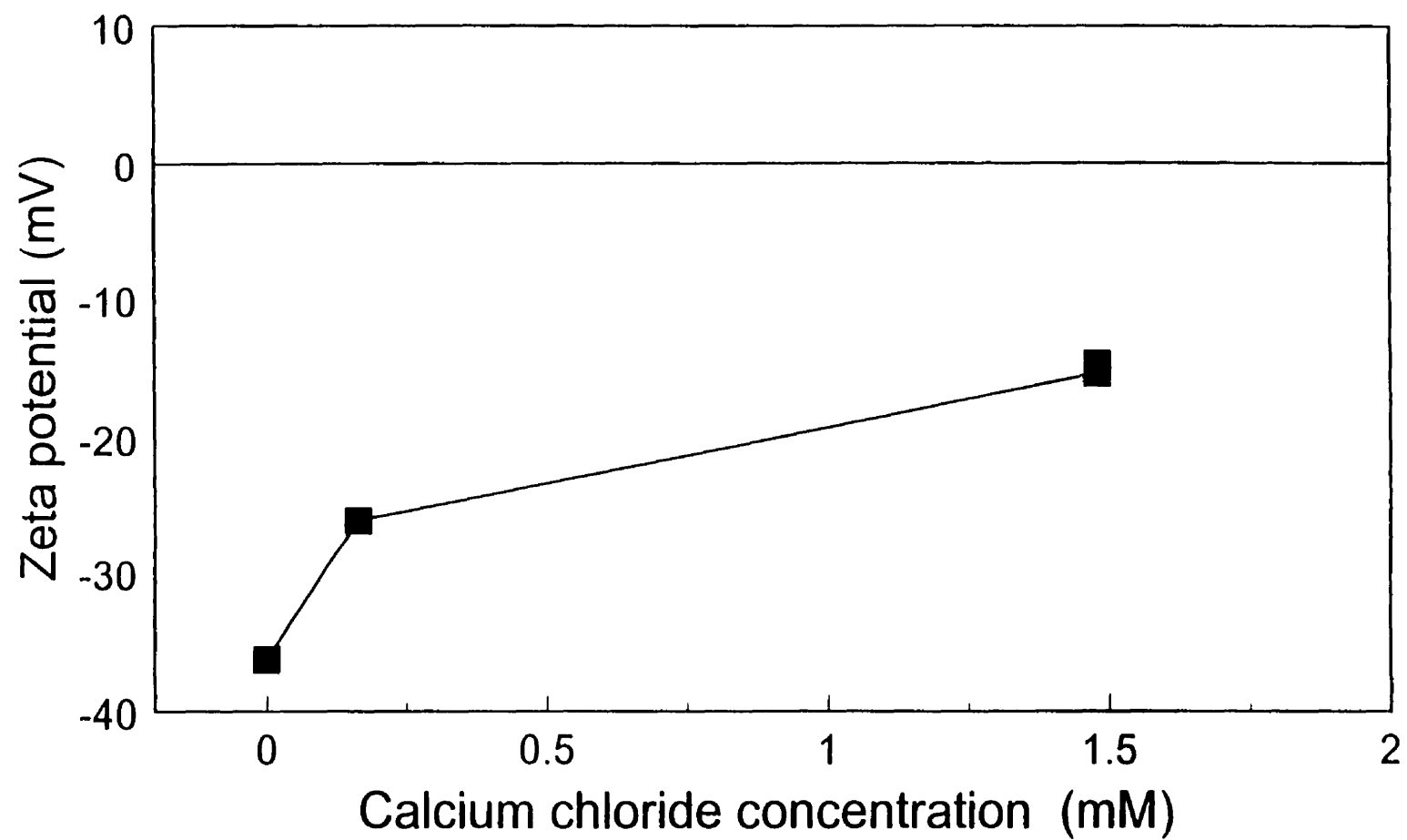


Fig.11 Effect of calcium chloride concentration on the zeta potential of calcium oleate particles.



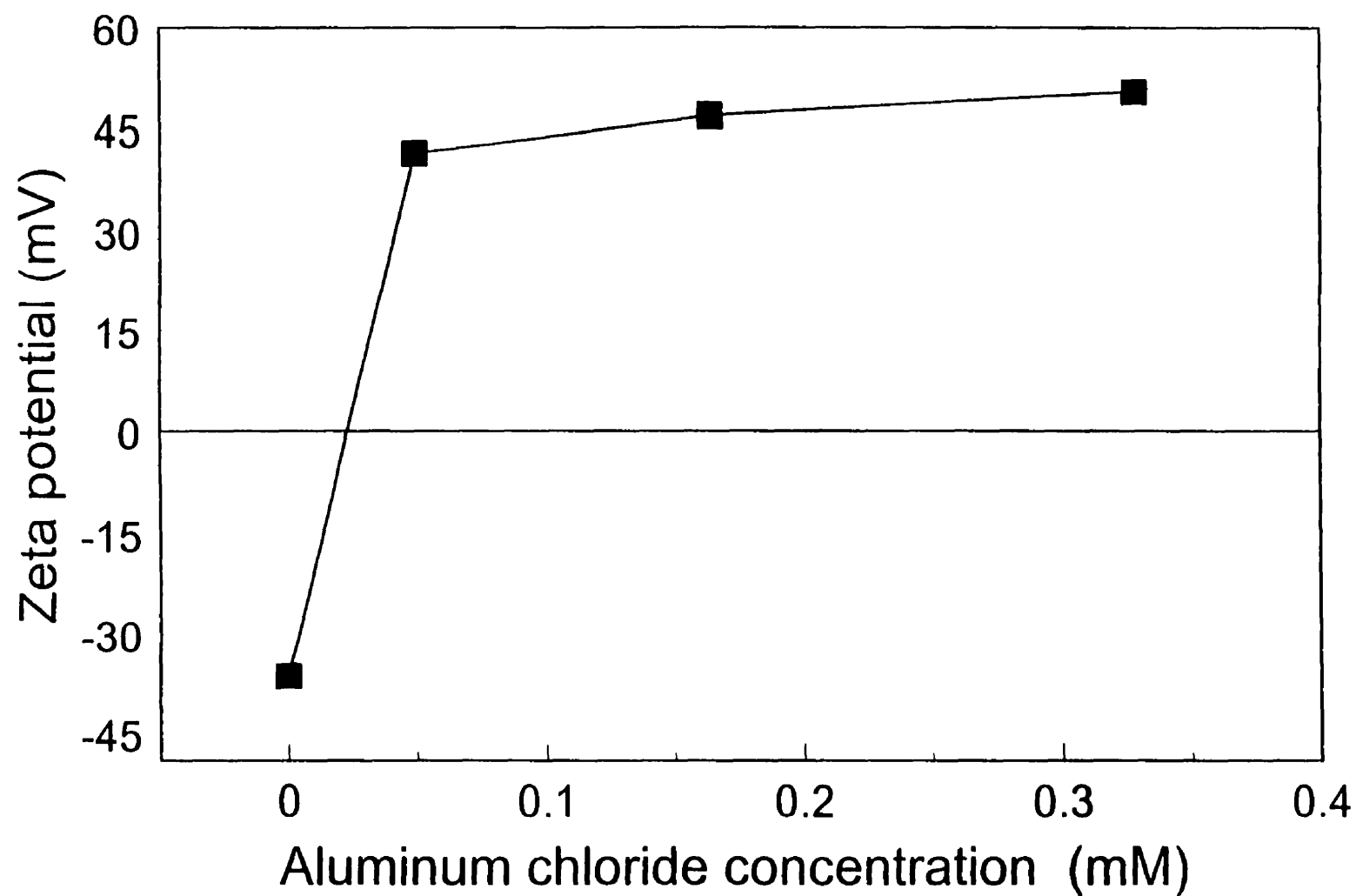


Fig.12 Effect of aluminum chloride concentration on the zeta potential of calcium oleate particles.

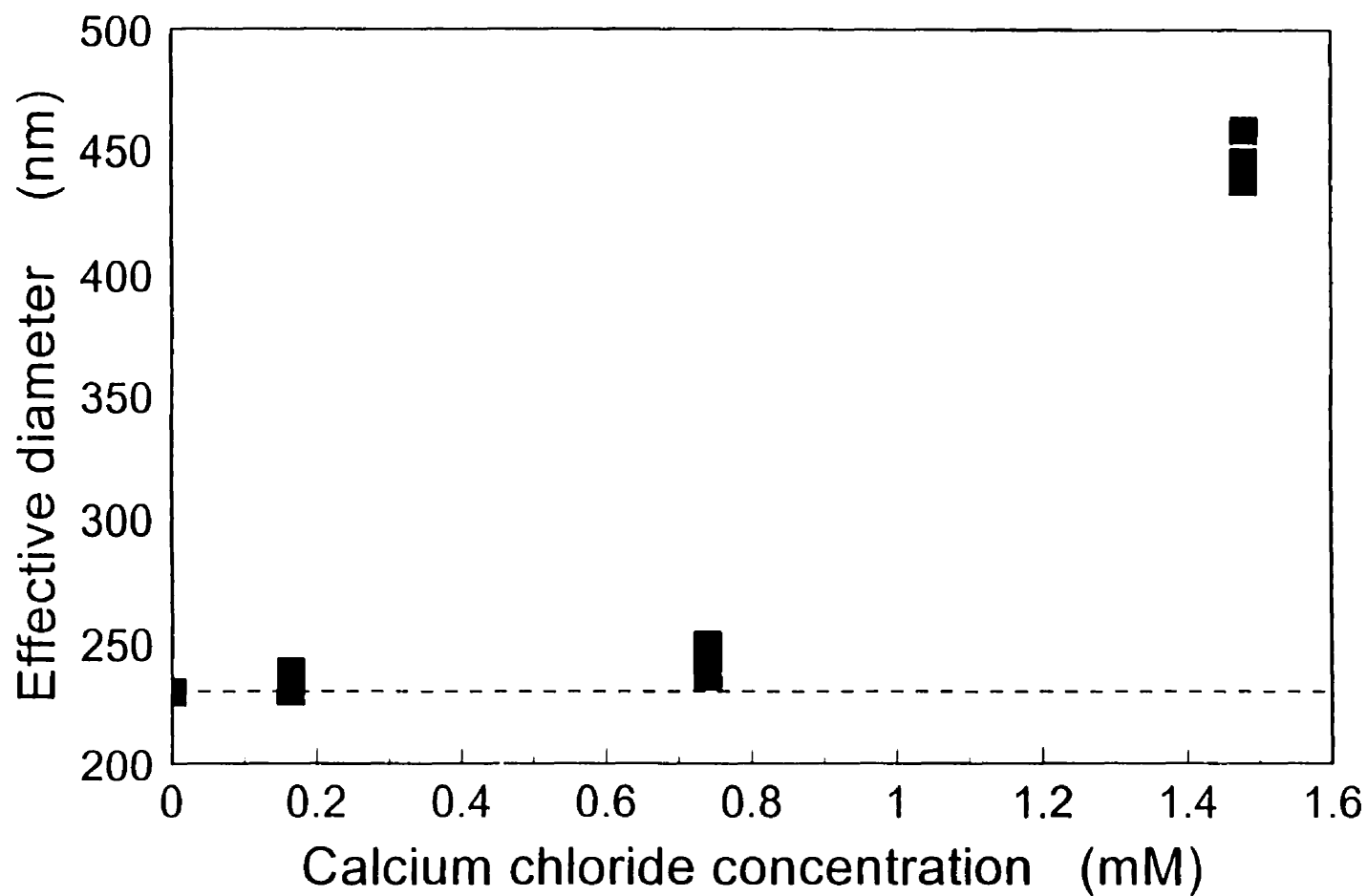


Fig.13 Effect of calcium chloride concentration on the calcium oleate particle diameter measured by DLS (0.164 mM calcium oleate).

particle size (Figure 14).

### 3.5.8 Stability study

The stability plot for calcium oleate at different calcium chloride concentrations was obtained by Harwott and van de Ven [19]. The critical coagulation concentration in free suspension was found to be 3.8 mmol/L  $\text{CaCl}_2$ . At this concentration, we measured the time required to reach steady state coagulation rate with the PDA to be about 6.7 minutes, as shown in Figure 15. This time is measured from the time of electrolyte addition (time=0) to the time passed before the signal reaches 95 % of its final value.

## 3.6 DISCUSSION

### 3.6.1 Particle Suspension Stability

Colloids undergo coagulation at high electrolyte concentrations. As a result, the size distribution changes as a function of the electrolyte concentration. The stability of a suspension can be followed with the size distribution and related to the surface charge of the particles. From Figure 11, the 0.16 mmol/L calcium oleate suspension is stable without excess calcium chloride (-30 mV). As  $\text{CaCl}_2$  is added, some calcium ions adsorb onto the negative particles and screen their electrostatic repulsion (reduced effective charge). This charge neutralization occurs at different rates depending on the salt concentration. At 1.48 mmol/L already, the zeta potential is close to -10 mV and the particle size is 450 nm (Figure 13). As the surface charge decreases, the suspension forms some doublets or triplets.

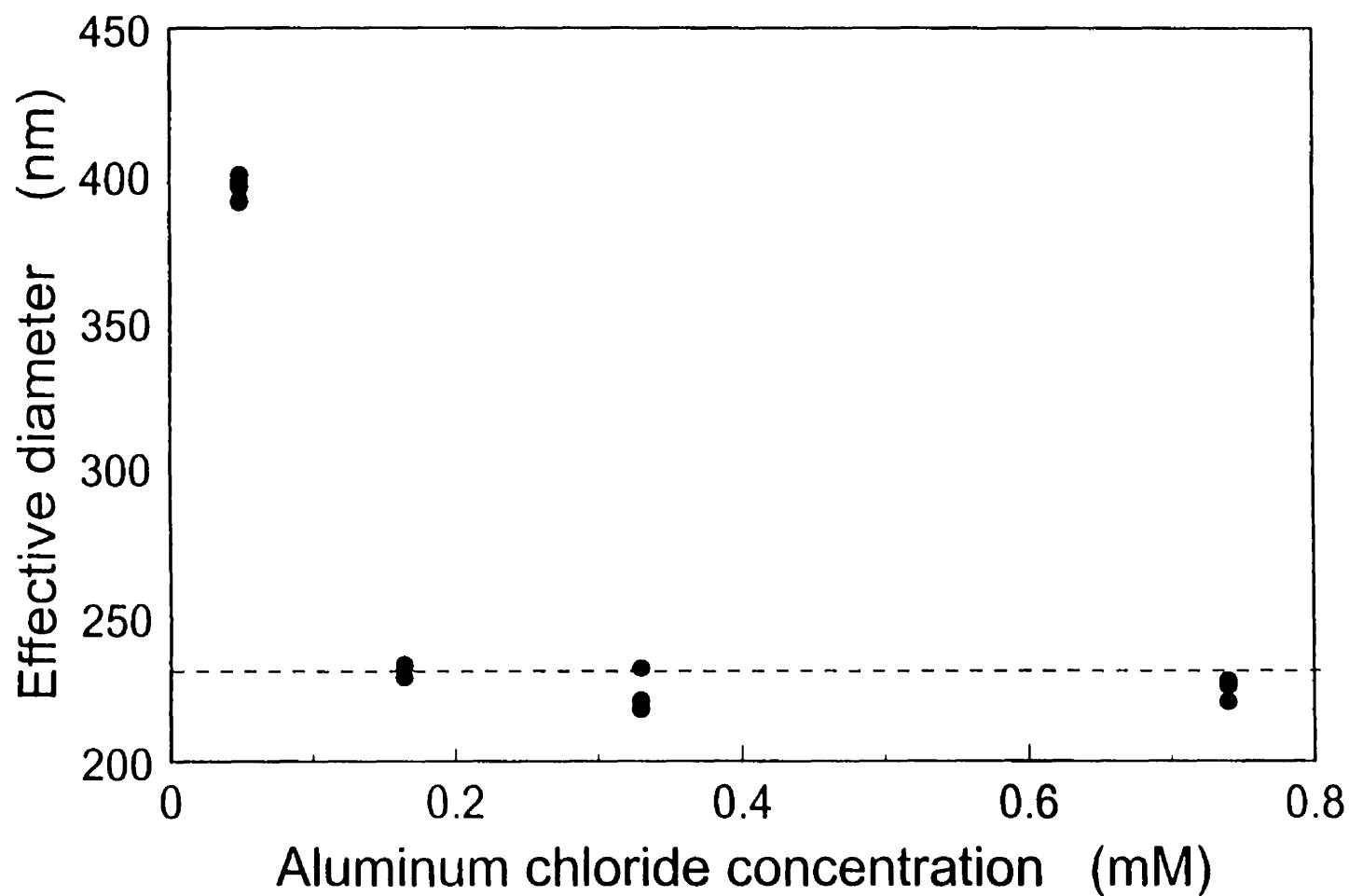


Fig. 14 Effect of aluminum chloride concentration on the calcium oleate particle diameter measured by DLS (0.164 mM calcium oleate).

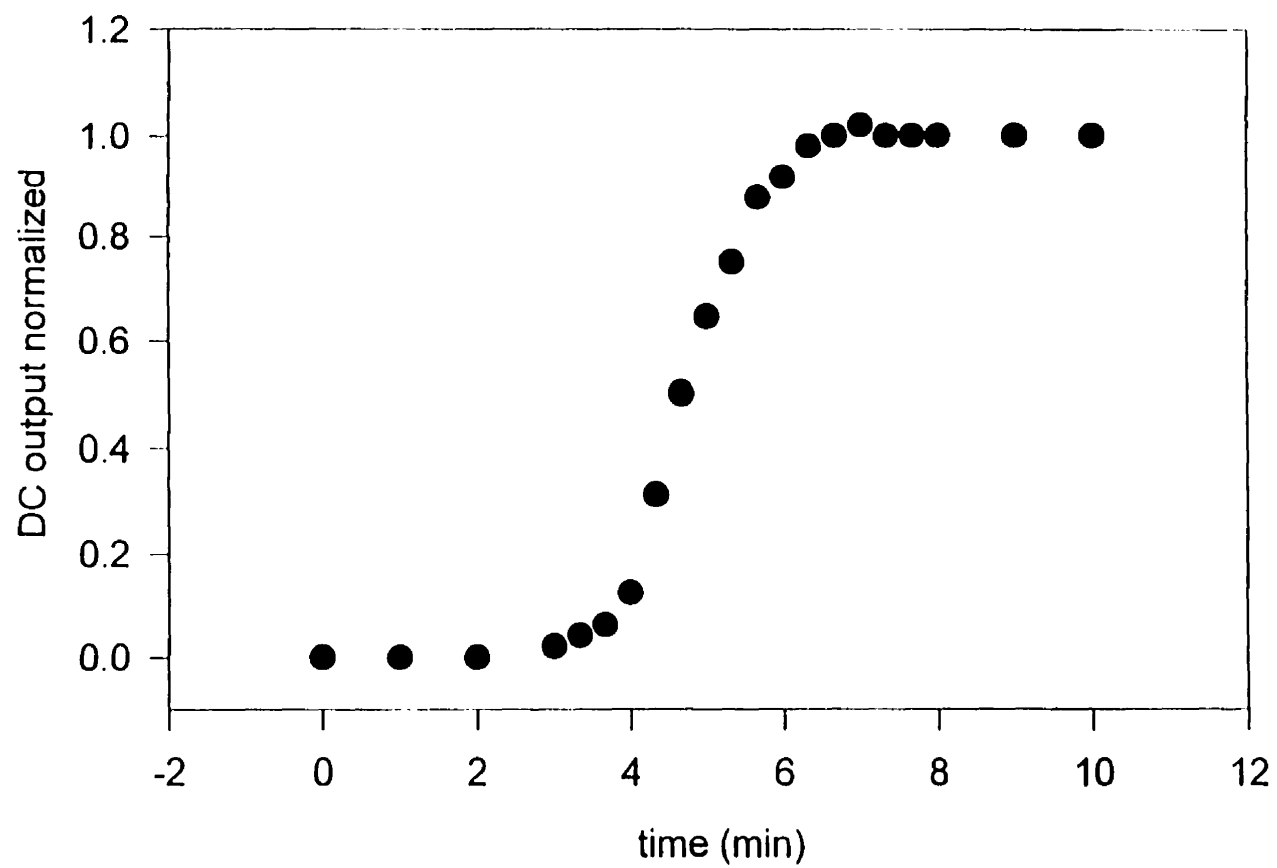


Fig.15 Soap suspension stability (PDA) for 0.16 mM calcium oleate at  $[\text{CaCl}_2]=3.8 \text{ mM}$

When  $\text{AlCl}_3$  is added to the soap suspension, the particle zeta potential is first neutralized (around 0.02 mmol/L) and then its charge reversed to +50 mV at 0.1 mmol/L (Figure 12). This is coupled with an initial particle size increase to 400 nm and followed by a particle size decrease at about 0.05 mmol/L (Figure 14). Thus, at a very low  $\text{AlCl}_3$  concentration (0.02 mmol/L), the particle charge is neutralized by ion adsorption and a limited coagulation occurs. The subsequent increase in zeta potential (restabilization) is likely due to ion-exchange between the free  $\text{Al}^{3+}$  ions and the  $\text{Ca}^{2+}$  ions on the particles' surface. At this point, the soap particles are stable again due to repulsive positive charges on their surface (back to initial particle size). It is expected that upon further addition of  $\text{AlCl}_3$ , coagulation will happen again.

### 3.6.2 The Effect of Electrolyte concentration ( $\text{CaCl}_2$ ) on soap retention

The effect of electrolyte concentration on the soap retention can best be analyzed by following the fraction of soap retained as a function of the salt concentration. The retention isotherm shown in Figure 16, displays two distinct regions which suggests two different mechanisms or kinetics of retention. It is obvious that the individual soap particles are too small (230 nm) to be retained between fibers by mechanical filtration and too large to be entrapped within the fibre wall pores (less than 40 nm). Retention is thus expected to occur only by physisorption on the fibre surface due to charge screening by excess electrolyte.

A similar partial retention pattern is observed with the various BTC's as we increase the  $\text{CaCl}_2$  concentration up to 0.58 mmol/L (Figure 14). The BTC at 1.48 mmol/L displays a different behavior with an almost complete retention. The different shapes of BTC's

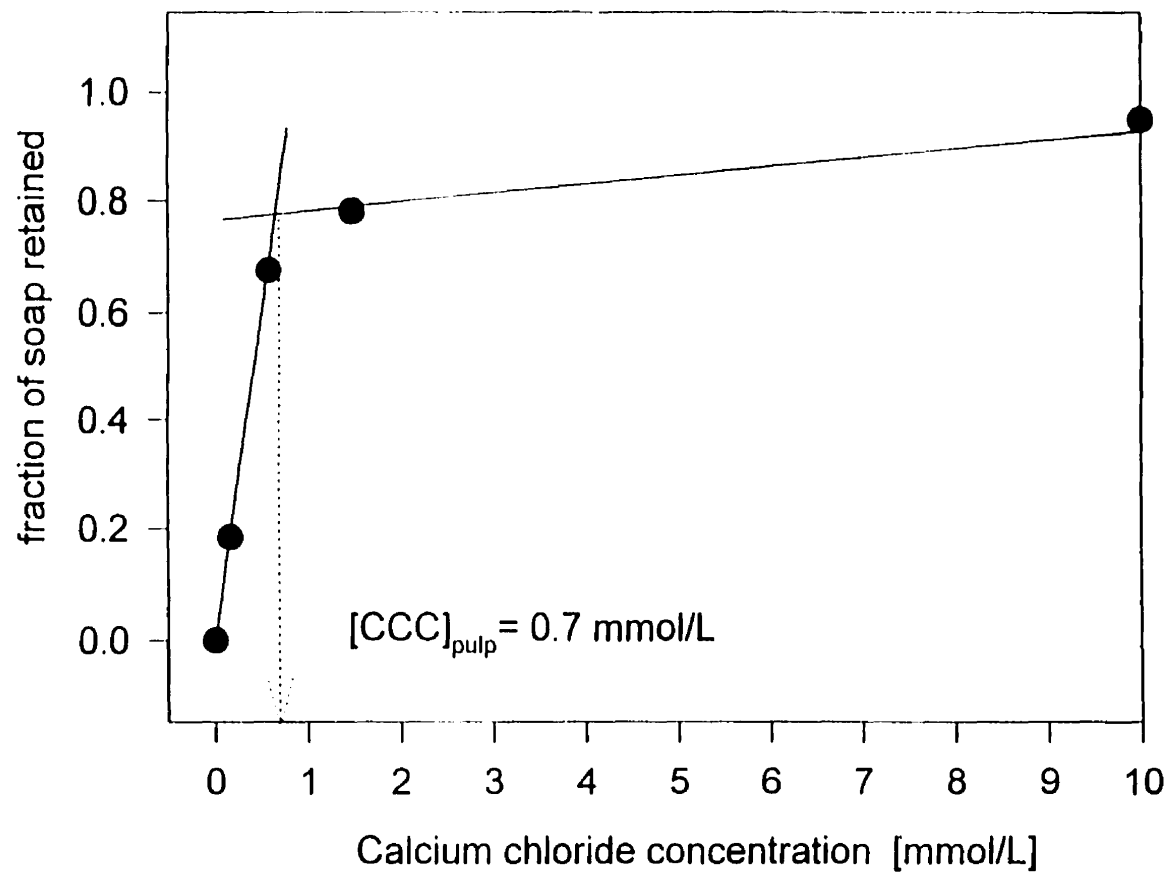


Fig.16 Retention isotherm for 0.16 mM calcium oleate (10-minute pulses).

indicate a transition from one mechanism to another. From the inflection point of the retention isotherm (Figure 16), we obtained a *Critical coagulation concentration* for soap retention within a fibre network,  $CCC_{\text{surface}}$  of 0.7 mmol/l. This concentration is lower than the CCC of 3.8 mmol/L measured without fibers (PDA). The lower magnitude of this critical coagulation could be due to:

- 1) The soap particle concentration is higher near the fiber surface due to osmotic pressure differences. A recent study modelled the particle concentration polarization near membranes [20]. Their results strongly suggest this mechanism (Figure 17).
- 2) High shear conditions are expected inside a porous medium, thus increasing the rate of shear induced coagulation (orthokinetic coagulation) due to improved collision frequencies [7].
- 3) Interference of surface potential between two adjacent particles already deposited on the fibre which may result in spatial locations with higher surface potential [21,22].

Because the above phenomena require at least one bed volume to reach an equilibrium state, the initial small peak eluted could be accounted for this way. Thus, coagulation inside the fibre network can be induced close to the fibre surface at high electrolyte concentrations ( above 0.7 mmol/L ) but only once certain conditions in the fiber bed reach an equilibrium (time  $> \theta_{avg}$ ).



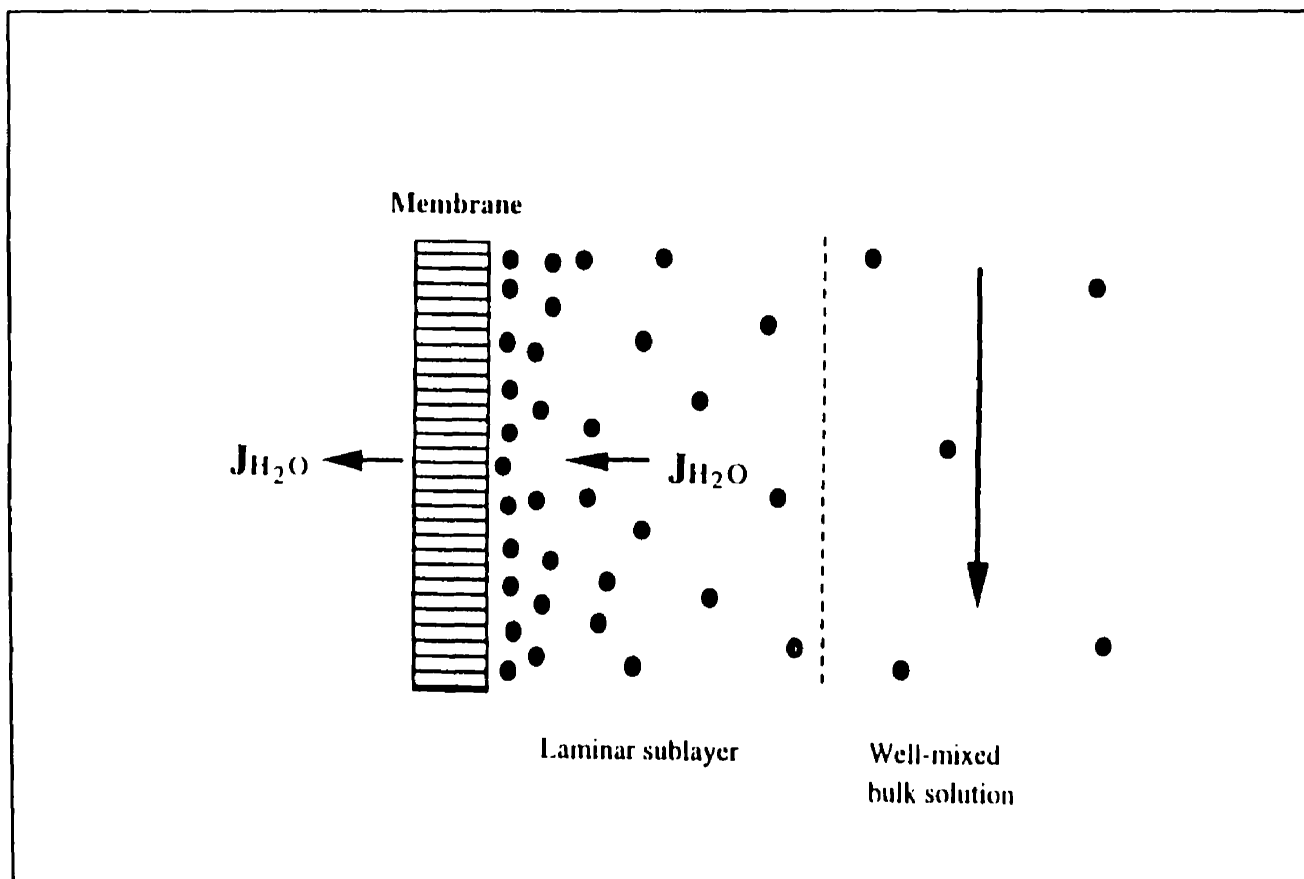


Fig. 17 Particle concentration polarization at the surface of a membrane [20].

The tailing behavior of the BTC when coagulation occurs may be explained by a reversible coagulation due to dilution at the end of the 10-minute soap concentration pulse. The outer particles of the aggregates are mobile. When the water pulse is introduced in the rinsing period, the outer "piled up" particles are the ones mostly affected by the dilution effects (see Figure 18). This could explain why we observe partial irreversible deposition only in some cases. Thus, the tailing peak depends on :

- 1) The rinsing water salt concentration (dilution effects)
- 2) Feed flowrate and bed porosity (shear forces on the aggregates).

The mechanism for soap retention in the presence of calcium chloride involves a combination of several processes that occur simultaneously:

- A. Adsorption of counter-ions onto the anionic fiber surface. Ions in contact with wood fibers undergo ion-exchange until an equilibrium is reached [23].
- B. Deposition of soap particles onto the surface of fibers above a CDC. The zeta potential measurements confirm the screening of negative charges in fibers.
- C. Establishment of a particle concentration gradient close to the fibre surface due to osmotic pressure gradient (could explain a  $CCC_{\text{surface}} < 3.8 \text{ mmol/l}$ ).
- D. Coagulation of particles at the fiber surface at high electrolyte concentration due to

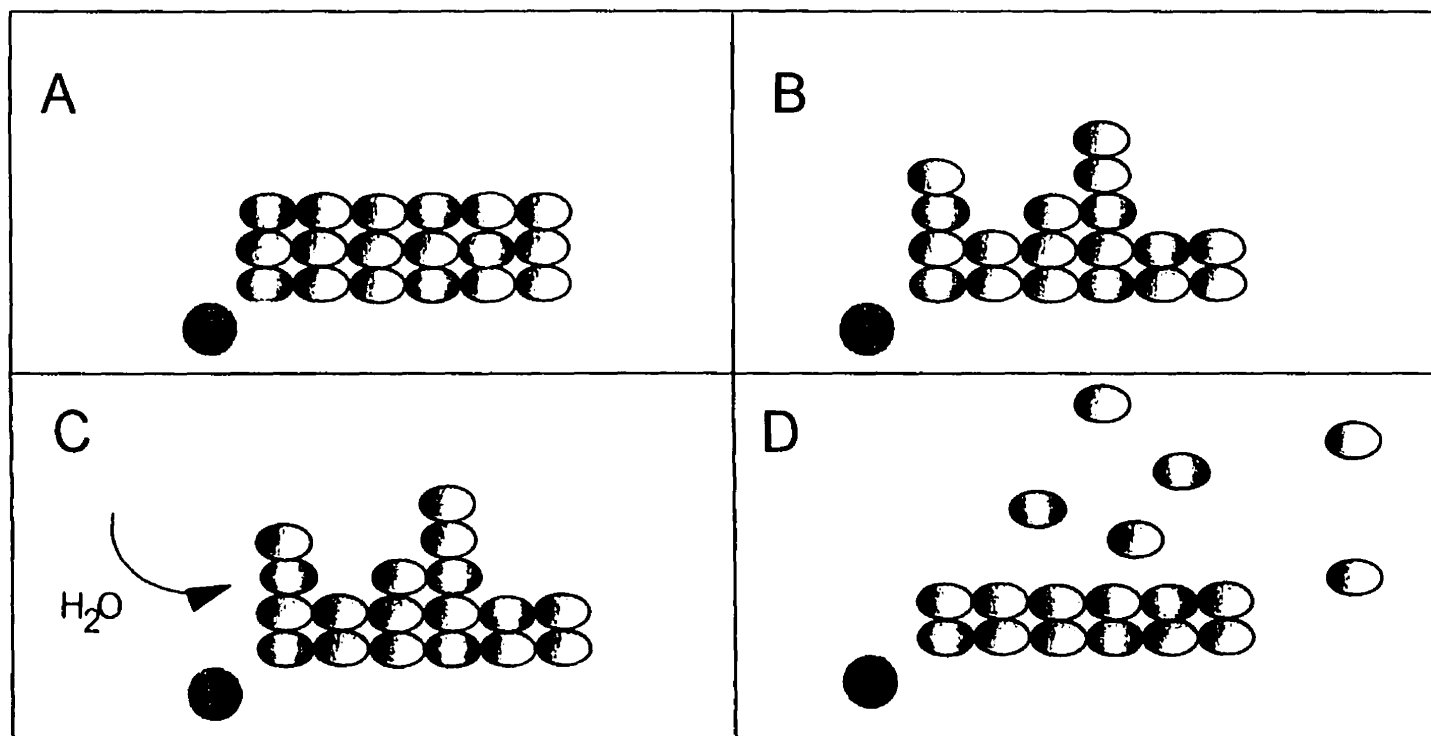


Fig. 18 Schematic of mechanism showing (A,B) piling-up of mobile particles and (C,D) dilution effects causing particle release.

charge neutralization and shear-induced coagulation. Particles deposited in step B may act as “nuclei” for aggregate formation [24].

- E. Re-conformation of particles on outer aggregate layer. The piling up of mobile particles at the outermost layer of soap may also occur [25].
- F. Dissociation of weakly bonded particles exposed to dilution (re-stabilization). Consequently, some particles deposited in step B may be detached. This partially reversible behavior is displayed in all the BTC's for soaps at 1.48 mmol/l  $\text{CaCl}_2$  where retention occurs via coagulation.

It should be noticed that although no extra electrolyte was added to the soap suspension (stoichiometric), NaCl is still present at a concentration of 0.08 mmol/L due to the soap formation stoichiometry. However, sodium does not affect the effective charge (zeta potential) of the fibers or the soap particles to the same extent that calcium or aluminum does.

### **3.6.3 Effect of valency on soap retention**

Soap retention in the presence of  $\text{AlCl}_3$  involves a more complex mechanism. For instance, the soap particles in the suspension containing aluminum undergo charge reversal (Figure 12). The nature of the particles themselves changes as the external layer of Calcium oleate is ion-exchanging with the Aluminum ions (this is seen for instance in rosin sizing

with alum) [28]. In addition, zeta potential measurements support the evidence for complex aluminum ion formation [26,27]. The aluminum precipitates formed could then compete against soap particles for deposition sites.

Thus, the retention kinetics also depend on competing rates of ion exchange (aluminum to fibers), and the rate of particle deposition on the fiber surface. These processes occur simultaneously at specific rates depending on the concentrations of particles, electrolyte and pulp, on pH and temperature.

Figure 5 shows the BTC of ten-minute soap pulses containing 0.10 and 2.0 mmol/L of aluminum chloride. The BTC at 2 mmol/L displays a different behavior with practically complete retention. The different shape of BTCs indicates a transition from a deposition mechanism to surface coagulation. The irreversible nature of soap retention on the fibers, indicated by the missing tailing peak (2 mmol/L) is an indication of strong electrostatic forces keeping the particle aggregates on the surface. This behavior is typical of heterogeneous coagulation [29]. According to the Schultze-Hardy rule, the CCC for the  $\text{AlCl}_3$  in the presence of fibers should be about 0.07 mmol/L. However, the 0.1 mmol/l feed soap suspension does not display this type of behavior. This could be because the rule assumes a symmetric electrolyte which is not the case for  $\text{AlCl}_3$ . Furthermore, the pulp is mainly under its calcium form and not the aluminum form. In any case, it is well known that Aluminum can complex and hydrolyze into many compounds. Therefore, certain conclusions are difficult.

The mechanism for soap retention with Aluminum chloride is different from that in the presence of calcium. It still results from a balance of several process kinetics:

- A. Adsorption of free/excess counterions (aluminum) onto the anionic fiber surface. This step could be in competition with the ion-exchange between free cations ( $Al^{+3}$ ) and bound cations ( $Ca^{+2}$ ) of the soap particles which renders the soap particles positively charged.
- B. Deposition of soap particles onto the surface of fibers due to heterocoagulation. This step occurs spontaneously (net attractive forces). Thus, the particle-fiber bonds are very strong. This type of particle deposition results in a uniform surface coverage.
- C. The first layer of soap deposited renders the surface hydrophobic which has higher affinity for the “free” hydrophobic particles. This enhances the retention of a second soap particle layer. Rogan’s experimental work on “cooperative adsorption” support this mechanism [30]. Furthermore, the high electrolyte concentration screens the electrostatic repulsion between particles.
- D. Dilution will not easily detach the first deposited layer. This explains the irreversible nature of retention.

#### 3.6.4 Feed flowrate and consistency

When no  $CaCl_2$  is added to the feed suspension, the initial slope of the BTC is virtually infinite (considering a small axial dispersion) and a plateau is soon reached. The soap concentration at the outlet rapidly reaches that of the inlet. When a 0.16 mmol/L  $CaCl_2$

are added to the feed suspension, the outlet concentration rapidly reaches a plateau: no coagulation occurs, irrespectively of the feed flowrate (Figure 8).

A different BTC behavior is observed at high salt concentration as function of the flowrate (Figure 9). For a constant consistency, the retention of soap seems to increase at lower flowrates as indicated by the slope decrease. Figure 19 shows a plot of the BTC's as a function of the residence time (corresponding to each flowrate). The BTC slopes decay exponentially as a function of the residence time. At a residence time of 6.4 minutes (30 mL/min), the slope of the BTC becomes zero. This means that all the soap introduced (at that flowrate) accumulates inside the fiber network. Thus, to reach complete retention, a sufficiently long contact time (long residence time) is necessary.

At high flowrates, the particles are fed to the packed bed faster than they can be captured, thus a lower retention efficiency would be expected. Figure 20 confirms this explanation. It shows the percentage of soap introduced that stays in the bed (calculated using equation [9]). The percentage of soap retained increases as the flowrate decreases until a residence time of 6.4 minutes where all of the soap is retained. We define 6.4 minutes as the Critical Residence Time (CRT) at 10 % consistency and 0.16 mmol/L calcium oleate. The CRT can be viewed as the time required for complete coagulation.

From the PDA measurements, it takes 6.7 minutes to reach steady state for a 0.16 mmol/L soap suspension at the CCC of 3.8 mmol/L  $\text{CaCl}_2$ . Further investigation is required to determine whether a logical correlation links these critical times or not. In addition, retention in the packed bed at high electrolyte concentration does not necessarily occur only by coagulation. Deposition of individual soap particles may occur simultaneously.

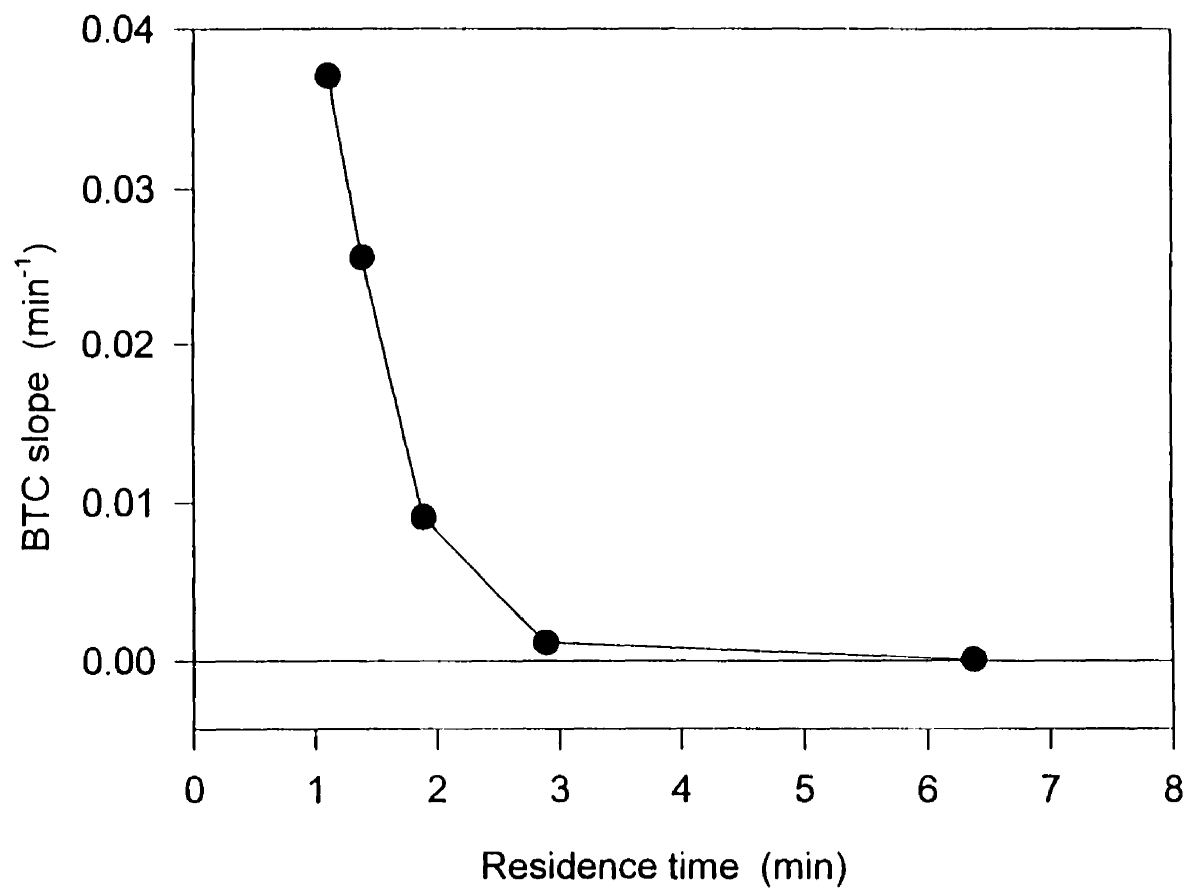


Fig. 19 Initial response slope as a function of residence time (1.48 mM  $\text{CaCl}_2$  ).



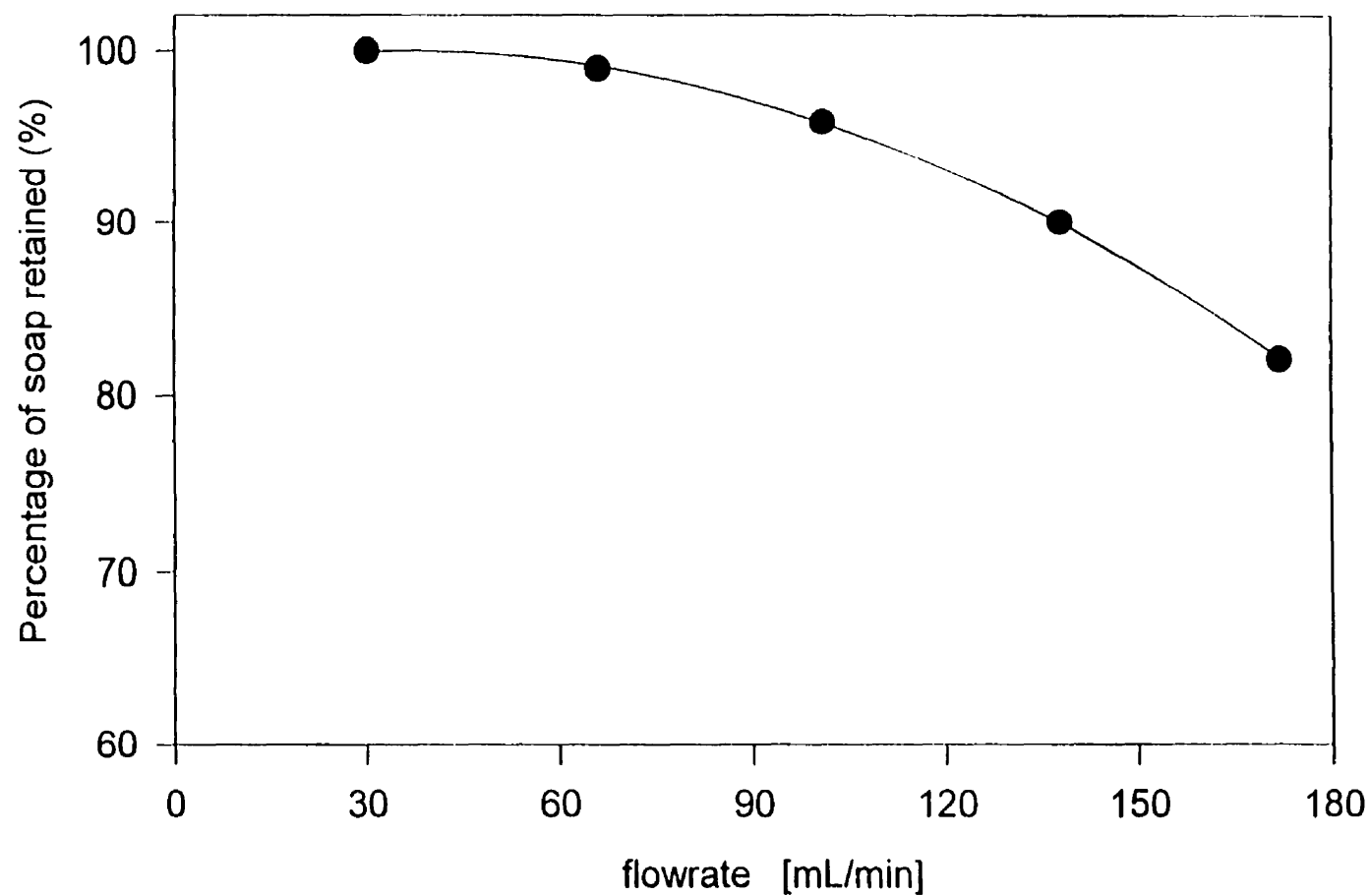


Fig.20 Effect of flowrate on percentage of soap retained

Retention due to coagulation phenomena may depend on the shear rate (orthokinetic coagulation) or on particle diffusion (perikinetic coagulation). Orthokinetic coagulation is the mechanism of particle aggregation brought about by high collision frequencies [18]. The rate of coagulation is expected to increase as the flowrate increases due to higher shear rates. Therefore, in order to determine if soap retention at high  $\text{CaCl}_2$  concentration occurs via orthokinetic coagulation, it is necessary to obtain measure the rate of soap retention at different flowrates. For our system, the rate of retention (mmol/min) can be calculated from:

$$\text{Rate of retention}_i = \text{soap molar flow (inlet)}_i - \text{soap molar flow (outlet)}_i \quad [10]$$

The soap molar flowrate (inlet) is known from the feed conditions. The number of moles of soap exiting the bed can be obtained from the BTC's ( $C/C_o * C_o * Q_i * t_i$ ) and are plotted as function of time for each flowrate  $i$  (Figure 21). Using the initial slopes (units mmol/min) as an approximation for the soap molar flow (outlet), the rate of retention can be estimated from equation [10]. As shown in Table III, the rate of retention increases at higher flowrates. The resulting rates are shown in Figure 22. These results suggest that the retention mode is by orthokinetic coagulation below 101 mL/min (where the retention rate increases with increasing flowrates).

It would be expected that the rate of retention would continue increasing with flowrate. However, Figure 22 shows that the rate of retention reaches a maximum above 101 mL/min. This is probably because for particle coagulation to occur, there should be enough calcium chloride available in the system to reach the  $\text{CCC}_{\text{surface}}$ . It is possible that at the

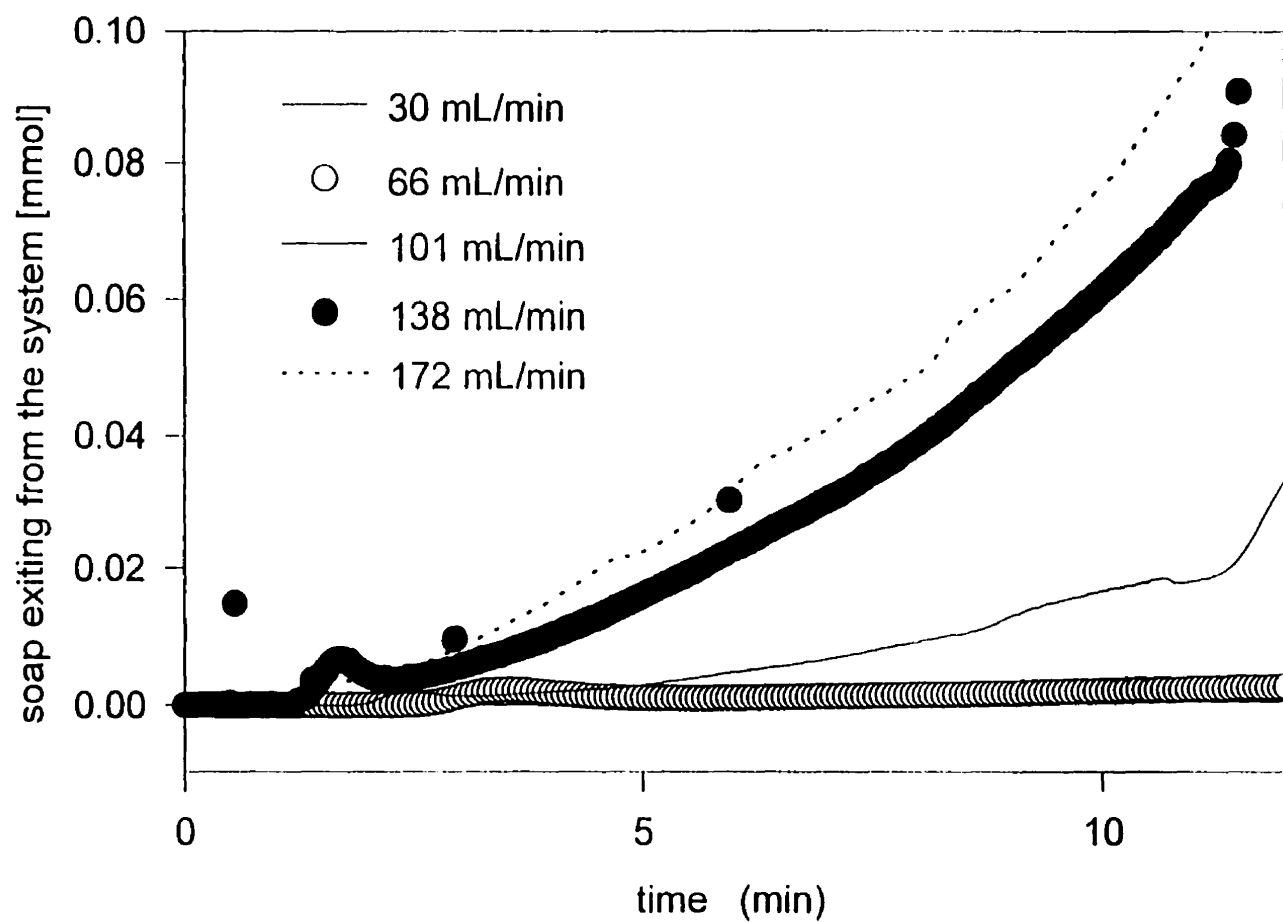


Fig.21 Number of moles exiting from the packed bed at time  $t$  as a function of flowrate

TABLE III			
RATE OF SOAP RETENTION AT DIFFERENT FLOWRATES			
FLOWRATE	INLET SOAP FLOWRATE (From feed conditions)	OUTLET SOAP FLOWRATE (From slope of Fig. 21)	RATE OF SOAP RETENTION
[mL/min]	[mmol/min]	[mmol/min]	[mmol/min]
30	0.005	0	0.005
66	0.011	2.5 e(-4)	0.011
101	0.016	2.4 e(-3)	0.014
138	0.023	7.4 e(-3)	0.015
172	0.028	1.3 e(-2)	0.015

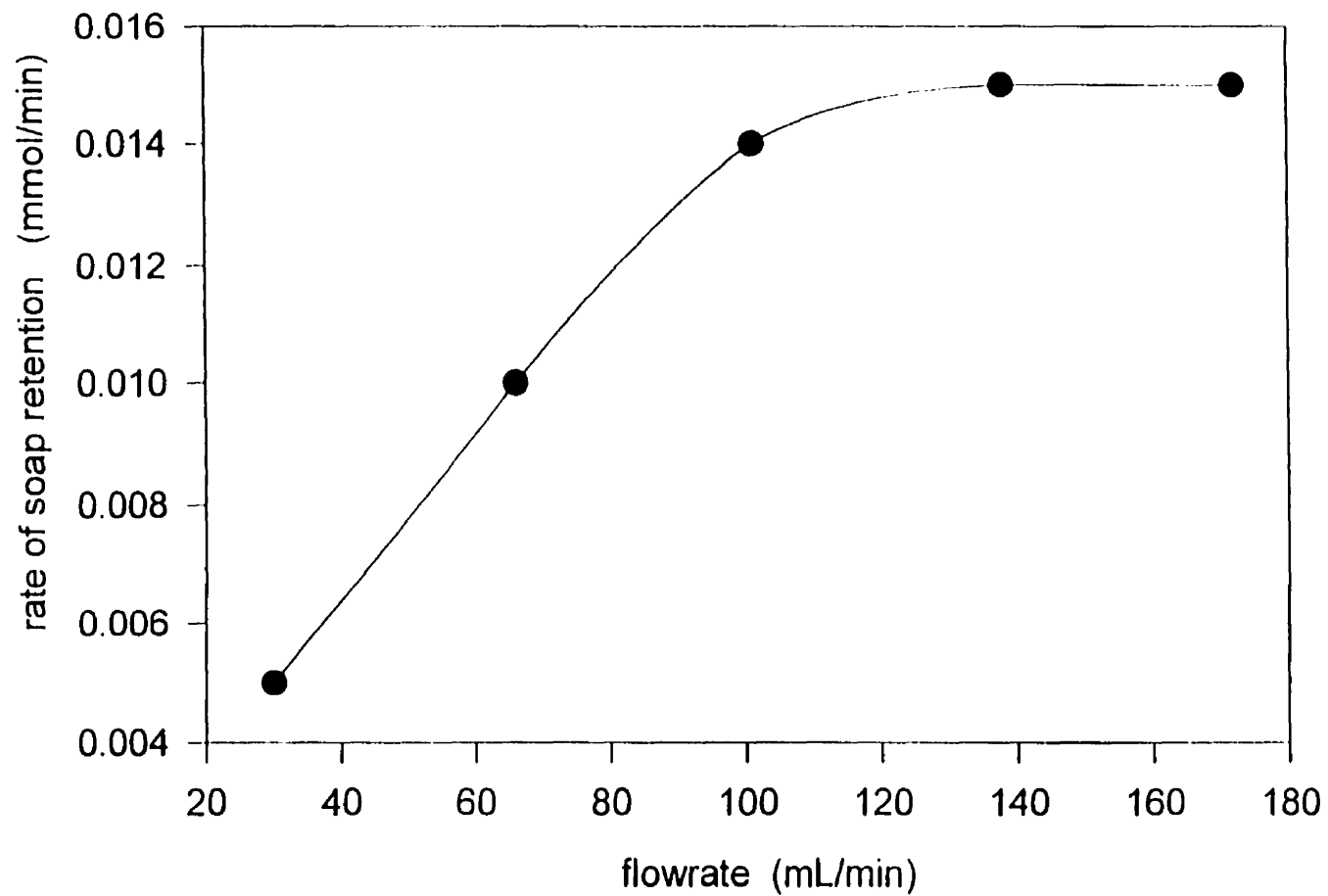


Fig.22 Rate of soap retention as a function of flowrate for 0.16 mM calcium oleate.

higher flowrates, the calcium ions in the feed soap suspension do not have enough time to diffuse to the fiber surface. In other words, at the higher flowrates, the particle collision frequency is high, but there is not enough electrolyte available to screen repulsive electrostatic forces (see Figure 21 for schematic explanation). Therefore, 101 ml/L is a transition flowrate between two regimes of coagulation.

From these results, it is evident that a transport equation for the electrolyte salt component (whose diffusion coefficient is not negligible) should be included in the mathematical model of soap retention.

A similar trend is expected for the retention behavior as a function of consistency. As the pulp consistency increases, higher shear rates are expected, thus increased retention levels due to orthokinetic coagulation. Also, the residence time inside the bed increases as the consistency decreases. Figure 6 shows the BTC's at 5, 10 and 15 % consistencies. The initial slopes of the BTC's were calculated and are shown in Figure 7. The percentage of soap retained in the bed is shown in Figure 23 (percentage is defined as the ratio between total retained and total introduced soap, calculated from the area under the BTC's). As the consistency increases, more soap is retained.

Although the residence time is longer at 5% consistency, retention percentage is the smallest and is weakly dependent on the consistency. Between 10 and 15 % consistency, however, the percentage of soap retention is a strong function of the consistency (shear rates) which suggests, an orthokinetic coagulation mechanism at high pulp consistency. The 10 % consistency could mark the transition between orthokinetic and perikinetic coagulation.

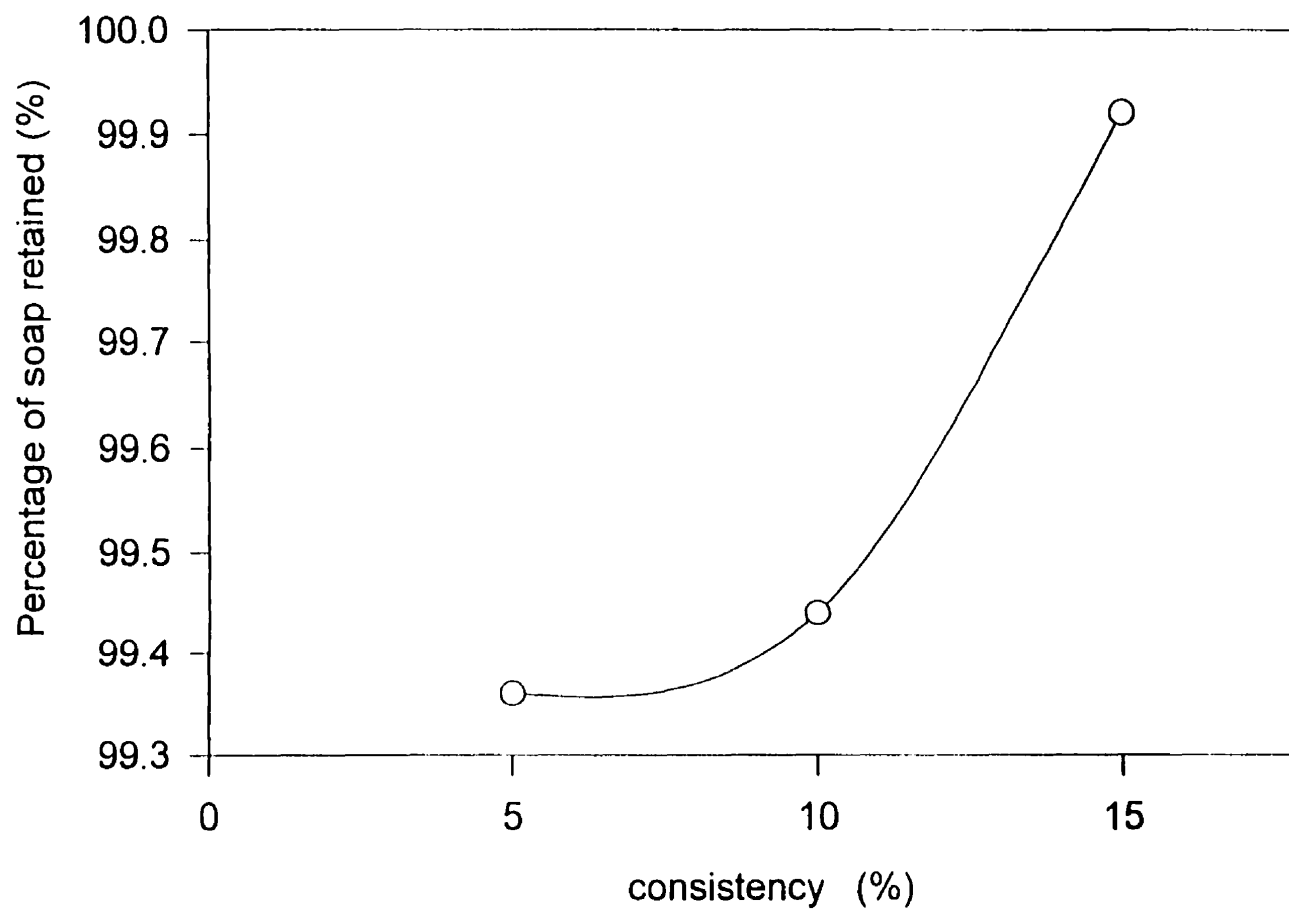


Fig.23 Effect of consistency on percentage of soap retained

### 3.6.5 Mathematical model parameters

Figures 1 through 3 show the effect of the model parameters  $P_1$ ,  $P_2$  and  $P_3$  on particle retention in packed beds of pulp fibers derived from a mathematical simulation. A parameter of importance in these simulations is the maximum retention capacity of the fibers' surface,  $N_{\max}$ . The theoretical monolayer coverage of calcium soap particles is calculated to be 60 mg/g, assuming a 230 nm particle diameter, the square packing model and no surface loss due to fiber-fiber contact. A qualitative comparison can be drawn from the model simulation and our results.

As the calcium chloride concentration increases, it is expected that the deposition rate constant ( $k_1$ ) will increase due to improved charge screening. This trend is reflected by the increase in  $P_3$ . The BTC of the 0.5 mM concentration is close to the result for  $P_3=100$ . Since the theoretical value of  $N_{\max}$  is 0.06 g/g, the equilibrium constant then is of the order  $10^3$  (very fast deposition) compared to 0.1 (slow deposition) for the case where there is no  $\text{CaCl}_2$  added to the soap suspension.

The same argument applies to the effect of valency, where a trivalent metal, aluminum, with a positive charge, deposits at a faster rate than the divalent calcium does. Thus, the aluminum chloride has even higher deposition constants than calcium.

As the pulp consistency is increased from 5 to 15 %, the void fraction,  $\epsilon$ , in the fiber bed is decreased.  $P_1$  decreases with a decrease in void fraction, which also results in higher levels of retention as was found experimentally. An increase in soap retention at lower void fraction can be attributed to an increase in particle collision frequency in the smaller



interstitial spaces where the degree of turbulence is expected to increase (shear-induced coagulation).

As the flowrate increases, for a constant consistency, the average residence time of the particles within the fiber bed decreases. According to the simulation (Figure 2), a shorter residence time would result in lower soap retention as described by  $P_2$ . This trend is not observed for the lower concentration of calcium chloride (0.164 mM) for which there is no direct relation between flowrate and soap retention. This could be caused by the fact that the increase in flowrate has opposing effects on  $k_1$  (which increases due to increased collision frequency at higher shear) and on  $\theta_{ave}$  (which decreases at higher flowrates).

However, when the calcium concentration is high enough that coagulation occurs (1.48 mM) the predicted behavior is observed. As the flowrate increases, retention decreases. This could be explained by soap coagulation kinetics. At this concentration, soap retention occurs via coagulation. Since the soap particles do not have enough time to contact the fibers (at high flowrates, the average residence time in the bed is small), the coagulation is incomplete (i.e.,  $\theta_{coag} > \theta_{avg}$ ). This phenomena was discussed earlier.

A complex model which incorporates retention by coagulation at high electrolyte concentrations would allow for a better quantitative analysis of these results. An important process that should be accounted for is the particle concentration polarization close to the fibre surface which depresses the CCC. Finally, the particle transport equation should be coupled to an equation describing electrolyte flow through the porous medium, including its diffusion term onto and out of the surface. The fact that the electrolyte salt may ion-exchange and diffuse into the porous wall of the fibre should be accounted for.

### 3.7 CONCLUSIONS

Soap retention in the pulp fibers results from the combination of simultaneous processes occurring at specific rates and to a different extent:

- A. Adsorption of free/excess cations (counterions) onto fiber wall. Could be coupled to the ion-exchange between free cations ( $\text{Al}^{+3}$ ) and bound cations ( $\text{Ca}^{+2}$ ) of the soap suspension.
- B. Deposition of particles onto pulp fiber surfaces due to either of:
  - 1. Charge neutralization above a CDC.
  - 2. Heterogeneous coagulation of positively charged particles on negatively charged fiber surface.
- C. Establishment of a concentration gradient of particles close to the fibre surface.
- D. Coagulation of particles at the fiber surface due to either of:
  - 1. Charge neutralization (colloidal destabilization).
  - 2. Shear-induced coagulation (orthokinetic).
  - 3. Hydrophobic surface of the first layer of soap favors subsequent deposition.
- E. Re-conformation of particles on the outer aggregate layer resulting in either of:
  - 1. Additional particle collisions resulting in continued aggregation.
  - 2. Piling up of particles in mobile layer of aggregate due to oriented coagulation.
  - 3. Dissociation of "outer" particles exposed to dilution effects during rinsing.

#### 4. Irreversible coagulation.

The experimental data was compared to a mathematical simulation of particle retention in packed beds. Our experimental results agree with the general trends predicted by the model. A more complete model is required to take into account the additional kinetic terms are relevant to soap retention such as: particle concentration polarization and coagulation close to the fibre surface; ion-exchange and adsorption mechanisms on fibers and soap, and shear-induced coagulation at high flowrate and consistency.

The rate of particle retention (coagulation) on the fiber surface was estimated for different flowrate levels. The results strongly suggest a retention mechanism by orthokinetic coagulation. The CRT of 6.4 min was defined as the minimum contact time necessary to attain complete coagulation at a specific particle concentration (0.16 mmol/l) and pulp consistency. At high flowrates, the rate of particle retention reaches a plateau, due to the reduced diffusion of calcium ions towards the fibre surface where a high electrolyte concentration is required for coagulation to occur.

A  $CCC_{\text{surface}}$  of soap particles inside a fiber network of 0.7 mmol/l CaCl<sub>2</sub> was estimated from our retention isotherms.

#### NOMENCLATURE

- $n_{\delta}$  soap concentration in the suspension ( $\text{kg/m}^3$ )
- $n$  dimensionless soap concentration in the suspension ( $n_{\delta}/n_0$ )
- $N_{\delta}$  soap content on fibers (g soap/g fibre)

$N$	dimensionless soap content on the fibers ( $N_\delta/N_{\max}$ )
$K$	steady-state constant ( $k_1/k_2$ )
$k_1$	deposition rate constant ( $s^{-1}$ )
$k_2$	detachment rate constant ( $s^{-1}$ )
$U$	superficial velocity ( $ms^{-1}$ )
$H$	bed height (m)
$t_\delta$	time (s)
$t$	dimensionless time ( $t_\delta/\theta_{ave}$ )
$x_\delta$	distance from the inlet in the direction of flow (m)
$x$	dimensionless distance from the inlet ( $x_\delta/H$ )
$\rho$	density of wood fibres (kg/m)
$\varepsilon$	void fraction in packed bed
$\theta_{avg}$	average residence time of liquid phase in the bed (s)

## ACKNOWLEDGEMENTS

The authors thank J. Wright and T. Forlini for their assistance in some of the laboratory work. We also wish to thank Dr. T.G.M. van de Ven for permission to reprint figures.

## REFERENCES

1. SUNBERG, K., PETTERSSON, C., ECKERMAN, C. and HOLMBOM, B., "Preparation and properties of a model Dispersion of Colloidal Wood Resin", *J. Pulp Pap. Sci.* 22(7):J248-J252 (1996).
2. JOHANSON, B., WICKMAN, M. and STRÖM, G., "Surface chemistry of Flotation deinking: Agglomeration Kinetics and Agglomerate Structure", *Nordic pulp Pap. Res. J.* 2:74-85 (1996).
3. SITHOLÉ, B., TRAN, T.N. and ALLEN, L.H., "Quantitative determination of Aluminum Soaps in pitch deposits", *Nordic pulp Pap. Res. J.* 1:64-69(1996).
4. CROW, R.D. and STRATTON, R.A., "The chemistry of Aluminum salts in Papermaking I: Aluminum adsorption", *TAPPI Papermakers Conf. (Denver) Proc.*, 183-187 (1985).
5. LINDSTRÖM, T., SÖREMARK, C., HEINEGÅRD, C. and MARTIN-LÖF, S., "The importance of Electrokinetic properties of Wood Fiber for Papermaking", *TAPPI* 57 (12):94-96 (1974).
6. LINDSTRÖM, T., "Chemical factors affecting the behaviour of Fibers during Papermaking", *Nordic Pulp Pap. Res. J.* 4:182-191(1992).
7. MARTON, J. and MARTON, T., "Some new principles to Optimize Rosin Sizing", *TAPPI* 65:105-109 (1982).
8. DOUEK, M. and ALLEN, L.H., "Calcium soap deposition in kraft mills", *Paprican Reports, PPR # 255*: 1-13 (1979).
9. FERNÁNDEZ, C. and GARNIER, G., "Retention of fatty acid soap during recycling. Part I: A study using Packed Beds of Pulp Fibers", *J. Pulp Pap. Sci.*, in review, 1996.
10. VAN DE VEN, T.G.M., "On the role of ion size in Coagulation", *J. Colloid Interface Sci.* 124(1):138-145 (1988).
11. HSU, J.P. and KUO, Y.C., "Critical Coagulation Concentration of Cations for negatively charged Particles with Ion-Penetrable Surface Layer", *J. Colloid Interface Sci.* 174:250-

- 257 (1995).
12. AL-JABARI, M., VAN HEININGEN, A. and VAN DE VEN, "Experimental study of Deposition of Clay Particles in Packed Beds of Pulp Fibers", *J. Pulp Pap. Sci.* 20(1):J289-J295 (1994).
  13. AL-JABARI, M., VAN HEININGEN, A. and VAN DE VEN, "Modeling the flow and the Deposition of Fillers in Packed Beds of Pulp Fibers", *J. Pulp Pap. Sci.* 20(9):J249-J253 (1994).
  14. PICARO, T. and VAN DE VEN, T.G.M., "The flow of dilute Polyethylene Oxide solutions through Packed beds of Pulp Fibers", *J. Pulp Pap. Sci.* 21(1):J13-J18 (1995).
  15. ELIMELECH, M., "Kinetics of capture of Colloidal Particles in Packed Beds under Attractive Double Layer Interactions", *J. Colloid Interface Sci.* 146(2): 337-352 (1991).
  16. BROKHAVEN INSTRUMENTS, "Electrokinetic Analyzer user manual" (1991).
  17. CARIGNAN, A., "The influence of cofactors on the flocculation properties of polyethylene oxide", Masters Thesis, *McGill University*, 120p.(1996).
  18. GREGORY, J., "Polymer Adsorption and Flocculation in Sheared Suspensions", *Colloids Surfaces* 31:231-253 (1988).
  19. HARWOTT, P. and VAN DE VEN, T.G.M., "Stability of latex suspensions", *J. Pulp Pap. Sci.*, to appear (1996).
  20. JÖNSSON, A. S. and JÖNSSON, B., "Ultrafiltration of Colloidal Dispersions-A Theoretical Model of the Concentration Polarization Phenomena", *J. Colloid Interface Sci.* 180: 504-518 (1996).
  21. STOLL, S. and BUFFLE, J., "Computer Simulation of Bridging Flocculation Processes", *J. Colloid Interface Sci.* 180: 548-563 (1996).
  22. CORNELL, R.M., GOODWIN, J.W. and OTTEWILL, R.H., "Direct Microscopic studies of Particle Motion in Stable Dispersions and in Floccules", *J. Colloid Interface Sci.* 71(2):254-26 (1979).
  23. TOWERS, M. and SCALLAN, A.M., "Predicting the Ion-Exchange of Kraft Pulps Using Donnan Theory", *Paprican Reports. PPR # 1170* (1995).
  24. ZHAOJING, D., CHUNYAN, P., JIAN, L., and YIPING, L., "Studies on the

- Spontaneous Evolution of Small Particle Aggregations", *J. Colloid Interface Sci.* 180:614-618 (1996).
25. THOMAS, L. and MCKORKLE, K.H., "Theory of Oriented Flocculation", *J. Colloid. Interface Sci.* 36 (1): 110-119 (1971).
  26. MELZER, J., "Zeta Potential and its importance in the Manufacture of Paper", *Das Papier* 26: 305-332 (1972).
  27. ARNO, J.N., FRANKLE, W.E. and SHERIDAN, J.L., "Zeta Potential and its application to Filler Retention", *TAPPI* 57 (12) :97-100 (1974).
  28. SCOTT, W.E., in *Pulp and Paper Manufacture*, "VII. Papermaking Chemistry":140-191 (1990).
  29. ALINCE, B., PETLICKI, J. and VAN DE VEN, T.G.M., "Kinetics of colloidal particle deposition on pulp fibers 1. Deposition of clay on fibers of opposite charge", *Colloids Surfaces* 59: 265-277 (1991).
  30. ROGAN, K.R., "Adsorption of oleic acid and triolein onto various minerals and surface treated minerals." *Colloid. Polym. Sci.* 272:82-98 (1994).

## **CHAPTER 4**

## **CONCLUSIONS**



#### 4.1 Overall conclusions

The objectives of this study were: (1) to develop an analytical technique that can be used to quantify contaminant retention in general, fatty acid soaps in specific; (2) to test if the hypothesis of surfactant retention on wood fibers is correct; and, if it is, (3) to propose a retention mechanism. The following conclusions were drawn from this study :

1. Retention of contaminants can be quantified by using a packed bed made of wood fibres and following the exit stream dynamics of a soap concentration pulse generated at the entrance. The area under a BTC is a sensitive measure of contaminant retention on the pulp. The system developed can analyze soap and sucrose tracer concentration on-line. The data is stored automatically in a PC.
2. Soap prepared by mixing equimolar amounts of sodium oleate and calcium chloride (1 Meq) do not adsorb on pulp fibers. This behavior goes according to theory as the negatively charged soap particles are repelled from the negatively charged fibers.
3. Calcium soap particles will deposit on the fiber at salt concentrations above a critical deposition concentration (CDC) and a critical coagulation concentration (CCC).
4. We proposed a diffusion mechanism by which the fiber micropores would be inaccessible to all species. The macropores could allow diffusion of hydrated calcium and micelles of sodium oleate. Calcium soap particles are too big to enter the pores inside the cell wall, thus they can only deposit on the external fiber surface.
5. Soap retention on the pulp increases the hydrophobicity of paper. This property may affect the printing potential of recycled fibers (ink absorption).

6. The weak adhesion strength of soap particles on paper combined with high adsorption and desorption rate constants of similar magnitude explain the carryover mechanism of fatty acid soaps. Carryover is the phenomenon responsible for water contamination, pitch deposition and reduced paper strength.
7. Sodium salts of fatty acids undergo ion-exchange with the calcium present in the pulp (forming calcium soaps).
8. Calcium ions present in tap water can be retained by the pulp by ion-exchange.
9. The availability of calcium and other ions within the pulp for ion-exchange is diffusion controlled.
10. Soap retention in the pulp fibers (at high salt concentration) will result from a combination of several processes that occur simultaneously at specific rates and to a different extent :
  - A. Adsorption of free/excess cations (counterions) onto fiber wall. Could be coupled to the ion-exchange between free cations ( $Al^{+3}$ ) and bound cations ( $Ca^{+2}$ ) of the soap suspension.
  - B. Deposition of particles onto pulp fiber surfaces due to either of:
    1. Charge neutralization above a CDC.
    2. Heterogeneous coagulation of positively charged particles on negatively charged fiber surface.
  - C. Establishment of a concentration gradient of particles close to the fibre surface.
  - D. Coagulation of particles at the fiber surface due to :
    1. Charge neutralization (colloidal destabilization). This step is diffusion

controlled because it depends on the diffusion of ions to and from the fibre surface. It is therefore a limiting step.

2. Shear-induced (orthokinetic) coagulation. This rate of coagulation increases at higher flowrates and pulp consistency.
3. The hydrophobic surface due to the first layer of soap (higher affinity for hydrophobic material than the “clean” hydrophilic surface.
4. Interference/interaction of surface potential distribution between two neighboring deposited particles (oriented coagulation).

E. Reformation of particles on the outer aggregate layer resulting in either of :

1. Additional particle collisions resulting in continued aggregation.
2. Piling up of particles in mobile layer of aggregate due to oriented coagulation .
3. Dissociation of “outer” particles exposed to dilution effects during the rinsing step. This phenomenon causes the reversible retention behavior when coagulation does occur.
4. Irreversible coagulation. This occurs when there is no aggregate layer (eg., salt concentration below the CCC).

11. The experimental data was compared to a mathematical simulation of particle retention in packed beds. Our experimental results agree with the general trends predicted by the model. A more complex model is required to take into account the additional kinetic terms that are relevant to soap retention such as: particle concentration polarization and coagulation close to the fibre surface; ion-exchange and adsorption on fibers and soap

in the presence of electrolytes, and shear-induced coagulation at high flowrate and consistency.

12. The rate of particle retention (coagulation) on the fiber surface was estimated (0.05-0.15 mmol/min) at different flowrates (30 - 178 mL/min). The results strongly suggest a retention mechanism by orthokinetic coagulation.
13. The fraction of soap introduced (during a 10-minute pulse) that is retained increases as the residence time (contact time) and the pulp consistency increase.
14. The CRT of 6.4 min was defined to be the minimum contact time necessary to attain complete coagulation at a specific particle concentration (0.16 mmol/l) and pulp consistency (10 %). This falls within the repulping duration of 30 minutes.
15. At high flowrates, the rate of particle retention reaches a plateau. This can be explained by the reduced diffusion of calcium ions towards the fibre surface (where a high electrolyte concentration is required for coagulation to occur) due to turbulent flow inside the porous medium. This is when charge neutralization becomes a limiting step.
16. A  $CCC_{\text{surface}}$  of soap particles (coagulation induced by the surface of the fibers) of 0.7 mmol/l  $\text{CaCl}_2$  was estimated from retention isotherms. This measure of a CCC inside porous medium was developed during the course of this work. The physical meaning and validity of this value should be confirmed by future work.

## 4.2 Future work

White water quality is a key factor determining soap deposition and detachment; thus, our observations are directly relevant for mills that having advanced water circuit closure

projects. Experiments at higher temperatures and different pH would be desirable to match closely the industrial operating conditions.

A  $CCC_{\text{surface}}$  of soap particles (coagulation induced by the surface of the fibers) of 0.7 mmol/l  $\text{CaCl}_2$  was estimated from retention isotherms. This technique to measure a CCC inside porous medium was developed during the course of this work. Its precise physical meaning and validity should be confirmed by future work.

The analytical technique developed to measure retention can be used for the selection of new deinking formulas. The interaction of other compounds with fibers can be studied in detail with this technique. The set up is flexible enough that it allows for a diverse range of manipulation. For instance, the input signal (feed concentration) need not be a square wave; it can be sinusoidal or a ramp. It would be sufficient to install two pumps in parallel at the inlet soap and water tanks and manipulate their flowrates with an automatic controller. Furthermore, one may add a flow through conductivity probe to monitor the conductivity of the effluent on-line for a complete kinetic study.

Energy Dispersive X-Ray Spectroscopy (EDX) can be a powerful tool to complement packed bed results. This technique allows to quantify and locate visually the distribution of individual elements (such as Calcium, Aluminum, Magnesium, and Sodium) across the fibre wall and on surface irregularities. X-ray mapping results can be compared before and after an experimental run. Then, it would be possible to learn even more about the formation of ion diffusion gradients, the stoichiometry of ion-exchange reactions, the relation between surface ion concentration and particle coagulation on the fiber surface, and other relevant phenomena.

Further soap retention studies should include the effect of fines which have a larger specific surface area (surface area per unit mass) than the larger fibers and are known to adsorb large quantities of process chemicals. Furthermore, it is desirable to confirm that the fibre morphology has a negligible effect on the surface properties of the fiber compared to the effects of the surface chemical composition.

The next step is to include the effect of ink particles on the retention study. It would be required to distinguish between the concentration of “free” soap particles, and the fatty acid component of ink particles. The development of an on-line analytical technique that can achieve this will be a challenge in itself. Still, a comprehensive simulation model should include the dynamic interactions between all the components of the deinking “chemical soup” (fibers, soaps, electrolyte salt and ink particles).

#### **4.3 Implications of this study on Paper Recycling**

In the mill, the water can contain alum, an aluminum compound. A process disturbance in its concentration may cause severe pitch deposition problems by means of chemical carryover by coagulation on the fibre surface (reversible deposition). Furthermore, patches of soap aggregates on the paper sheet (irreversible deposition) represents “weak spots” and may result in paper breakage in the paper machine. Sizing and lower paper strength can be a result of soap retention during recycling. Once the pulp fibers “pick up” the soap, they carry it from unit to unit until subjected to a shock in consistency, pH or ionic strength (desorption).

In order to avoid these commonly encountered problems, the input of inorganic salts

should be optimized (eg. calcium chloride, aluminum chloride, etc) by reducing their input as much as possible. The flowrate of white water through the press felt should be reduced to an optimum level. Finally, the input of fatty acid soaps should be lowered during flotation deinking by as much as possible.

The justification of this work was to search ways of preventing some of the detrimental effects of the paper recycling process. The sticky material (pitch) deposition on the equipment, the reduced strength, lower coefficient of friction, papermachine breaks and reduced water absorption may now be addressed at once. This study may also be used as a starting point to optimize the chemical input to the recycling process by means of mathematical modelling. The fulfilment of that objective would have a great impact on environmental and production costs.





## **APPENDIX A**

### **TECHNICAL DESIGN**

## APPENDIX A: TECHNICAL DESIGN

### I. Experimental strategy

A decision was made to study the interactions between fibers and a model chemical (calcium oleate). The technique developed for this purpose would have the following features:

1. Can visually inspect the fiber suspension. Need to use a transparent material.
2. Can operate at high pulp consistency (solid content 5-25 %) yet the system must be homogeneous.
3. Can analyze for the model chemical on-line to avoid sample collection and time-consuming analysis.
4. Wood fibers do not interfere with analytical method.
5. Can measure chemical retention amounts as well as perform kinetic studies (measure eluent concentration as a function of time).
6. Dead volumes (tubing and sampling port) must be negligible.

With these constraints in mind, a preliminary decision was made to use a packed bed reactor connected to a flow-through cell to measure absorbance and particle light scattering (see Chapter 2 for a description). Figure 1 shows a photograph of the final experimental set up.

### II. Packed bed design

A rough draft of the design was submitted to the Paprican machine shop staff. The specifications included the construction materials, detailed dimensions, and design of (3) types of liquid distribution discs for the piston (Figure 2). Technical drawings produced by

the machine shop are shown in appendix B.

### III. Trouble-Shooting

Once the equipment was installed, preliminary debugging experimentation was carried out. The results of that exercise were the following:

1. It was necessary to degas the pulp before utilization. Many packing procedures were tested for reproducibility. When the pulp slurry was not degassed, air bubbles were entrapped, adding a source of error to the RTD function.
2. The turbulence of the suspension within the tubing does not cause a noisy absorbance signal. The spectrophotometer produced smooth absorbance readings upto a flowrate of 230 mL/min.
3. A bleed line was connected to facilitate tubing rinsing and pad formation.
4. A three-way valve was installed at the feed to use the same pump for: water, soap, and tracer. This allows us to produce tracer and soap concentration pulses at the same exact flowrate without causing disturbances in fibre conformation due to flow changes.
5. A quartz flow-through cell was installed to avoid sample handling (Figure 3). The measurements were best performed in the "single beam" mode. The instrument zeroing could then be done on-line during the initial water "rinsing" step. A decay in absorbance was usually observed during this step, perhaps due to impurities exiting the system. A flat baseline was insured before beginning the runs.
6. It was not necessary to collect sucrose samples manually as the spectrophotometer was producing a well defined RTD curve at 105 nm with a sucrose feed of 15 g/L.

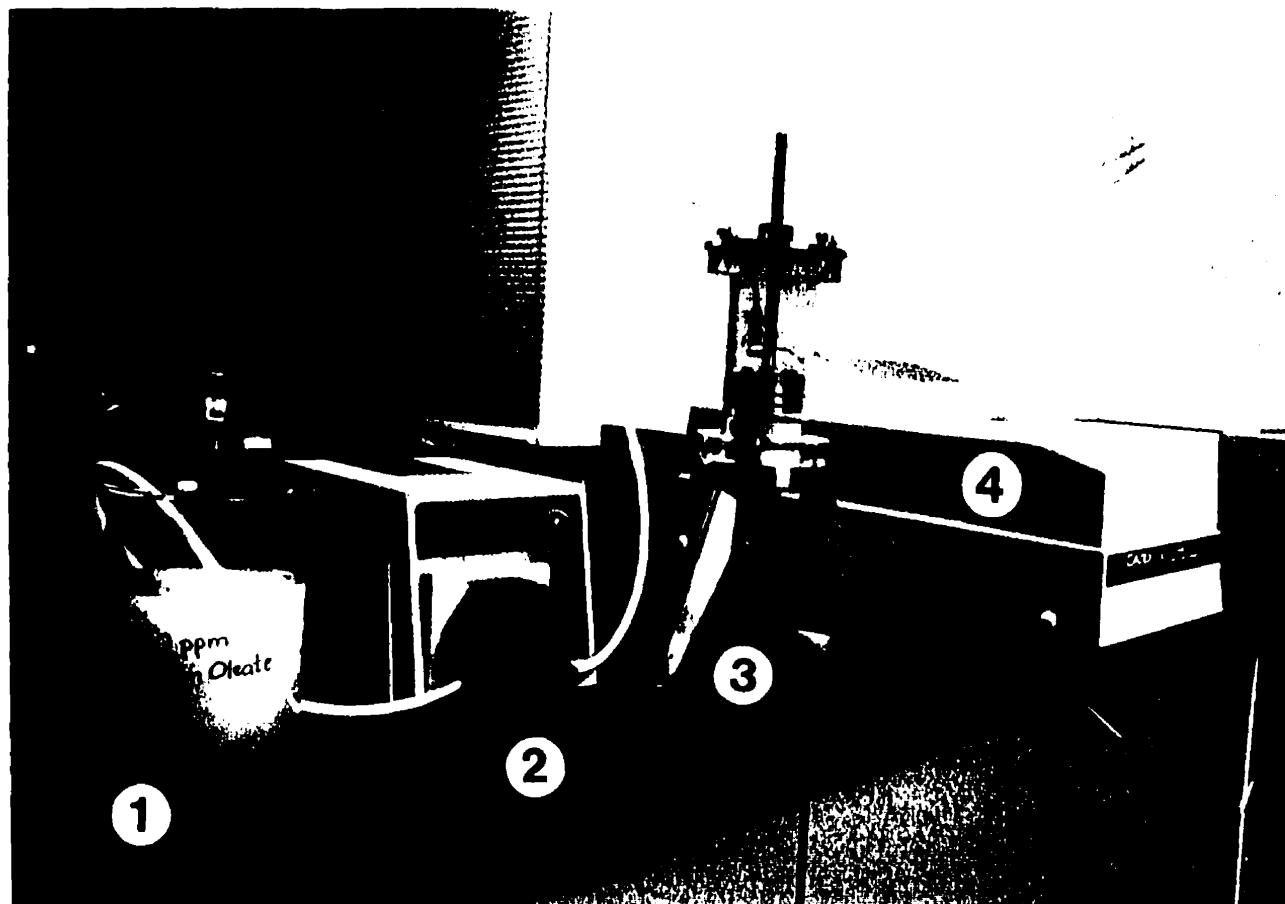


Figure 1. Photograph of experimental set-up showing:(1) feed soap suspension, (2) peristaltic pump, (3) packed bed, and (4) UV/Vis spectrophotometer.

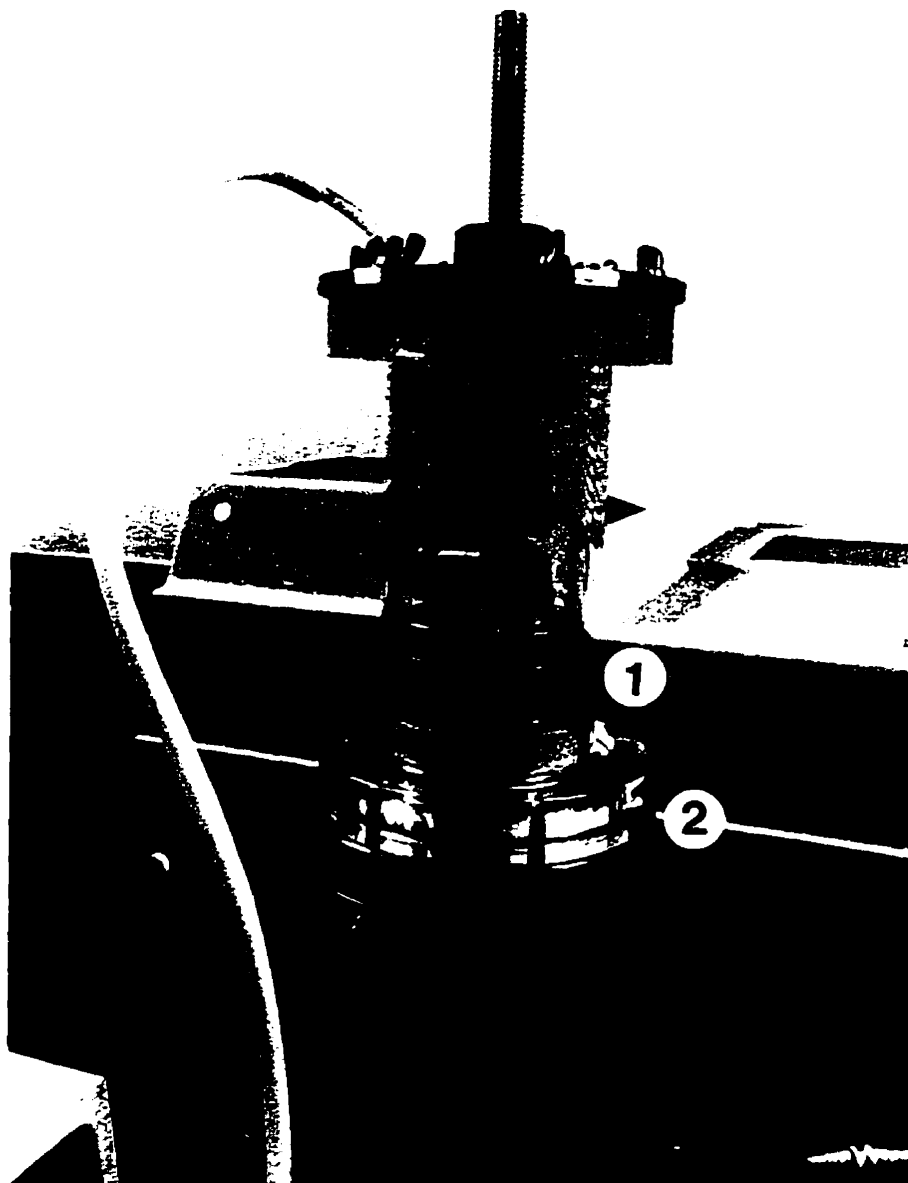


Figure 2. Photograph of packed bed showing:(1) liquid distribution disc/ piston, and (2) lower screening disc .



Figure 3. Close-up of spectrophotometer sample compartment showing quartz flow-through cell.

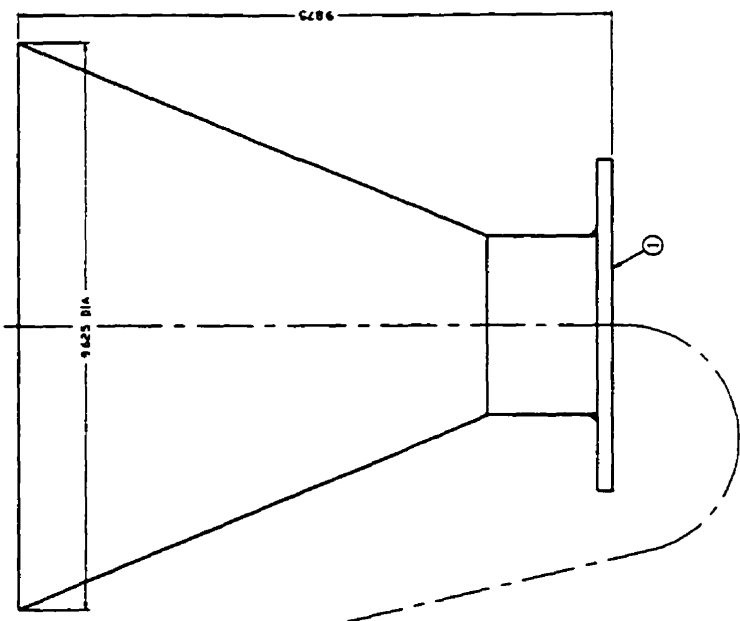


Figure 12b. Magnified image (white bar indicates 100 nm).

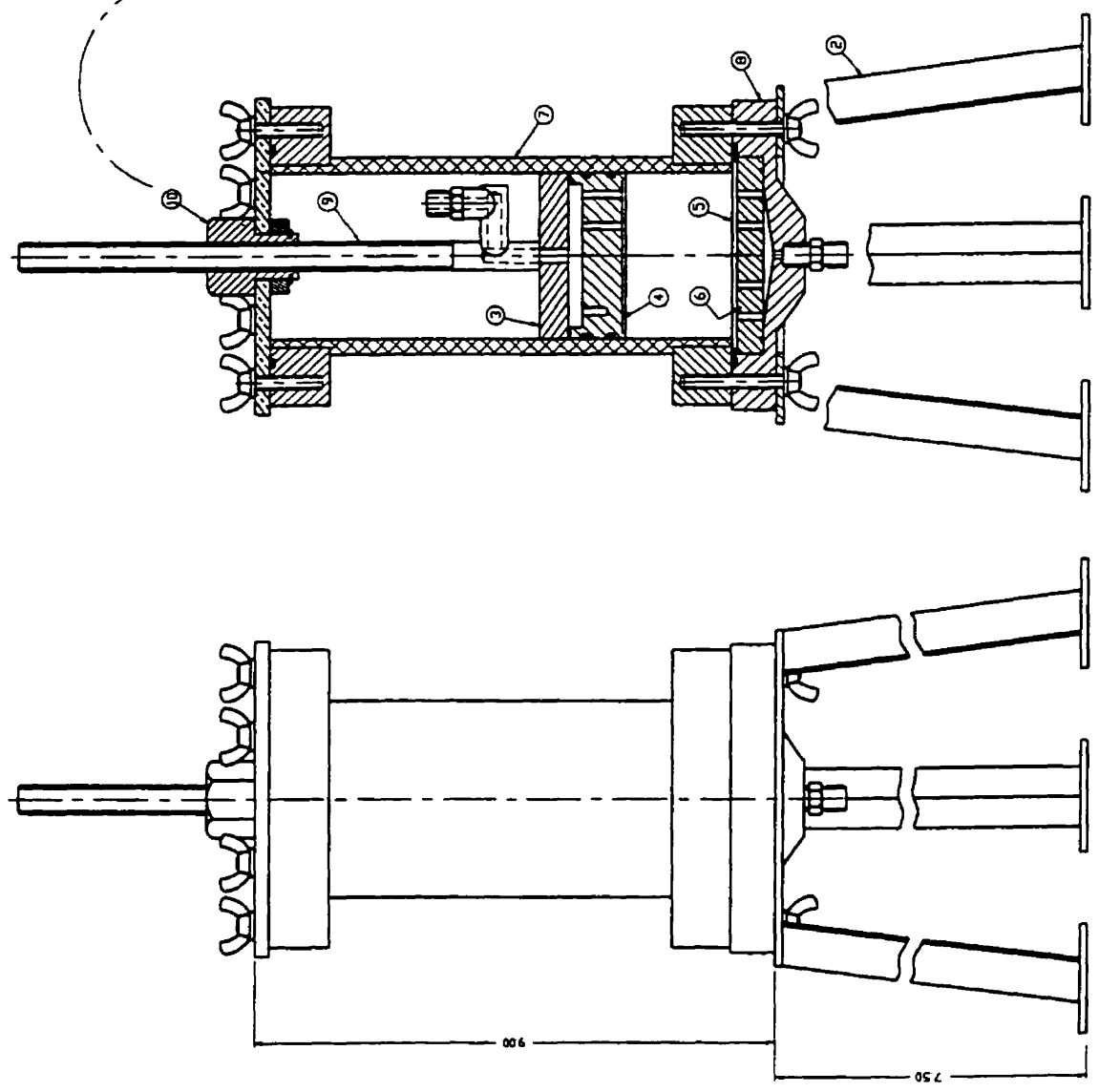
## **APPENDIX B**

### **PACKED BED TECHNICAL DRAWINGS**





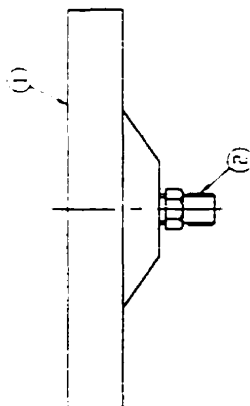
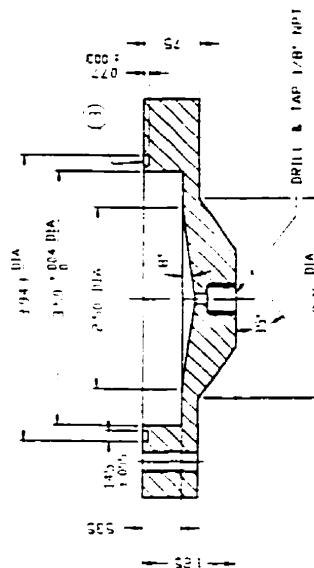
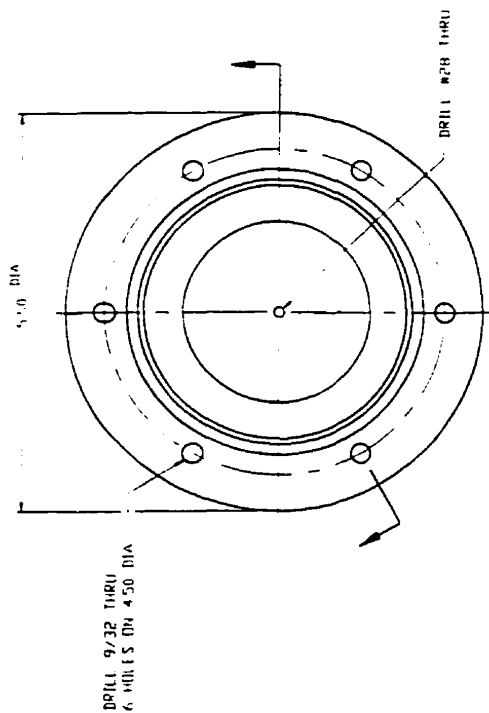
NOTES: 1) TO INSTALL FILLING FUNNEL (PART 1) IN REMOVE  
ADJUSTING NUT ASSY (PART 10) & PISTON ASSEMBLY  
2) PART 5 TO BE INSTALLED SUCH THAT MESH FACES UP



ITEM NO		DESCRIPTION		MATERIAL OR PART NO	
10	1	ADJUSTING NUT	BRASS-10	BRASS-10	
9	1	PISTON RING	BRASS-10	BRASS-10	
8	1	PISTON RING	BRASS-10	BRASS-10	
7	1	PISTON RING	BRASS-10	BRASS-10	
6	1	PISTON RING	BRASS-10	BRASS-10	
5	1	PISTON RING	BRASS-10	BRASS-10	
4	1	PISTON RING	BRASS-10	BRASS-10	
3	1	PISTON RING	BRASS-10	BRASS-10	
2	1	PISTON RING	BRASS-10	BRASS-10	
1	1	PISTON RING	BRASS-10	BRASS-10	
ITEM NO DESCRIPTION MATERIAL OR PART NO					
11	1	PISTON RING	BRASS-10	BRASS-10	
12	1	PISTON RING	BRASS-10	BRASS-10	
13	1	PISTON RING	BRASS-10	BRASS-10	
14	1	PISTON RING	BRASS-10	BRASS-10	
15	1	PISTON RING	BRASS-10	BRASS-10	
16	1	PISTON RING	BRASS-10	BRASS-10	
17	1	PISTON RING	BRASS-10	BRASS-10	
18	1	PISTON RING	BRASS-10	BRASS-10	
19	1	PISTON RING	BRASS-10	BRASS-10	
20	1	PISTON RING	BRASS-10	BRASS-10	
ITEM NO DESCRIPTION MATERIAL OR PART NO					
21	1	PISTON RING	BRASS-10	BRASS-10	
22	1	PISTON RING	BRASS-10	BRASS-10	
23	1	PISTON RING	BRASS-10	BRASS-10	
24	1	PISTON RING	BRASS-10	BRASS-10	
25	1	PISTON RING	BRASS-10	BRASS-10	
26	1	PISTON RING	BRASS-10	BRASS-10	
27	1	PISTON RING	BRASS-10	BRASS-10	
28	1	PISTON RING	BRASS-10	BRASS-10	
29	1	PISTON RING	BRASS-10	BRASS-10	
30	1	PISTON RING	BRASS-10	BRASS-10	
ITEM NO DESCRIPTION MATERIAL OR PART NO					
31	1	PISTON RING	BRASS-10	BRASS-10	
32	1	PISTON RING	BRASS-10	BRASS-10	
33	1	PISTON RING	BRASS-10	BRASS-10	
34	1	PISTON RING	BRASS-10	BRASS-10	
35	1	PISTON RING	BRASS-10	BRASS-10	
36	1	PISTON RING	BRASS-10	BRASS-10	
37	1	PISTON RING	BRASS-10	BRASS-10	
38	1	PISTON RING	BRASS-10	BRASS-10	
39	1	PISTON RING	BRASS-10	BRASS-10	
40	1	PISTON RING	BRASS-10	BRASS-10	
ITEM NO DESCRIPTION MATERIAL OR PART NO					
41	1	PISTON RING	BRASS-10	BRASS-10	
42	1	PISTON RING	BRASS-10	BRASS-10	
43	1	PISTON RING	BRASS-10	BRASS-10	
44	1	PISTON RING	BRASS-10	BRASS-10	
45	1	PISTON RING	BRASS-10	BRASS-10	
46	1	PISTON RING	BRASS-10	BRASS-10	
47	1	PISTON RING	BRASS-10	BRASS-10	
48	1	PISTON RING	BRASS-10	BRASS-10	
49	1	PISTON RING	BRASS-10	BRASS-10	
50	1	PISTON RING	BRASS-10	BRASS-10	
ITEM NO DESCRIPTION MATERIAL OR PART NO					
51	1	PISTON RING	BRASS-10	BRASS-10	
52	1	PISTON RING	BRASS-10	BRASS-10	
53	1	PISTON RING	BRASS-10	BRASS-10	
54	1	PISTON RING	BRASS-10	BRASS-10	
55	1	PISTON RING	BRASS-10	BRASS-10	
56	1	PISTON RING	BRASS-10	BRASS-10	
57	1	PISTON RING	BRASS-10	BRASS-10	
58	1	PISTON RING	BRASS-10	BRASS-10	
59	1	PISTON RING	BRASS-10	BRASS-10	
60	1	PISTON RING	BRASS-10	BRASS-10	
ITEM NO DESCRIPTION MATERIAL OR PART NO					
61	1	PISTON RING	BRASS-10	BRASS-10	
62	1	PISTON RING	BRASS-10	BRASS-10	
63	1	PISTON RING	BRASS-10	BRASS-10	
64	1	PISTON RING	BRASS-10	BRASS-10	
65	1	PISTON RING	BRASS-10	BRASS-10	
66	1	PISTON RING	BRASS-10	BRASS-10	
67	1	PISTON RING	BRASS-10	BRASS-10	
68	1	PISTON RING	BRASS-10	BRASS-10	
69	1	PISTON RING	BRASS-10	BRASS-10	
70	1	PISTON RING	BRASS-10	BRASS-10	
ITEM NO DESCRIPTION MATERIAL OR PART NO					
71	1	PISTON RING	BRASS-10	BRASS-10	
72	1	PISTON RING	BRASS-10	BRASS-10	
73	1	PISTON RING	BRASS-10	BRASS-10	
74	1	PISTON RING	BRASS-10	BRASS-10	
75	1	PISTON RING	BRASS-10	BRASS-10	
76	1	PISTON RING	BRASS-10	BRASS-10	
77	1	PISTON RING	BRASS-10	BRASS-10	
78	1	PISTON RING	BRASS-10	BRASS-10	
79	1	PISTON RING	BRASS-10	BRASS-10	
80	1	PISTON RING	BRASS-10	BRASS-10	
ITEM NO DESCRIPTION MATERIAL OR PART NO					
81	1	PISTON RING	BRASS-10	BRASS-10	
82	1	PISTON RING	BRASS-10	BRASS-10	
83	1	PISTON RING	BRASS-10	BRASS-10	
84	1	PISTON RING	BRASS-10	BRASS-10	
85	1	PISTON RING	BRASS-10	BRASS-10	
86	1	PISTON RING	BRASS-10	BRASS-10	
87	1	PISTON RING	BRASS-10	BRASS-10	
88	1	PISTON RING	BRASS-10	BRASS-10	
89	1	PISTON RING	BRASS-10	BRASS-10	
90	1	PISTON RING	BRASS-10	BRASS-10	
ITEM NO DESCRIPTION MATERIAL OR PART NO					
91	1	PISTON RING	BRASS-10	BRASS-10	
92	1	PISTON RING	BRASS-10	BRASS-10	
93	1	PISTON RING	BRASS-10	BRASS-10	
94	1	PISTON RING	BRASS-10	BRASS-10	
95	1	PISTON RING	BRASS-10	BRASS-10	
96	1	PISTON RING	BRASS-10	BRASS-10	
97	1	PISTON RING	BRASS-10	BRASS-10	
98	1	PISTON RING	BRASS-10	BRASS-10	
99	1	PISTON RING	BRASS-10	BRASS-10	
100	1	PISTON RING	BRASS-10	BRASS-10	

PULP AND PAPER RESEARCH  
INSTITUTE OF CANADA  
DRAWING NO. 9501A00-100

ITEM	QTY	DESCRIPTION	MATERIAL OR PART NO
WET ASSY TO PENDING DOG	FINAL	ASSY TO RFR	
DRAWN 11	CHECKED RJS	APPROVED SCALE	NOT NAME CLASSIFIED DATE 9/20/75
PULP AND PAPER RESEARCH INSTITUTE OF CANADA			PACKED BY D. VASIA R DETAIL OF FRTING, FIBRE I DRAWING No.: 9-001A00D (70)



ITEM	QTY	DESCRIPTION	UNIT	QTY	PRICE	TOTAL
1	1	FLANGE	EA	1	1.00	1.00
2	1	DRILL #28 THRU	EA	1	1.00	1.00
3	1	DRILL & TAP 1/8" NPT	EA	1	1.00	1.00
4	1	DRILL 9/32 THRU	EA	1	1.00	1.00
5	1	DRILL 5/16" DIA	EA	1	1.00	1.00
6	1	DRILL 3/8" DIA	EA	1	1.00	1.00
7	1	DRILL 1/2" DIA	EA	1	1.00	1.00
8	1	DRILL 5/8" DIA	EA	1	1.00	1.00
9	1	DRILL 3/4" DIA	EA	1	1.00	1.00
10	1	DRILL 7/8" DIA	EA	1	1.00	1.00
11	1	DRILL 1" DIA	EA	1	1.00	1.00
12	1	DRILL 1 1/8" DIA	EA	1	1.00	1.00
13	1	DRILL 1 1/4" DIA	EA	1	1.00	1.00
14	1	DRILL 1 3/8" DIA	EA	1	1.00	1.00
15	1	DRILL 1 1/2" DIA	EA	1	1.00	1.00
16	1	DRILL 1 5/8" DIA	EA	1	1.00	1.00
17	1	DRILL 1 3/4" DIA	EA	1	1.00	1.00
18	1	DRILL 1 7/8" DIA	EA	1	1.00	1.00
19	1	DRILL 2" DIA	EA	1	1.00	1.00
20	1	DRILL 2 1/8" DIA	EA	1	1.00	1.00
21	1	DRILL 2 1/4" DIA	EA	1	1.00	1.00
22	1	DRILL 2 3/8" DIA	EA	1	1.00	1.00
23	1	DRILL 2 1/2" DIA	EA	1	1.00	1.00
24	1	DRILL 2 5/8" DIA	EA	1	1.00	1.00
25	1	DRILL 2 3/4" DIA	EA	1	1.00	1.00
26	1	DRILL 2 7/8" DIA	EA	1	1.00	1.00
27	1	DRILL 3" DIA	EA	1	1.00	1.00
28	1	DRILL 3 1/8" DIA	EA	1	1.00	1.00
29	1	DRILL 3 1/4" DIA	EA	1	1.00	1.00
30	1	DRILL 3 3/8" DIA	EA	1	1.00	1.00
31	1	DRILL 3 1/2" DIA	EA	1	1.00	1.00
32	1	DRILL 3 5/8" DIA	EA	1	1.00	1.00
33	1	DRILL 3 3/4" DIA	EA	1	1.00	1.00
34	1	DRILL 3 7/8" DIA	EA	1	1.00	1.00
35	1	DRILL 4" DIA	EA	1	1.00	1.00
36	1	DRILL 4 1/8" DIA	EA	1	1.00	1.00
37	1	DRILL 4 1/4" DIA	EA	1	1.00	1.00
38	1	DRILL 4 3/8" DIA	EA	1	1.00	1.00
39	1	DRILL 4 1/2" DIA	EA	1	1.00	1.00
40	1	DRILL 4 5/8" DIA	EA	1	1.00	1.00
41	1	DRILL 4 3/4" DIA	EA	1	1.00	1.00
42	1	DRILL 4 7/8" DIA	EA	1	1.00	1.00
43	1	DRILL 5" DIA	EA	1	1.00	1.00
44	1	DRILL 5 1/8" DIA	EA	1	1.00	1.00
45	1	DRILL 5 1/4" DIA	EA	1	1.00	1.00
46	1	DRILL 5 3/8" DIA	EA	1	1.00	1.00
47	1	DRILL 5 1/2" DIA	EA	1	1.00	1.00
48	1	DRILL 5 5/8" DIA	EA	1	1.00	1.00
49	1	DRILL 5 3/4" DIA	EA	1	1.00	1.00
50	1	DRILL 5 7/8" DIA	EA	1	1.00	1.00
51	1	DRILL 6" DIA	EA	1	1.00	1.00
52	1	DRILL 6 1/8" DIA	EA	1	1.00	1.00
53	1	DRILL 6 1/4" DIA	EA	1	1.00	1.00
54	1	DRILL 6 3/8" DIA	EA	1	1.00	1.00
55	1	DRILL 6 1/2" DIA	EA	1	1.00	1.00
56	1	DRILL 6 5/8" DIA	EA	1	1.00	1.00
57	1	DRILL 6 3/4" DIA	EA	1	1.00	1.00
58	1	DRILL 6 7/8" DIA	EA	1	1.00	1.00
59	1	DRILL 7" DIA	EA	1	1.00	1.00
60	1	DRILL 7 1/8" DIA	EA	1	1.00	1.00
61	1	DRILL 7 1/4" DIA	EA	1	1.00	1.00
62	1	DRILL 7 3/8" DIA	EA	1	1.00	1.00
63	1	DRILL 7 1/2" DIA	EA	1	1.00	1.00
64	1	DRILL 7 5/8" DIA	EA	1	1.00	1.00
65	1	DRILL 7 3/4" DIA	EA	1	1.00	1.00
66	1	DRILL 7 7/8" DIA	EA	1	1.00	1.00
67	1	DRILL 8" DIA	EA	1	1.00	1.00
68	1	DRILL 8 1/8" DIA	EA	1	1.00	1.00
69	1	DRILL 8 1/4" DIA	EA	1	1.00	1.00
70	1	DRILL 8 3/8" DIA	EA	1	1.00	1.00
71	1	DRILL 8 1/2" DIA	EA	1	1.00	1.00
72	1	DRILL 8 5/8" DIA	EA	1	1.00	1.00
73	1	DRILL 8 3/4" DIA	EA	1	1.00	1.00
74	1	DRILL 8 7/8" DIA	EA	1	1.00	1.00
75	1	DRILL 9" DIA	EA	1	1.00	1.00
76	1	DRILL 9 1/8" DIA	EA	1	1.00	1.00
77	1	DRILL 9 1/4" DIA	EA	1	1.00	1.00
78	1	DRILL 9 3/8" DIA	EA	1	1.00	1.00
79	1	DRILL 9 1/2" DIA	EA	1	1.00	1.00
80	1	DRILL 9 5/8" DIA	EA	1	1.00	1.00
81	1	DRILL 9 3/4" DIA	EA	1	1.00	1.00
82	1	DRILL 9 7/8" DIA	EA	1	1.00	1.00
83	1	DRILL 10" DIA	EA	1	1.00	1.00
84	1	DRILL 10 1/8" DIA	EA	1	1.00	1.00
85	1	DRILL 10 1/4" DIA	EA	1	1.00	1.00
86	1	DRILL 10 3/8" DIA	EA	1	1.00	1.00
87	1	DRILL 10 1/2" DIA	EA	1	1.00	1.00
88	1	DRILL 10 5/8" DIA	EA	1	1.00	1.00
89	1	DRILL 10 3/4" DIA	EA	1	1.00	1.00
90	1	DRILL 10 7/8" DIA	EA	1	1.00	1.00
91	1	DRILL 11" DIA	EA	1	1.00	1.00
92	1	DRILL 11 1/8" DIA	EA	1	1.00	1.00
93	1	DRILL 11 1/4" DIA	EA	1	1.00	1.00
94	1	DRILL 11 3/8" DIA	EA	1	1.00	1.00
95	1	DRILL 11 1/2" DIA	EA	1	1.00	1.00
96	1	DRILL 11 5/8" DIA	EA	1	1.00	1.00
97	1	DRILL 11 3/4" DIA	EA	1	1.00	1.00
98	1	DRILL 11 7/8" DIA	EA	1	1.00	1.00
99	1	DRILL 12" DIA	EA	1	1.00	1.00
100	1	DRILL 12 1/8" DIA	EA	1	1.00	1.00

PULP AND PAPER RESEARCH  
INSTITUTE OF CANADA

DETAIL OF OUTLET FLANGE  
DRAWING No. 65,01400 (178)

DETAIL OF PART 1

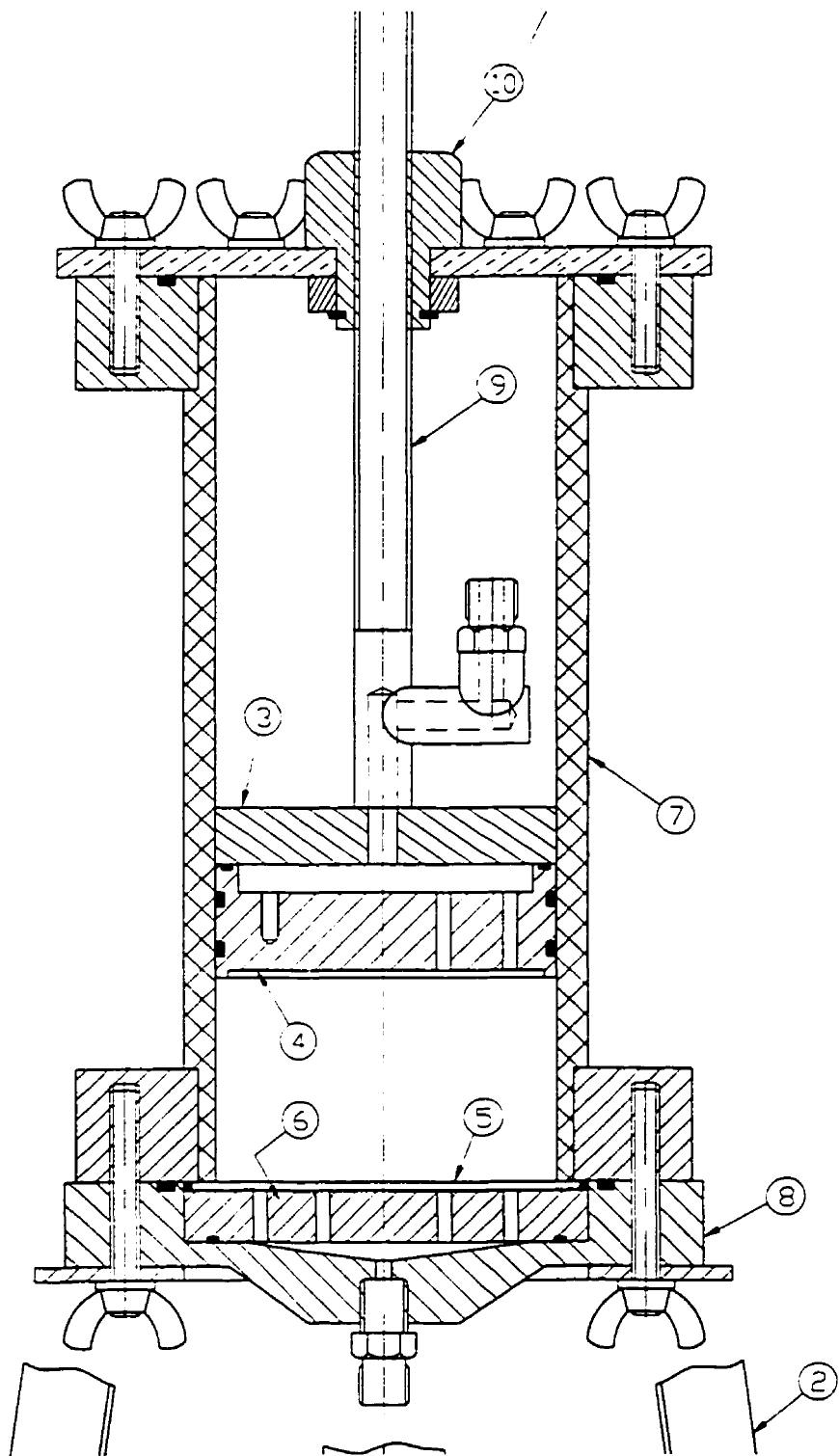
DETAIL OF PART 2

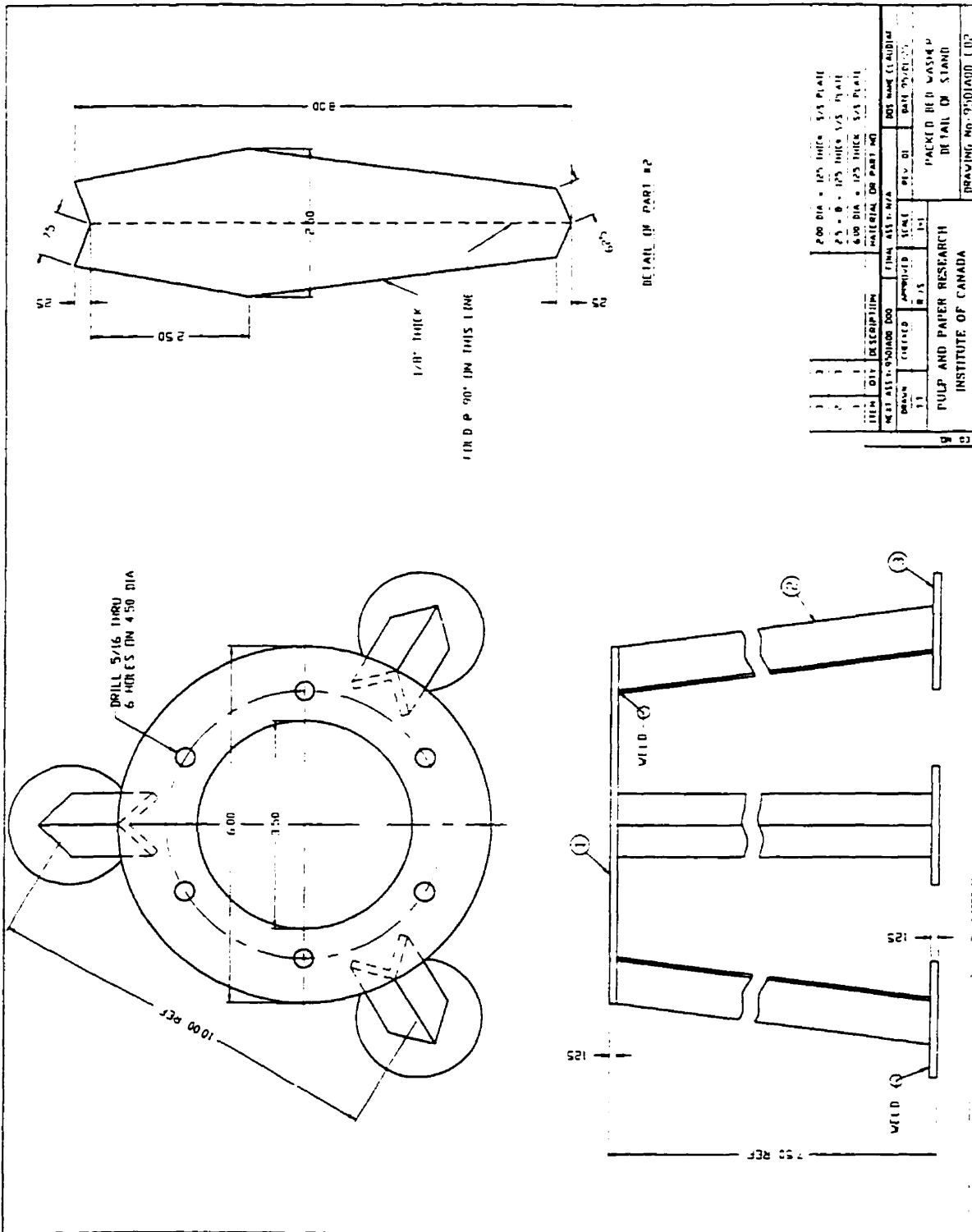
SWAGelok Fitting, to be modified  
as shown above

ASSEMBLY IT BE WITHD AS RECD

ASSEMBLY SCALE 11)

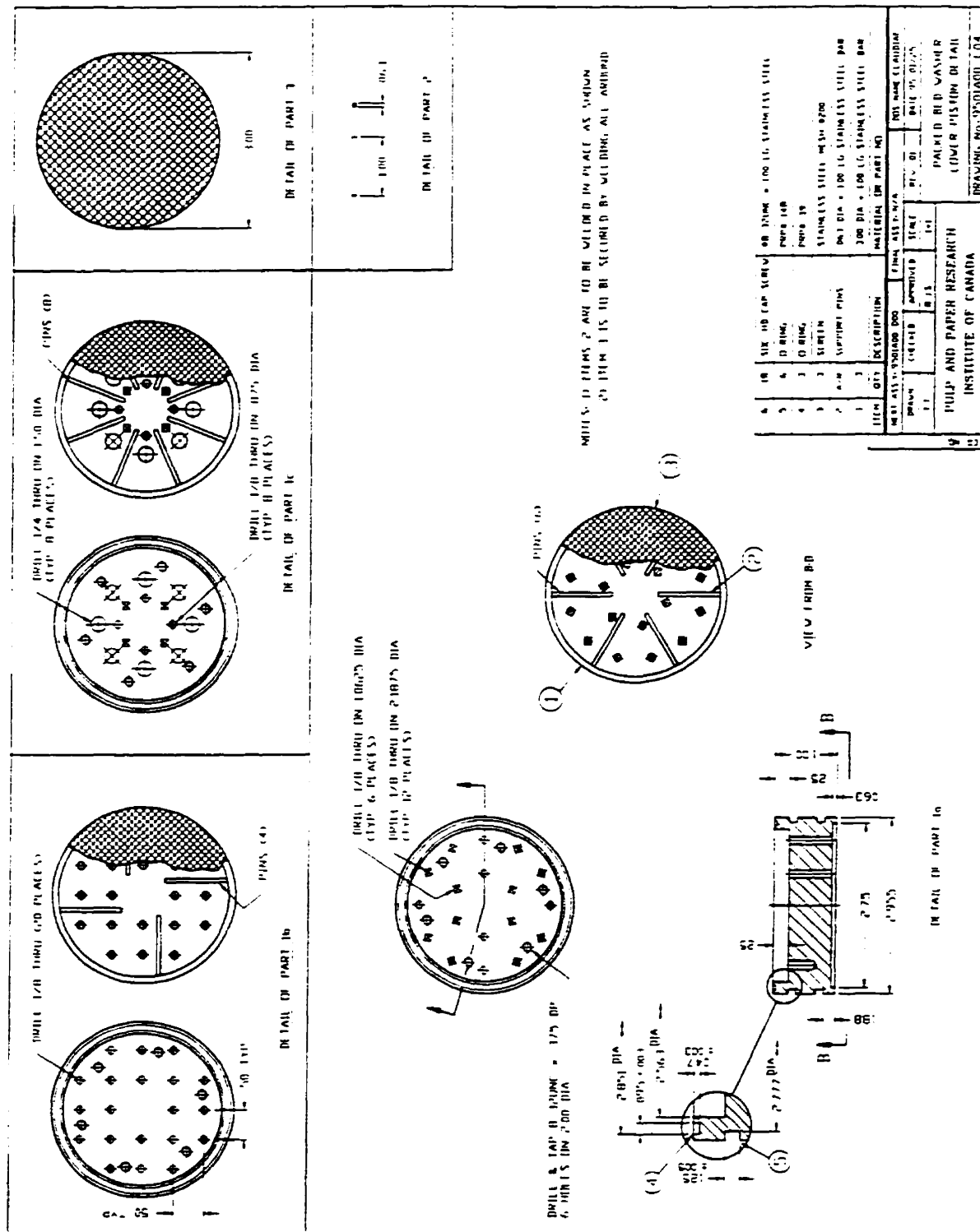
3	1	SWAGE OF FITTING	CAT# 55-000-1	4W INCH	PUMP WELD COMM. (100)
2	1	30 DIA. x 150 LG. STAINLESS STEEL BAR			
1	1	30 DIA. x 950 LG. STAINLESS STEEL BAR			
ITEM	QTY	DESCRIPTION	MATERIAL OR PART NO.		
MEET ASS. TO 910-0400-000		FINAL ASS. NO.		300 INCH WASHER	
DRAWN	CHECKED	APPROVED	SCALE	REV. Q2	DATE 9/10/17
1		R. S.	2:1		
PULP AND PAPER RESEARCH					
INSTITUTE OF CANADA					
DISPLACEMENT WASHER					
DETAIL OF BLEED LINE ASS. V					
DRAWING NO. 910-0400-C02					

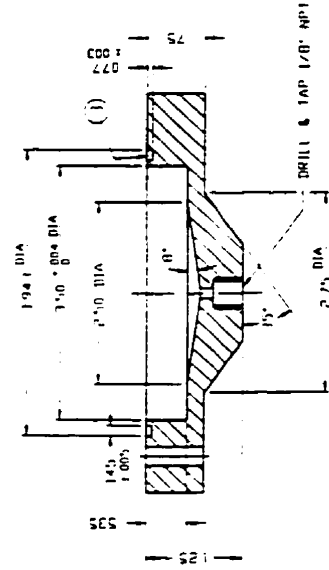
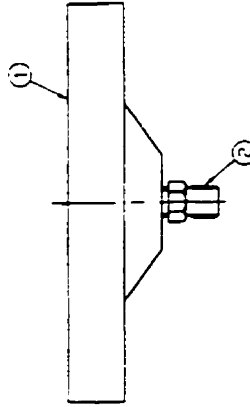




ITEM NO.		DESCRIPTION		FINAL ASSY. N/A		MATERIAL OF PART NO.		MATERIAL OF PART NO.		MATERIAL OF PART NO.	
1	1	DRILL	5/16 TORRU	6	Holes	IN 4.50 DIA					
2	2	DRILL	5/16 TORRU	6	Holes	IN 4.50 DIA					
3	3	DRILL	5/16 TORRU	6	Holes	IN 4.50 DIA					
4	4	DRILL	5/16 TORRU	6	Holes	IN 4.50 DIA					
5	5	DRILL	5/16 TORRU	6	Holes	IN 4.50 DIA					
6	6	DRILL	5/16 TORRU	6	Holes	IN 4.50 DIA					
7	7	DRILL	5/16 TORRU	6	Holes	IN 4.50 DIA					
8	8	DRILL	5/16 TORRU	6	Holes	IN 4.50 DIA					
9	9	DRILL	5/16 TORRU	6	Holes	IN 4.50 DIA					
10	10	DRILL	5/16 TORRU	6	Holes	IN 4.50 DIA					
11	11	DRILL	5/16 TORRU	6	Holes	IN 4.50 DIA					
12	12	DRILL	5/16 TORRU	6	Holes	IN 4.50 DIA					
13	13	DRILL	5/16 TORRU	6	Holes	IN 4.50 DIA					
14	14	DRILL	5/16 TORRU	6	Holes	IN 4.50 DIA					
15	15	DRILL	5/16 TORRU	6	Holes	IN 4.50 DIA					
16	16	DRILL	5/16 TORRU	6	Holes	IN 4.50 DIA					
17	17	DRILL	5/16 TORRU	6	Holes	IN 4.50 DIA					
18	18	DRILL	5/16 TORRU	6	Holes	IN 4.50 DIA					
19	19	DRILL	5/16 TORRU	6	Holes	IN 4.50 DIA					
20	20	DRILL	5/16 TORRU	6	Holes	IN 4.50 DIA					
21	21	DRILL	5/16 TORRU	6	Holes	IN 4.50 DIA					
22	22	DRILL	5/16 TORRU	6	Holes	IN 4.50 DIA					
23	23	DRILL	5/16 TORRU	6	Holes	IN 4.50 DIA					
24	24	DRILL	5/16 TORRU	6	Holes	IN 4.50 DIA					
25	25	DRILL	5/16 TORRU	6	Holes	IN 4.50 DIA					
26	26	DRILL	5/16 TORRU	6	Holes	IN 4.50 DIA					
27	27	DRILL	5/16 TORRU	6	Holes	IN 4.50 DIA					
28	28	DRILL	5/16 TORRU	6	Holes	IN 4.50 DIA					
29	29	DRILL	5/16 TORRU	6	Holes	IN 4.50 DIA					
30	30	DRILL	5/16 TORRU	6	Holes	IN 4.50 DIA					
31	31	DRILL	5/16 TORRU	6	Holes	IN 4.50 DIA					
32	32	DRILL	5/16 TORRU	6	Holes	IN 4.50 DIA					
33	33	DRILL	5/16 TORRU	6	Holes	IN 4.50 DIA					
34	34	DRILL	5/16 TORRU	6	Holes	IN 4.50 DIA					
35	35	DRILL	5/16 TORRU	6	Holes	IN 4.50 DIA					
36	36	DRILL	5/16 TORRU	6	Holes	IN 4.50 DIA					
37	37	DRILL	5/16 TORRU	6	Holes	IN 4.50 DIA					
38	38	DRILL	5/16 TORRU	6	Holes	IN 4.50 DIA					
39	39	DRILL	5/16 TORRU	6	Holes	IN 4.50 DIA					
40	40	DRILL	5/16 TORRU	6	Holes	IN 4.50 DIA					
41	41	DRILL	5/16 TORRU	6	Holes	IN 4.50 DIA					
42	42	DRILL	5/16 TORRU	6	Holes	IN 4.50 DIA					
43	43	DRILL	5/16 TORRU	6	Holes	IN 4.50 DIA					
44	44	DRILL	5/16 TORRU	6	Holes	IN 4.50 DIA					
45	45	DRILL	5/16 TORRU	6	Holes	IN 4.50 DIA					
46	46	DRILL	5/16 TORRU	6	Holes	IN 4.50 DIA					
47	47	DRILL	5/16 TORRU	6	Holes	IN 4.50 DIA					
48	48	DRILL	5/16 TORRU	6	Holes	IN 4.50 DIA					
49	49	DRILL	5/16 TORRU	6	Holes	IN 4.50 DIA					
50	50	DRILL	5/16 TORRU	6	Holes	IN 4.50 DIA					
51	51	DRILL	5/16 TORRU	6	Holes	IN 4.50 DIA					
52	52	DRILL	5/16 TORRU	6	Holes	IN 4.50 DIA					
53	53	DRILL	5/16 TORRU	6	Holes	IN 4.50 DIA					
54	54	DRILL	5/16 TORRU	6	Holes	IN 4.50 DIA					
55	55	DRILL	5/16 TORRU	6	Holes	IN 4.50 DIA					
56	56	DRILL	5/16 TORRU	6	Holes	IN 4.50 DIA					
57	57	DRILL	5/16 TORRU	6	Holes	IN 4.50 DIA					
58	58	DRILL	5/16 TORRU	6	Holes	IN 4.50 DIA					
59	59	DRILL	5/16 TORRU	6	Holes	IN 4.50 DIA					
60	60	DRILL	5/16 TORRU	6	Holes	IN 4.50 DIA					
61	61	DRILL	5/16 TORRU	6	Holes	IN 4.50 DIA					
62	62	DRILL	5/16 TORRU	6	Holes	IN 4.50 DIA					
63	63	DRILL	5/16 TORRU	6	Holes	IN 4.50 DIA					
64	64	DRILL	5/16 TORRU	6	Holes	IN 4.50 DIA					
65	65	DRILL	5/16 TORRU	6	Holes	IN 4.50 DIA					
66	66	DRILL	5/16 TORRU	6	Holes	IN 4.50 DIA					
67	67	DRILL	5/16 TORRU	6	Holes	IN 4.50 DIA					
68	68	DRILL	5/16 TORRU	6	Holes	IN 4.50 DIA					
69	69	DRILL	5/16 TORRU	6	Holes	IN 4.50 DIA					
70	70	DRILL	5/16 TORRU	6	Holes	IN 4.50 DIA					
71	71	DRILL	5/16 TORRU	6	Holes	IN 4.50 DIA					
72	72	DRILL	5/16 TORRU	6	Holes	IN 4.50 DIA					
73	73	DRILL	5/16 TORRU	6	Holes	IN 4.50 DIA					
74	74	DRILL	5/16 TORRU	6	Holes	IN 4.50 DIA					
75	75	DRILL	5/16 TORRU	6	Holes	IN 4.50 DIA					
76	76	DRILL	5/16 TORRU	6	Holes	IN 4.50 DIA					
77	77	DRILL	5/16 TORRU	6	Holes	IN 4.50 DIA					
78	78	DRILL	5/16 TORRU	6	Holes	IN 4.50 DIA					
79	79	DRILL	5/16 TORRU	6	Holes	IN 4.50 DIA					
80	80	DRILL	5/16 TORRU	6	Holes	IN 4.50 DIA					
81	81	DRILL	5/16 TORRU	6	Holes	IN 4.50 DIA					
82	82	DRILL	5/16 TORRU	6	Holes	IN 4.50 DIA					
83	83	DRILL	5/16 TORRU	6	Holes	IN 4.50 DIA					
84	84	DRILL	5/16 TORRU	6	Holes	IN 4.50 DIA					
85	85	DRILL	5/16 TORRU	6	Holes	IN 4.50 DIA					
86	86	DRILL	5/16 TORRU	6	Holes	IN 4.50 DIA					
87	87	DRILL	5/16 TORRU	6	Holes	IN 4.50 DIA					
88	88	DRILL	5/16 TORRU	6	Holes	IN 4.50 DIA					
89	89	DRILL	5/16 TORRU	6	Holes	IN 4.50 DIA					
90	90	DRILL	5/16 TORRU	6	Holes	IN 4.50 DIA					
91	91	DRILL	5/16 TORRU	6	Holes	IN 4.50 DIA					
92	92	DRILL	5/16 TORRU	6	Holes	IN 4.50 DIA					
93	93	DRILL	5/16 TORRU	6	Holes	IN 4.50 DIA					
94	94	DRILL	5/16 TORRU	6	Holes	IN 4.50 DIA					
95	95	DRILL	5/16 TORRU	6	Holes	IN 4.50 DIA					
96	96	DRILL	5/16 TORRU	6	Holes	IN 4.50 DIA					
97	97	DRILL	5/16 TORRU	6	Holes	IN 4.50 DIA					
98	98	DRILL	5/16 TORRU	6	Holes	IN 4.50 DIA					
99	99	DRILL	5/16 TORRU	6	Holes	IN 4.50 DIA					
100	100	DRILL	5/16 TORRU	6	Holes	IN 4.50 DIA					

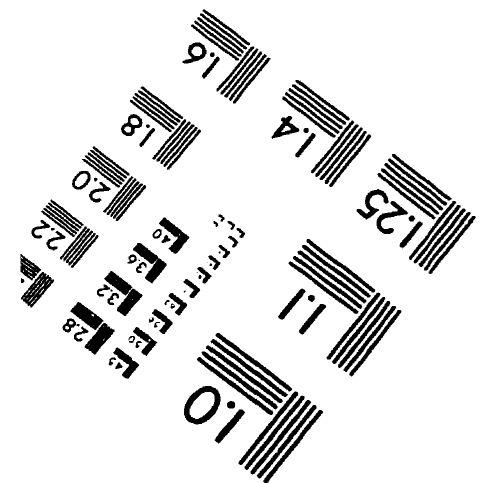
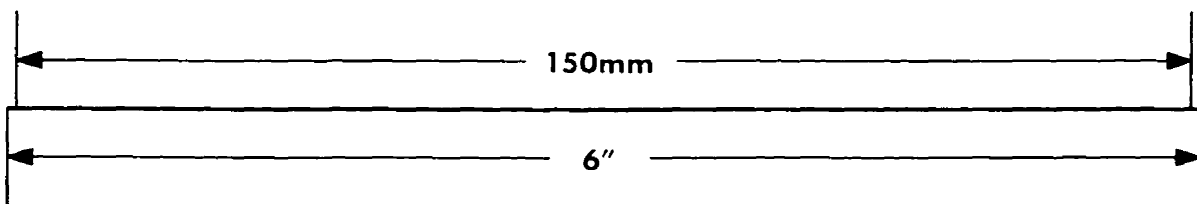
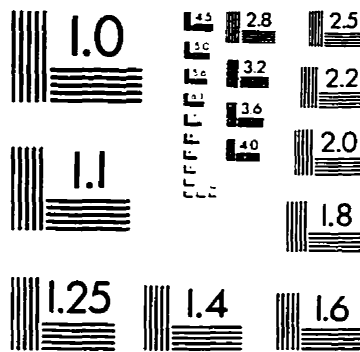
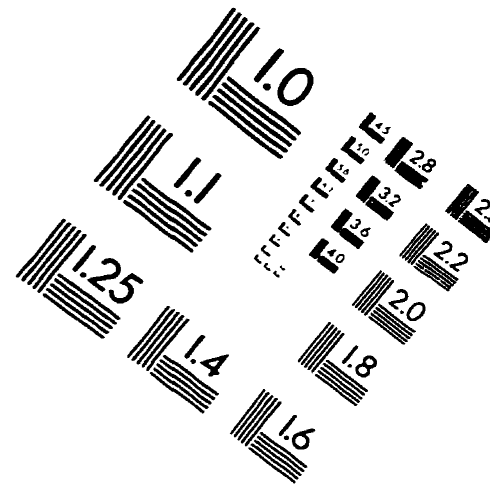
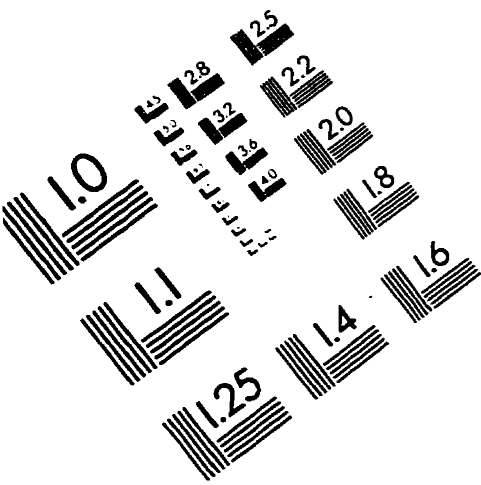
INSTITUTE OF CANADA  
DRAWING No. 9301A001 102



[illegible]



# IMAGE EVALUATION TEST TARGET (QA-3)



APPLIED IMAGE, Inc.  
1653 East Main Street  
Rochester, NY 14609 USA  
Phone: 716/482-0300  
Fax: 716/288-5989

© 1993, Applied Image, Inc., All Rights Reserved

